A Combination of Linear and Quadratic Time-Frequency Techniques for Time-Varying Signals

by

Muhammad Ajab
PE093007

A thesis submitted to the
Electronic Engineering Department
in partial fulfillment of the requirements for the degree of
DOCTOR OF PHILOSOPHY IN ELECTRONIC ENGINEERING

Faculty of Engineering
Mohammad Ali Jinnah University
Islamabad
July, 2013

Dedicated to Hazrat Syedna Ghaus- e-Azam Shaikh Abdul Qadir Jilani
(Sarkar Ghaus Pak)

ACKNOWLEDGMENT

ABSTRACT

Majority of the time-frequency representations (TFRs) make some kind of compromise between auto-component's resolution and cross-terms suppression during the analysis of time varying signals. Linear TFRs offer no cross-terms but have low resolution of auto-components. Quadratic TFRs offer better resolutions of auto-components but have cross-terms. The proposed research focuses on TFRs that can combine the advantages of both linear and quadratic TFRs.

In the first part of this research, a modified form of Gabor Wigner Transform (GWT) has been proposed by using adaptive thresholding in Gabor Transform (GT) and Wigner Distribution (WD). The proposed GWT combines the advantages of both GT and WD and provides a powerful analysis tool for analyzing multi-component signals. This technique is however not very efficient for multi-component signals having large abrupt amplitude variation in its auto-components.

In multi-component signal analysis where GWT fails to extract auto-components, the combination of signal processing techniques such as fractional Fourier transform (FRFT) and image processing techniques such as image thresholding and segmentation have proven their potential to extract auto-components. In the second part of this research, an algorithm is proposed for an effective representation in time-frequency domain called Modified Fractional GWT that combines the strengths of GWT, image segmentation and FRFT. This representation maintains the resolution of auto-components besides recognizing FRFT, a powerful tool for signal analysis. Performance analysis of proposed fractional GWT reveals that it provides solution of cross-terms of WD and worst resolution faced by linear TFRs.

In the third part of this work, a novel algorithm for effective representation of multi-component signals in time-frequency domain is proposed. The scheme not only suppresses the cross terms but also ensures that all the auto-components even very weak ones are properly shown in time-frequency domain. The scheme also results in much localized time frequency representation (TFR). The algorithm uses the strengths of GWT and linear time-varying (LTV) filtering in time domain to design a filter in time-frequency domain that suppresses cross terms and enhances auto components through an iterative approach. Performance analysis of proposed algorithm reveals

that it provides concentrated and high resolution auto-components which are desirable for a TFR.

The TFRs are used to separate and extract signal's auto-components which are buried in noise and are used to estimate the instantaneous frequency of a multi-component signal in low SNR scenarios. The modified GWT can be used for detection, identification and classification of power quality disturbances (such as voltage sag, voltage swell, transients and harmonics). The LTV based GWT and modified fractional GWT can be extended for IF estimation of auto-components of EEG Seizure.

LIST OF PUBLICATIONS AND SUBMISSIONS

[1]   **M. Ajab**, I. A. Taj and N. A. Khan, "Comparative Analysis of Variants of GWT for Cross-Terms Reduction," Metrology and Measurement Systems, vol. 19, no.3, 499-508, 2012 (ISSN 0860-8229, Impact Factor 0.982).

[2]   **M. Ajab,** I. A. Taj , I. Shafi and S.Stankovic, "A new form of Gabor Wigner Transform by adaptive thresholding in Gabor Transform and Wigner Distribution and the power of signal synthesis techniques to enhance the strengths of GWT," Metrology and Measurement Systems, vol. 20, no.2, 99-106, 2013 (ISSN 0860-8229, Impact Factor 0. 982).

[3]   **M. Ajab**, I. A. Taj and N. A. Khan, "On efficacy of combining linear and quadratic time frequency representations for time-varying signal analysis: A Review," Metrology and Measurement Systems, (accepted, ISSN 0860-8229, Impact Factor 0. 982).

[4]   **M. Ajab**, I. A. Taj and N. A. Khan, "A highly localized time-frequency representation scheme for dynamic signal with multiple components of varying strengths," Signal Processing, (submitted, ISSN 0165-1684, Impact Factor 1.851).

Table of Contents

List of Figures

List of Tables

List of Acronyms

FT   Fourier Transform

TFR   Time-Frequency Representation

TFRs   Time-Frequency Representations

STFT   Short-time Fourier Transform

GT   Gabor Transform

WT   Wavelet Transform

WD   Wigner Distribution

SWD   Smoothed Wigner Distribution

SPWD   Smoothed Pseudo Wigner Distribution

FRFT   Fractional Fourier Transform

GWT   Gabor Wigner Transform

ICI   Intersection of the confidence interval

SVM   Support vector machine

MFT   Multi-resolution Fourier transform

IF   Instantaneous Frequency

LTV   linear time varying

Chapter 1

Introduction

1.1 Background

Representation and analysis of a signal play a vital role in various applications of signal processing. Signals are commonly represented either in time domain or in frequency domain. Time representation of one dimensional signal does not contain the frequency description of the signal. Similarly frequency domain representation of the signal cannot tell how the frequency contents of the signal change with respect to time. This information may be critical in many non-stationary signals found in various practical applications, like seismic signals, radar signals, voice communication signals, biomedical signals, etc. Therefore a time variable is induced in Fourier transform (FT) to obtained information about the changes of frequency content with respect to time. Hence, the basic goal of a time frequency representation (TFR) is to find out the concentration of signal' auto-components along the frequency axis for a given time [1].

A TFR is a two-dimensional (2D) function which provides simultaneously, temporal and spectral information and therefore is used to analyze the non-stationary signals. It provides the information which is unavailable in time or frequency representation alone. Time frequency representations (TFRs) provide information, such as number of auto-components, time duration, frequency band and relative amplitude of the considered signal [2].

TFRs are classified as Linear TFRs and Quadratic TFRs. Linear TFRs including short time Fourier transform, Gabor transform (GT), wavelet transform, etc., obey the principle of superposition. Linear TFRs offer no cross-terms but have low resolution of auto- components. Quadratic TFRs including Wigner distribution (WD), spectrogram, etc., offer better resolutions of auto-components but have cross-terms [1, 3]. Therefore there is no unique TFR that tackles all types of non-stationary signals and the selection of a particular TFR is highly dependent upon specific application at hand. However, TFRs have proven their utility in successful identification, extraction and classification of signals' auto-components in various

applications. TFRs are often compared in terms of their ability to suppress cross-terms, resolution performance and mathematical properties [2].

1.2 Objectives

As discussed on the basis of general merits and demerits of linear and quadratic TFRs, there is a no unique TFR that tackles all possible applicational requirements. WD, which is the most popular quadratic TFR, has high resolution of auto-component in case of mono-component signal and it has cross-terms in case of multi-component signal and also suffers from inner interference due to non-liner frequency modulation. On the other hand linearity of GT avoids cross-terms, but GT has low resolution of auto-components than WD. A detailed analysis of most widely used linear and quadratic TFRs, their strengths and limitations and the need to combine linear and quadratic TFRs is discussed in the initial chapters of this thesis. Two main goals for a desirable TFR are,

- high concentration of auto-components and
- elimination of the cross-terms.

For achieving the above desirables, it is necessary to combine the strengths of both linear and quadratic TFRs [4].

The objective of this research is to propose a TFR with the following features.

- It should preserve the quality of auto-components for a multi-component signal.
- Eliminate the cross-terms and inner interference due to non-liner frequency modulation which is the main bottleneck of quadratic TFRs.
- It provides better features of both linear and quadratic TFRs
- The computational requirements should be in acceptable range.

1.3 Contributions

The research presented in this thesis contributes in the field of time-frequency signal analysis as follows.
.
- <u>Critical review of widely used linear and quadratic TFRs and their combinations</u>

2

As the first part of this research a comprehensive comparative analysis of widely used linear and quadratic TFRs, including their merits and demerits has been done. In this part, discussion on fractional Fourier transform (FRFT) and signal synthesis technique are given, which are used for time varying-filtering. This part also provides critical analysis of recent cross-terms suppression techniques. In addition comparative analysis of variants of Gabor Wigner transform (GWT) defined in [4] have been done by using various performance measures.

- Modified Gabor Wigner transform

    A modified form of Gabor Wigner Transform (GWT) has been developed by using adaptive thresholding in GT and WD. The proposed GWT combines the advantages of both GT and WD and proves itself as a powerful tool for analyzing multi-component signals. Performance analysis of modified GWT shows to have high resolution as well as cross-terms suppression of WD. All above techniques are applicable for slowly time varying signals.

- Modified fractional GWT

    In multi-component signal analysis where most widely used variants of GWT fail to extract auto-components, the combination of signal processing techniques (FRFT) and image processing techniques including image thresholding and segmentation have proven their potential to extract auto-components. The proposed algorithm maintains the resolution of auto-components and readability of weak components. This work also shows that fractional Fourier transform (FRFT) domain is a powerful tool for signal analysis. Performance analysis of modified fractional GWT reveals that it provides solution of cross-terms of WD and resolution problem of linear TFRs.

- GWT and linear time-varying (LTV) filtering based TFR

    In this part, the advantages of GWT are analyzed by using linear time varying filtering techniques. In this approach a filter in time-frequency domain is designed using an iterative approach in both time-frequency and time

domains. This filter is specifically designed in order to suppress cross-terms and enhances concentration of auto-components even weaker ones. In this approach the strengths of time varying filtering, GWT and image processing are exploited.

1.4 Thesis Overview

The thesis is organized as follows.

Chapter 1 gives introduction of joint time-frequency signal analysis, problem formulation and contributions in this thesis.

Literature review is described in Chapter 2. It starts with the review of time domain signal representation, Fourier transform and TFRs. This chapter also includes discussion and comparison of some of linear TFTRs, quadratic TFRs, cross-terms suppression techniques, reduced interference TFRs and IF estimation techniques. It also includes a comprehensive discussion on FRFT domain.

Chapter 3 presents performance measures regarding to TFRs. It includes readability criteria, cross-terms suppression criteria, energy concentration criteria and resolution criteria.

Chapter 4 describes the need for combination of linear and quadratic TFRs. It describes different ways to combine GT and WD as proposed in [4] and modified form of GWT by using adaptive thresholding in GT and WD.

Chapter 5 describes the advantages of GWT in FRFT domain for a multi-component signal analysis where GWT fails to extract auto-components. This chapter also describes combination of signal processing and image processing techniques to extract auto-components.

Chapter 6 presents another novel iterative technique to find a TFR which fuses GWT and LTV filtering techniques.

Chapter 7 concludes the thesis. It includes limitations and future work.

Chapter 2

Review of widely used TFRs

This chapter includes a thorough review of some of the most popular linear and quadratic TFRs. It also reviews some of the common signal processing techniques which are often combined with TFRs in order to get a better signal representation. These techniques include fractional Fourier transform for analysis of time varying signals, cross-terms suppression techniques and reduce interference TFRs. In this chapter signal synthesis techniques and IF estimation techniques are also discussed.

2.1 Time and Frequency representation of a signal

Time representation of a signal is a function of time which may be written in the form $x(t)$. Time domain signal indicates how a signal's amplitude changes over time. This representation leads immediately to the instantaneous power, which shows how the energy of the signal is distributed over time, the total signal energy (E) is given by the integration of instantaneous power over time and E is expressed as,

$$E = \int_{-\infty}^{\infty} |x(t)|^2 \ dt. \tag{2.1}$$

$Eq\,(2.1)$ does not show how the frequency varies with time [3, 5].

Fourier transform (FT) maps the signal into a set of frequency components and transforms the signal $x(t)$ onto the domain of orthogonal basis $\exp(-j\omega t)$. FT is expressed as,

$$X(\omega) = \int_{-\infty}^{\infty} x(t)) \exp(-j\omega t) dt, \tag{2.2}$$

where $X(\omega)$ is FT of $x(t)$ and the inverse FT is given by,

$$x(t) = 1/2\pi \int_{-\infty}^{\infty} X(\omega) \exp(j\omega t) d\omega. \tag{2.3}$$

The problem of FT is that it does not show where frequency components occur in time domain. For stationary signals FT is a favorable representation, since the frequency components of the stationary signals do not change with time [3, 5].

2.2 Time-Frequency Representations (TFRs)

A TFR is a two-dimensional (2D) function which provides simultaneously, temporal and spectral information and therefore is used to analyze the non-stationary signals.

As a simple demonstration of a TFR, consider a signal consisting of three quadratic components. Fig 2.1(a, b) describes time domain analysis of the signal. This representation only tells varying amplitude with respect to time and has no information about number of auto-components in the signal. Similarly FT (Fig 2.1 (c)) of the signal describes frequency contents of the multi-component signal. Fig 2.1(d) clearly indicates that there are three quadratic components are present in the signal. In this simple example we have shown that how a combined TFR is more descriptive and abstract representation as compared to other representations.
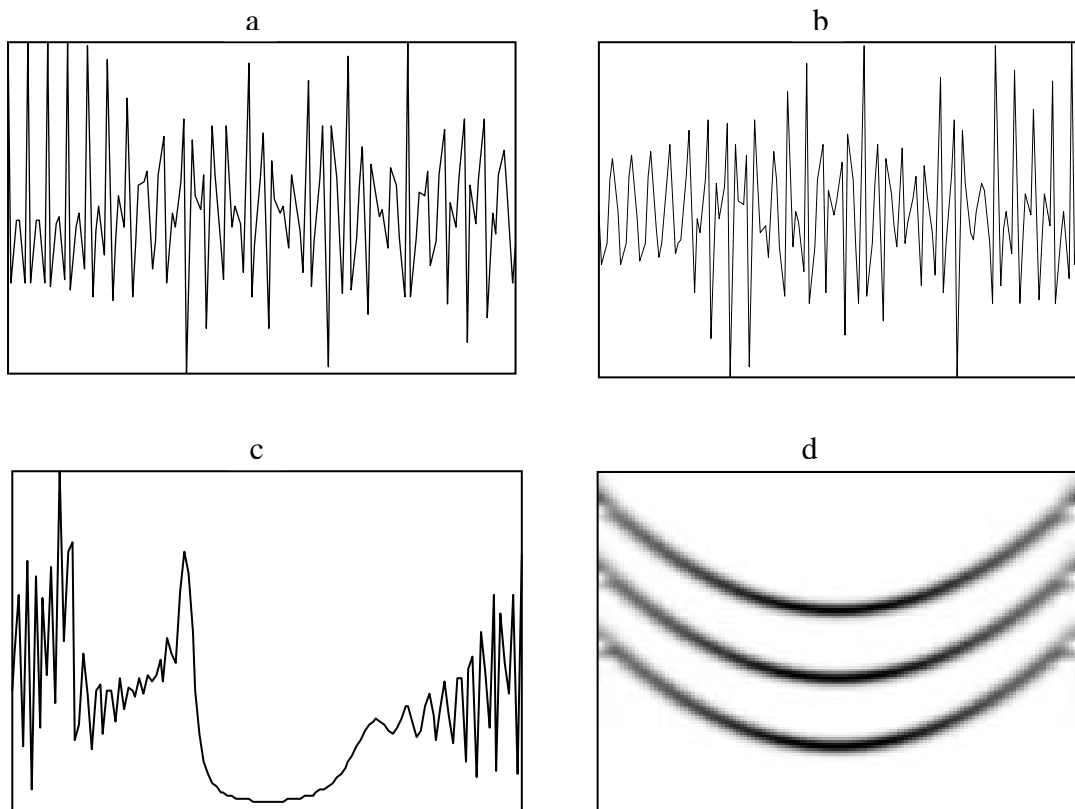
Fig 2.1 Analysis of a multi-component signal (a) time-domain analysis (real part), (b) time-domain analysis (imaginary part), (c) FT analysis and (d) TFR analysis.

Four desired properties [2] of an ideal time frequency representation are:

(a) Readability

This property depends upon concentration and resolution of auto-component.

(b) Free of Cross-terms

This property distinguishes noise and auto-component.

(c) Fulfilling mathematical properties

It is required that a given TFR fulfills mathematical properties including energy constraints and marginal characteristics etc.

(d) Low computational cost

Low computational complexity is required to show a signal on time frequency plane.

Two main analysis approaches for TFRs are Linear and Quadratic techniques.

2.2.1 Linear TFRs

Linear TFRs obey the principle of superposition. For a signal, $x(t)$ the TFR is given by,

$$TFR_x(t,\omega) = \int\limits_{-\infty}^{\infty} x(\tau)\varphi^*_{t,\omega}(\tau)d\tau, \tag{2.4}$$

where $x(t)$ represent signal, $\varphi_{t,\omega}(\tau)$ represents the basis functions and '*' represents the complex conjugate. Short-time Fourier transform (STFT), wavelet transform (WT), and matching pursuit algorithms are typical examples in this category [6, 7, 8].

2.2.1.1 Short-time Fourier transform

STFT [3, 5], the simplest TFR, is a two-dimensional representation that has been introduced for better time localization of the frequency contents of a signal by using a suitable time window. By using STFT, we can observe how the frequency of a signal changes with time. It multiplies the signal with a symmetric sliding window $w(t-\tau)$ and then transforms it to the frequency domain. STFT of a signal $x(t)$ is defined as:

$$STFT_x(t,\omega) = \int\limits_{-\infty}^{\infty} x(\tau)w(t-\tau)\exp(-j\omega\tau)d\tau. \tag{2.5}$$

Implementation issues of STFT include how to choose the shape and size of window function. Wide window provides high frequency resolution (Fig 2.2) while narrow window has high time resolution (Fig 2.3). Once the analysis window is chosen, the resolution is set for both time and frequency. We cannot have a window function that corresponds to   an arbitrary short time duration and narrow frequency bandwidth at the same time. According to Uncertainty Principal it is impossible to get both frequency and time resolution at the same time [9].
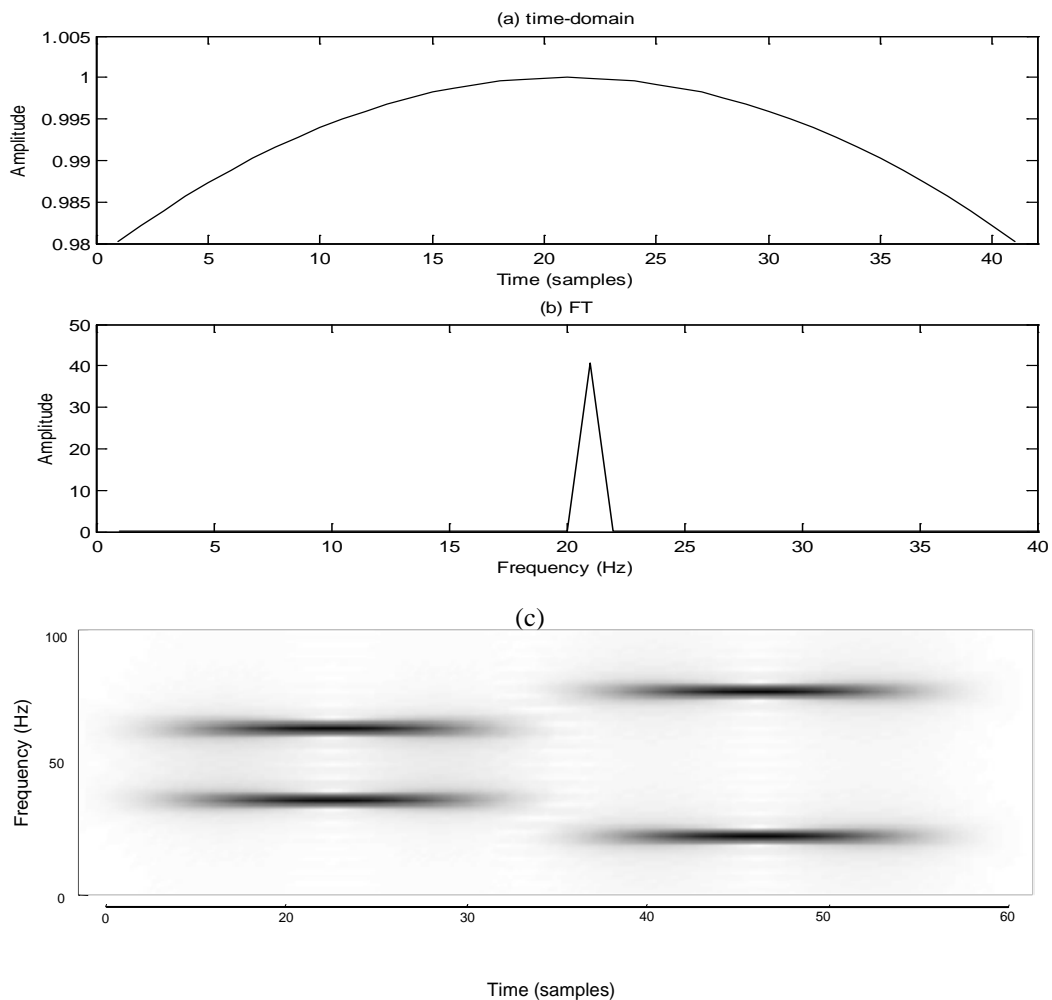
Fig 2.2: Tradeoff between time resolution and frequency resolution (a) the time function of the wide Hamming window. (b) The Fourier Transform of the wide Hamming window. (c) The amplitude of STFT.

8
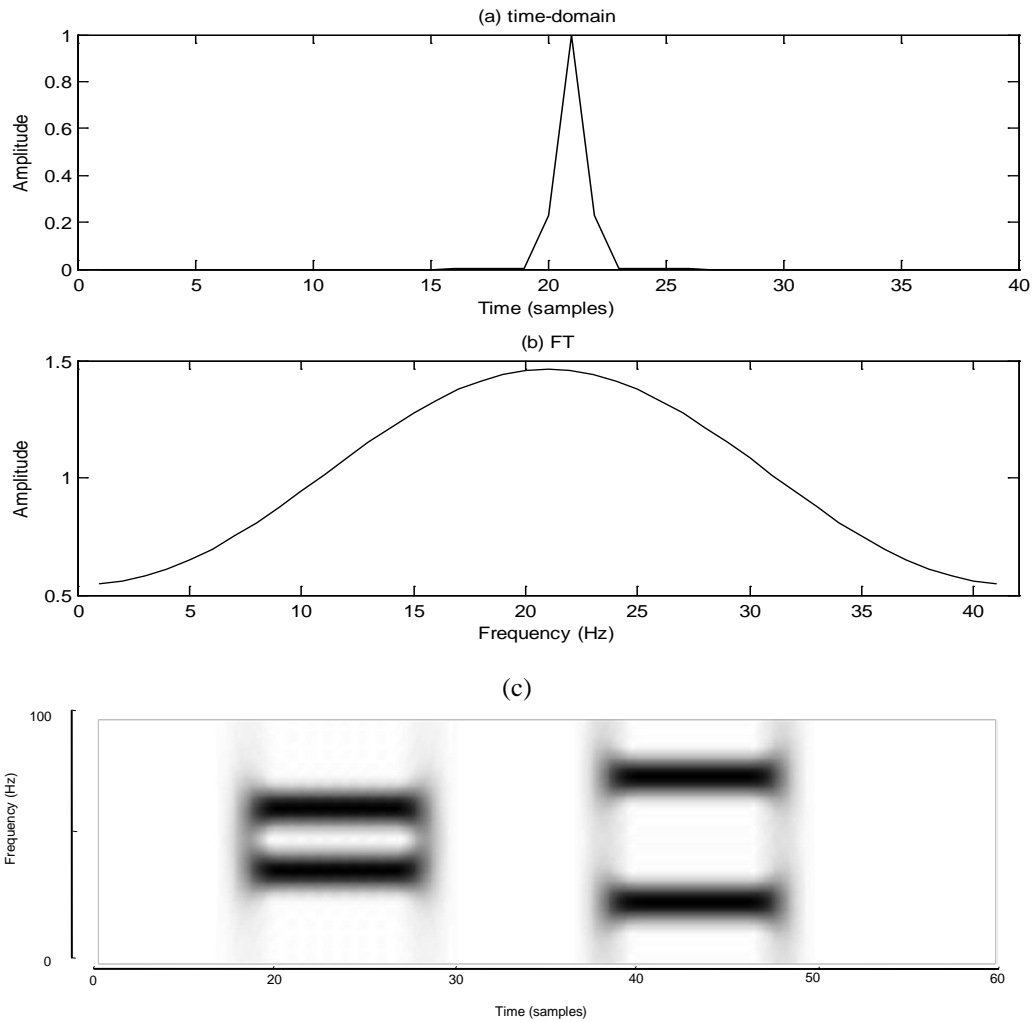
Fig 2.3: Tradeoff between time resolution and frequency resolution (a) the time function of the narrow Hamming window. (b) The Fourier Transform of the narrow Hamming window. (c) The amplitude of STFT.

2.2.1.2 Gabor transform (GT)

As discussed in previous section, as an outcome of Uncertainty Principal [9], it can generally be state that, it is impossible to achieve both time and frequency resolution at the same time. However Gaussian window achieves an optimal joint time- frequency concentration with maximum possible resolution in both domains. For example, consider a Gaussian window $w(t)$

$$w(t) = e^{-at^2/2}. \tag{2.6}$$

In Fig 2.4 we can analyze the behavior of parameter "a" in $Eq\,(2.6)$. Window parameter "a"control the balance of the time-frequency concentration. The small value of "a"gives narrow frequency bandwidth. The large value of "a"gives short time duration.
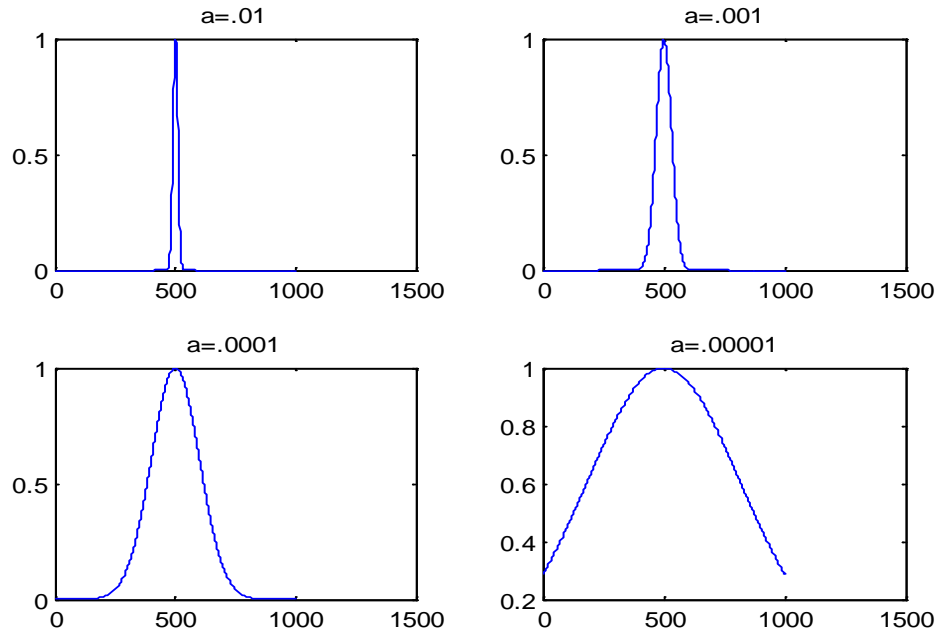
Fig 2.4 the behavior of controlling parameter "a" of a Gaussian Window, which balance the time frequency concentration.

As a reason of choosing a Gaussian mask, further significance of a Gaussian function is discussed. The Gaussian function gives the following main benefits.

- Among all functions, the Gaussian function has the advantage that the area in time-frequency distribution is minimal.
- FT of a Gaussian function is also Gaussian function

$$\int_{-\infty}^{\infty} e^{-t^2/2} e^{-j\omega t} dt = e^{-\omega^2/2}. \tag{2.7}$$

Gaussian function fulfills the lower limit of uncertainty principle [9]

$$\Delta_t \Delta_\omega = \frac{1}{2}, \quad where\, \Delta_t = time\ duration\ and\ \Delta_\omega = frequency\ bandwidth \tag{2.8}$$

The variant of STFT with Gaussian window is called as Gabor transform [4, 10]. The main feature of the GT is its linearity but GT has less resolution of auto-components than WD. On the other hand GT does not have the cross-term problem. Mathematically GT of $x(t)$ is defined as,

$$GT_x(t,\omega) = \sqrt{\frac{1}{2\pi}} \int_{-\infty}^{\infty} e^{-(\tau-t)^2/2} e^{-j\omega(\tau-t/2)} x(\tau) d(\tau). \tag{2.9}$$

Implementation wise GT may consume less computation time after a little optimization that exploits the nature of Gaussian function. Gaussian window outside a certain boundary can be ignored. Note that, although from $Eq(2.9)$, range of integration for GT is $(-\infty,\infty)$, but we know that

$$e^{-x^2/2} < 0.00001, \; when \; |x| > 4.7985 \tag{2.10}$$

Therefore, modified GT can be well approximated by

$$GT_x(t,\omega) \approx \sqrt{\frac{1}{2\pi}} \int_{t-4.7985}^{t+4.7985} e^{-(\tau-t)^2/2} e^{-j\omega(\tau-t/2)} x(\tau) d(\tau). \tag{2.11}$$

This modification, as given in $Eq(2.11)$, reduces the computational time of GT significantly.

As GT is a linear operator and the cross-term problem is avoided. If $x(t)$ consists of two components then the following equation is fulfilled showing no cross-terms in case of GT.

$$GT_x(t,\omega) = GT_{x_1}(t,\omega) + GT_{x_2}(t,\omega). \tag{2.12}$$

Let us consider the example of (linear component (chirp), transient component (Gaussian atom), quadratic component and multiple quadratic components). Analysis of these signals through GT (Fig 2.5) shows the effect of linear time frequency transformation. GT eliminates cross-terms in case of linear component, Gaussian component and quadratic component at the cost of component's blurring. Our analysis reveals that in case of multiple quadratic components, GT blurring, makes it difficult to extracts the individual auto-components which are closely placed.

a b c d

Fig 2.5 GT Analysis of (a) linear component (b) atom or transient (c) quadratic component (d) multiple quadratic components

In summary merits of GT are

➢ it avoids cross-terms problem (GT is a linear operator)and

➢ consumes less computation time.

➢ The drawback GT is that it has low resolution than WD because of blurring. However, the resolution of GT is better than WD for a particular signal of the form $e^{(jat^k + \phi_k)}$, where ϕ_k are remaining terms and $k \geq 3$ [4].

2.2.1.3 Multi-resolution Fourier transform (MFT)

This method [11] has a variable resolution and is defined as:

$$MFT_x(t,\omega) = \int\limits_{-\infty}^{\infty} x(\tau)\sqrt{s}h(s(\tau - t))\exp(-j\omega\tau)d\tau. \tag{2.13}$$

In $Eq(2.13)$, $h(.)$ is a window and s a is scale. Since this method is a function of multiple variables, it is not very suitable for various applications.

2.2.1.4 S-transform

This method [12] also has variable resolution and is defined as:

$$S-transform_x(t,\omega) = \int_{-\infty}^{\infty} x(\tau)h(\tau-t,\sigma(\omega))\exp(-j\omega\tau)d\tau. \qquad (2.14)$$

In $Eq(2.14)$, σ is a standard deviation of Gaussian window $h(.)$. The parameter $\sigma(\omega)$ in $Eq(2.14)$ provides further flexibility for signal analysis however the drawback of this technique is single analysis window.

2.2.1.5 Wavelet Transform

Due to the sliding window function the spectrum generated by STFT is limited in resolution. WT is a TFR which gives variable resolution. It is based on the so called "wavelet theory". It is an advancement of the STFT where length of window is made a frequency dependent parameter. The main feature of the WT is its scale which provides information about the frequency. So WT is "time-scale representation". The scale is the main parameter of WT for time varying signals. High values of frequency correspond to small values of scale and vice-versa [13, 14]. Mathematically,

$$WT_x(t,\omega) = \int_{\tau} x(\tau)\sqrt{|\omega/\omega_0|}f^*(\omega/\omega_0(\tau-t))d\tau, \qquad (2.15)$$

where $f(t)$ is the analyzing wavelet and ω/ω_0 is scale parameter. WT decomposes the signal $x(t)$ into shifted and dilated wavelets. Multi-resolution property of WT is a main feature of WT over FT. WT may improve resolution of STFT, but it also suffers from same resolution limit as that of STFT due to uncertainty principle.

In summary, as discussed in the review of some famous linear TFRs, these TFRs are cross-terms free but have low resolution of auto-components.

2.2.2 Quadratic TFRs

Quadratic TFRs are expected to fulfill the following marginal criteria [5]. Mathematically,

$$|x(t)|^2 = \int TFR_x(t,\omega)d\omega, \tag{2.16}$$

$$|X(\omega)|^2 = \int TFR_x(t,\omega)dt. \tag{2.17}$$

Apart from marginal criteria, Quadratic TFRs offer better resolution and are expected to fulfill large number of other mathematical properties. Quadratic TFRs were originally proposed by Cohen [5, 15]. Mathematically these TFRs are generally given as,

$$TFR_x(t,\omega) = \frac{1}{4\pi^2} \iiint x(u+\tau/2\tau)x*(u-\tau/2\tau)\varphi(\theta,\tau)e^{-j(\theta t+\omega\tau+\theta u)}dud\tau d\theta, \tag{2.18}$$

where $\varphi(\theta,\tau)$ is a kernel function which determines a particular TFR [1]. Commonly used methods for obtaining these TFRs are Wigner distribution, S-method and Spectrogram.

2.2.2.1 Spectrogram and its mathematical properties

Spectrogram [1] is defined as,

$$SPEC_x(t,\omega) = \left| \int_{-\infty}^{\infty} x(\tau)w(t-\tau)\exp(-j\omega\tau)d\tau \right|^2. \tag{2.19}$$

It is frequently used in the time-frequency analysis. This TFR also obeys the uncertainty principle [9] and it is impossible to achieve a high resolution in both time and frequency domains at the same time. Various versions of spectrogram was proposed to improve auto-components' resolution. A 2-D de-convolution operator is applied on the STFT spectrogram in [16], but this technique is highly dependent upon de-convolution method. Spectrogram' de-blurring by using neural networks [17] and by using fractional windows [18]. All above techniques [16, 17, 18] have low resolution of auto-components.

If a signal $x(t)$ consist of two auto-components then $STFT$ of $x(t)$ is

$$STFT_x(t,\omega) = STFT_{x_1}(t,\omega) + STFT_{x_2}(t,\omega). \tag{2.20}$$

Now,

$$SPEC_x(t,\omega) = \left| STFT_{x_1}(t,\omega) + STFT_{x_2}(t,\omega) \right|^2. \tag{2.21}$$

By expanding $Eq(2.21)$,

$$SPEC_x(t,\omega) = SPEC_{x_1}(t,\omega) + SPEC_{x_2}(t,\omega) +$$
$$2\,\mathrm{Re}[STFT_{x_1}(t,\omega)STFT_{x_2}^*(t,\omega)]. \tag{2.22}$$

14

In $Eq(2.22)$ $STFT_{x_2}^*(t,\omega)$ is transpose of $STFT_{x_2}(t,\omega)$. For $i = 1, 2$, $Eq(2.20)$ takes the form,

$$STFT_{x_i}(t,\omega) = \left| STFT_{x_i}(t,\omega) \right| e^{j\phi_{x_i}(t,\omega)}. \tag{2.23}$$

In $Eq(2.23)$ $\left| STFT_{x_i}(t,\omega) \right|$ is the amplitude and $\phi_{x_i}(t,\omega)$ is the phase. Putting $Eq(2.22)$ and $Eq(2.23)$ in $Eq(2.21)$ we have,

$$SPEC_x(t,\omega) = SPEC_{x_1}(t,\omega) + SPEC_{x_2}(t,\omega) +$$
$$2\left| STFT_{x_1}(t,\omega) \right|\left| STFT_{x_2}(t,\omega) \right| \cos(\phi_{x_1}(t,\omega) - \phi_{x_2}(t,\omega)). \tag{2.24}$$

In $Eq(2.24)$, the first and second terms on right hand side are auto-components and the third term is a cross-term. In case of spectrogram, the cross-term is zero if STFT of two auto-components have no overlap. Similarly its cross-term, if present, occurs always at the intersection of auto-components [19].

Let us consider the same example of four signals including a linear chirp, Gaussian atom, quadratic component and multiple quadratic components. Analysis of these signals through spectrogram (Fig 2.6) shows that auto-components has low resolution, and in case of multiple quadratic components it is difficult to extract the individual auto-components which are closely placed.

Fig 2.6 Spectrogram Analysis of (a) linear component (b) atom or transient (c) quadratic component (d) multiple quadratic components.

2.2.2.2 Wigner Distribution and its mathematical properties

WD is the most popular TFR [5, 20]. Mathematically, WD of a signal $x(t)$ is defined as,

$$WD_x(t,\omega) = \int_{-\infty}^{\infty} x(t+\tau/2)x^*\ (t-\tau/2)e^{-j\omega\tau}d\tau, \tag{2.25}$$

where $x^*(t)$ is the complex conjugate of $x(t)$. WD is not a linear operator since it contains an autocorrelation term. If a signal $x(t)$ consist of two components then WD of $x(t)$ is given by,

$$WD_x(t,\omega) \neq WD_{x_1}(t,\omega) + WD_{x_1}(t,\omega). \tag{2.26}$$

In $Eq(2.26)$,

$$x(t) = x_1(t) + \ x_2(t). \tag{2.27}$$

WD exhibits its high resolution for analysis of a linear chirp and a Gaussian atom, while in case of multiple quadratic components, WD has a severe cross terms problem [3, 6].

We consider the same example of four signals including a linear chirp, Gaussian atom, quadratic component and multiple quadratic components. Analysis of these signals through WD reveals that in case of linear chirp and Gaussian atom WD shows its high resolution property, while in case of quadratic component and multiple quadratic components, WD has a severe cross-term as shown in Fig 2.7.

Fulfillment of mathematical properties including reality, time invariance, frequency shift invariance, time marginal, frequency marginal, signal energy, instantaneous frequency, group delay, time support, frequency support, convolution invariance, modulation invariance and inner product invariance etc. are the strengths of WD. This is shown in Table 2.1. These strengths have made WD a powerful tool for analysis of signals [20, 21]. Similarly WD has a drawback of its quadratic nature and introduces the cross-terms which makes difficult to visualize the time-frequency plane [22].
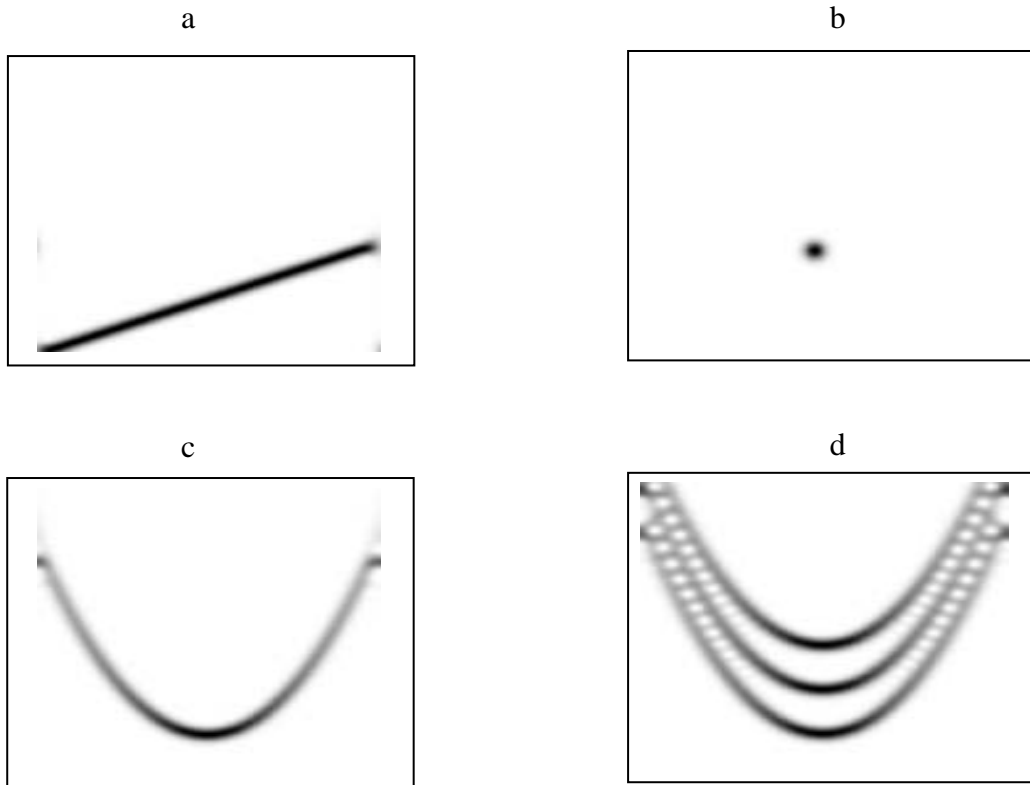
Fig 2.7 WD Analysis of (a) linear component (b) atom or transient (c) quadratic component (d) multiple quadratic components

Consider a signal $x(t)$ consisting of M auto-components given as follows,

$$x(t) = \sum_{i=1}^{M} x_i(t).$$ (2.28)

The WD of $x(t)$ is given by

$$WD_x(t,\omega) = \sum_{i=1}^{M} WD_{x_i}(t,\omega) + \sum_{k=1}^{M-1} \sum_{l=k+1}^{M} 2\operatorname{Re}(WD_{x_k x_l}(t,\omega)).$$ (2.29)

$Eq(2.29)$ shows that the WD of the multi-component signal $x(t)$ has M auto-components and $M(M-1)/2$ cross-components. The properties of cross- terms are defined in [23]. Now consider a signal $x_0(t)$. Let $x_1(t)$ and $x_2(t)$ be the time and frequency shifted version of $x_0(t)$ then these signals are given as,

17

$$x_0(t) = e^{j(\omega_o t + \frac{1}{2}\beta t^2)},$$ (2.30)

$$x_1(t) = x_o(t-t_1)e^{j\omega_1 t},$$ (2.31)

$$x_2(t) = x_o(t-t_2)e^{j\omega_2 t}.$$ (2.32)

The composition of $x_1(t)$ and $x_2(t)$ is $x(t)$ which given in $Eq(2.27)$. WD of the composite signal $x(t)$ is given by,

$$WD_x(t,\omega) = 2\pi\delta(\omega-(\omega_1+\omega_o)-\beta(t-t_1)) + 2\pi\delta(\omega-(\omega_2+\omega_o)-\beta(t-t_2)) +$$
$$4\pi\delta(\omega-(\omega_m+\omega_o)-\beta(t-t_m)) \times \cos(\omega_d(t-t_m)-t_d(\omega-\omega_m)+\omega_d t_m,$$ (2.33)

where $\delta(\omega)$ is impulse which is zero everywhere except at origin, $\omega_d = \omega_2 - \omega_1$,

$t_d = t_2 - t_1, t_m = (t_1+t_2)/2$ and $\omega_m = (\omega_1+\omega_2)/2$.

$Eq(2.33)$ shows that,

➢ cross-terms occur at mid-frequency and mid-time,

➢ cross-terms oscillates at a frequency proportional to the difference in time-shift and frequency- shift of the signal,

➢ cross-terms oscillates in the direction perpendiculars to the line that connects the signal auto-components, and

➢ The amplitude of cross-term is twice that of signal component.

The integration range of the WD ($Eq(2.25)$) is $(-\infty,\infty)$, means that due to $FT(x(t+\tau/2)x^*(t-\tau/2))$, the computation time of the WD is very high as compared to GT ($Eq(2.11)$), which can be time limited due to limited span of Gaussian window.

In summary WD has the advantage of:

• Infinite time and frequency resolution.

• WD gives direct information about time-frequency localization

• Ideal mono-component signal analysis tool.

• Nice mathematical properties.

The disadvantages of WD are:

• WD is not a linear operator.

• WD has cross-terms in case of quadratic and multi-component signal.

• High computation time.

Table 2. 1 Properties of WD

Property	Description
Reality	$WD(t,\omega)$ is real
Time Invariance	$x_\lambda(t) = x(t-t_0)$ $WD_x(t,\omega) = WD_x(t-t_0,\omega)$
Frequency Invariance	$x_m(t) = x(t)e^{j\omega t}$ $WD_x(t,\omega) = WD_x(t,\omega-\omega_0)$
Time Marginal	$\|x(t)\|^2 = \int WD_x(t,\omega)d\omega$
Frequency Marginal	$\|x(\omega)\|^2 = \int WD_x(t,\omega)dt$
Signal Energy	$E = \iint WD_x(t,\omega)dtd\omega$
Instantaneous Frequency	$\dfrac{\int \omega WD_x(t,\omega)d\omega}{\int WD_x(t,\omega)d\omega} = \dfrac{d}{d\omega}(\arg x(t))$
Group Delay	$\dfrac{\int \omega WD_x(t,\omega)dt}{\int WD_x(t,\omega)dt} = \dfrac{d}{d\omega}(\arg x(\omega))$
Time Support	If a signal exists in $[t_1,t_2]$ then it $WD(t,\omega)$ will also exist in this interval
Frequency Support	If a signal exists in $[\omega_1,\omega_2]$ then it $WD(t,\omega)$ will also exist in this interval
Convolution Invariance	$x(t) = x_1(t) * x_2(t)$ $WD_x(t,\omega) = WD_{x_1}(t,\omega)\,{}_t^*\,WD_{x_2}(t,\omega)$
Modulation Invariance	$x(t) = x_1(t)x_2(t)$ $WD_x(t,\omega) = WD_{x_1}(t,\omega)\,{}_\omega^*\,WD_{x_2}(t,\omega)$

2.3 Cross-terms suppression methods

In this section we will describe some of the most widely used cross-terms suppression techniques which have been proposed by researchers as extensions to WD.

2.3.1 Smoothed pseudo Wigner distribution (SPWD)

Different variants of WD were proposed to eliminate cross-terms of WD. Since cross-terms are highly oscillatory, the simple technique to remove them is, by applying a 2 dimensional low-pass filter on the signal processed through WD. Now the resultant WD is called as smoothed Wigner distribution (SWD) [24]. Mathematically SWD is,

$$SWD_x(t,\omega) = \int\limits_{-\infty}^{\infty} \int\limits_{-\infty}^{\infty} \phi(u,v)WD_x(t-u,\omega-v)dudv, \qquad (2.34)$$

where $\phi(u,v)$ is a 2D low-pass filter. The effect of this filtering is appeared as low resolution of auto-components. In separable form of $\phi(u,v)$ [$p(u)$ and $h(v)$] ,SWD is called as smoothed pseudo Wigner distribution (SPWD) [25]. Mathematically SPWD is defined as,

$$SPWD_x(t,\omega) = \int\limits_{-\infty}^{\infty} \int\limits_{-\infty}^{\infty} p(u)h(v)WD_x(t-u,\omega-v)dudv. \qquad (2.35)$$

The disadvantage of SPWD is degradation of original excellent time frequency resolution of WD. Moreover closely placed signal components cannot be separated due to smoothing effect.

In summary SPWD has the advantage of

- cross-terms reduction in case of quadratic component and multiple components.

The disadvantages of SPWD are

- worst resolution of auto-components
- cannot separates closely placed signal components

For the same example of four signals including a linear chirp, Gaussian atom, quadratic component and multiple quadratic components, the SWD is shown in Fig 2.8. Analysis of these signals through SWD reveals that in case of linear chirp, Gaussian atom and quadratic component it shows its high resolution property, while in case of multiple quadratic components SWD has cross-terms as shown in Fig 2.8. The behavior of SPWD for the same signal is shown in Fig 2.9. It is cleared that in case of multiple quadratic components it is impossible to extract individual auto-component as shown in Fig 2.9.

a   b

c   d
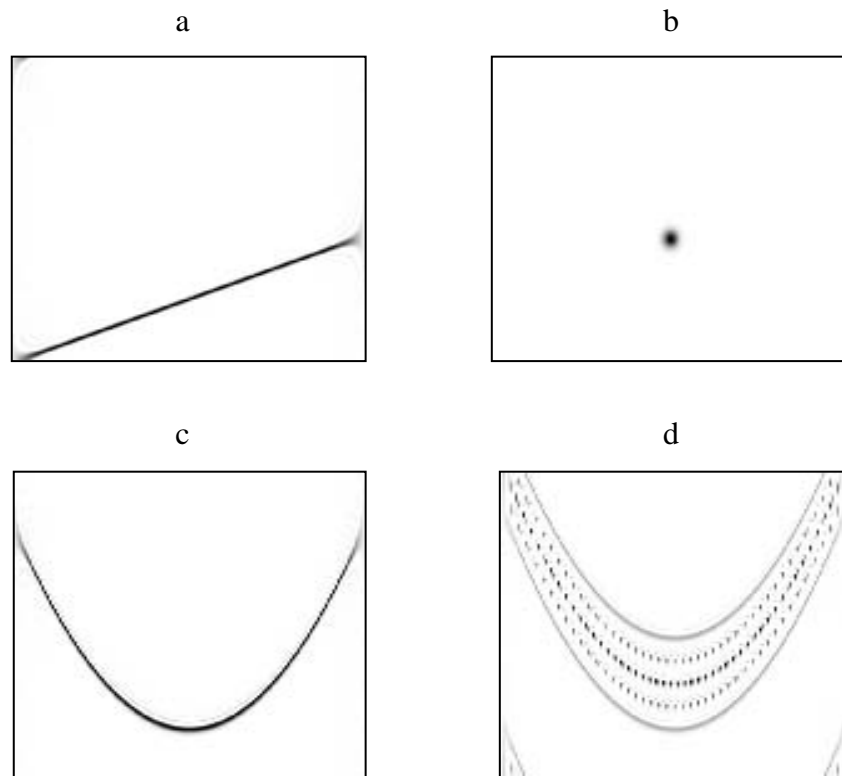
Fig 2.8 SWD Analysis of (a) linear component (b) atom or transient (c) quadratic
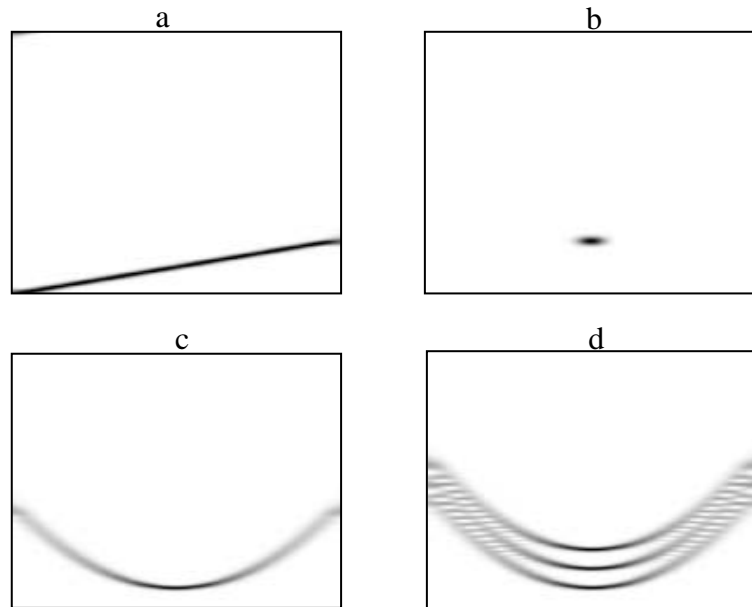component (d) multiple quadratic components
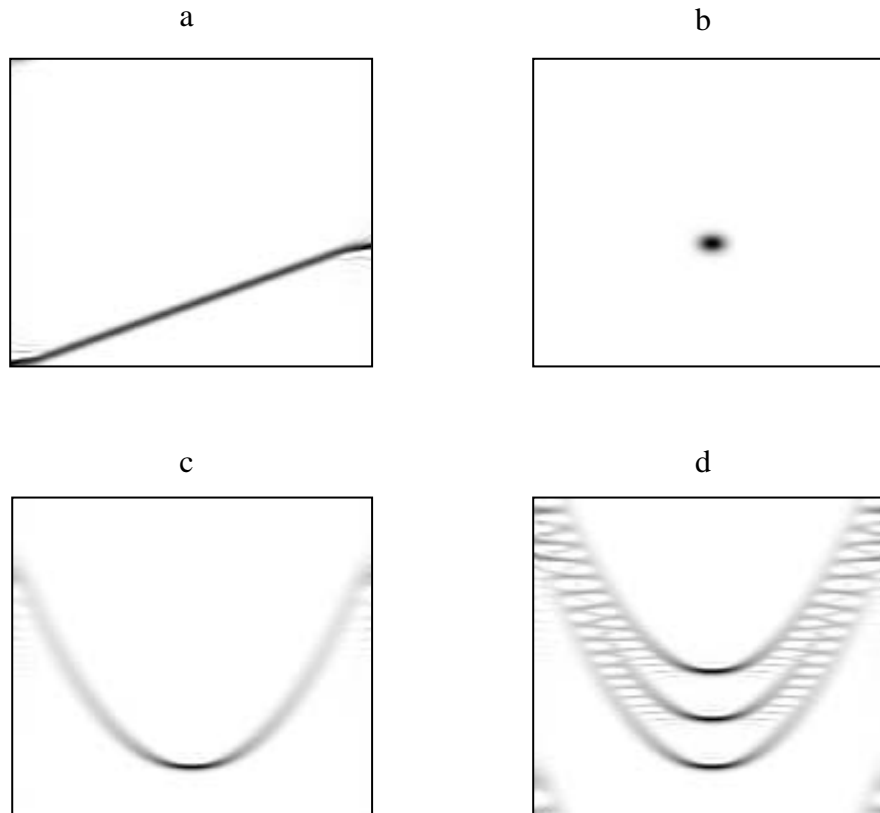
Fig 2.9 SPWD Analysis of (a) linear component (b) atom or transient (c) quadratic component (d) multiple quadratic components

2.3.2 Reassigned WD

Signal dependent or independent kernels suppress cross-terms at the cost of quality of auto-components. Reassignment technique [2, 26, 27] solves this problem by shifting back the auto-components. Eq. (2.9) shows that TFR at any time-frequency point is weighted sum of its neighboring points in time-frequency plane. The averaging of neighboring points may suppress cross-terms at the expense of disturbing the location of auto-components. Reassigned TFRs work on the rule that every point in a TFR is shifted back to the center of gravity of the TFR. The reassigned co-efficients are calculated as:

$$t'(t,\omega) = t - \frac{\iint t_0 \phi(t_0,\omega_0) WD_x(t-t_0,\omega-\omega_0) dt_0 d\omega_0}{\iint \phi(t_0,\omega_0) WD_x(t-t_0,\omega-\omega_0) dt_0 d\omega_0}, \qquad (2.36)$$

$$\omega'(t,\omega) = \omega - \frac{\iint \omega_0 \phi(t_0,\omega_0) WD_x(t-t_0,\omega-\omega_0) dt_0 d\omega_0}{\iint \phi(t_0,\omega_0) WD_x(t-t_0,\omega-\omega_0) dt_0 d\omega_0}. \qquad (2.37)$$

Now the affect of reassignment process is described as:

$$TFR_x(t,\omega) = \iint TFR_x(t_0,\omega_0)\delta(t-t'(t_0,\omega_0))\delta(\omega-\omega'(t_0,\omega_0)) dt_0 d\omega_0. \qquad (2.38)$$

Readability of reassigned TFR depends on cross-term reduction and auto-component preservation of the original TFR. The negative effect of this reassignment process is appeared as a loss of most of important mathematical properties of original TFR.

As in previous cases let us again consider the same example of four signals including a linear chirp, Gaussian atom, quadratic component and multiple quadratic components. Analysis of these signals through RSPWD reveals that in case of linear chirp, Gaussian atom and quadratic component RSPWD does not show its effect on auto-component resolution. In case of multiple quadratic components, it is impossible to extract individual auto-component as shown in Fig 2.10.
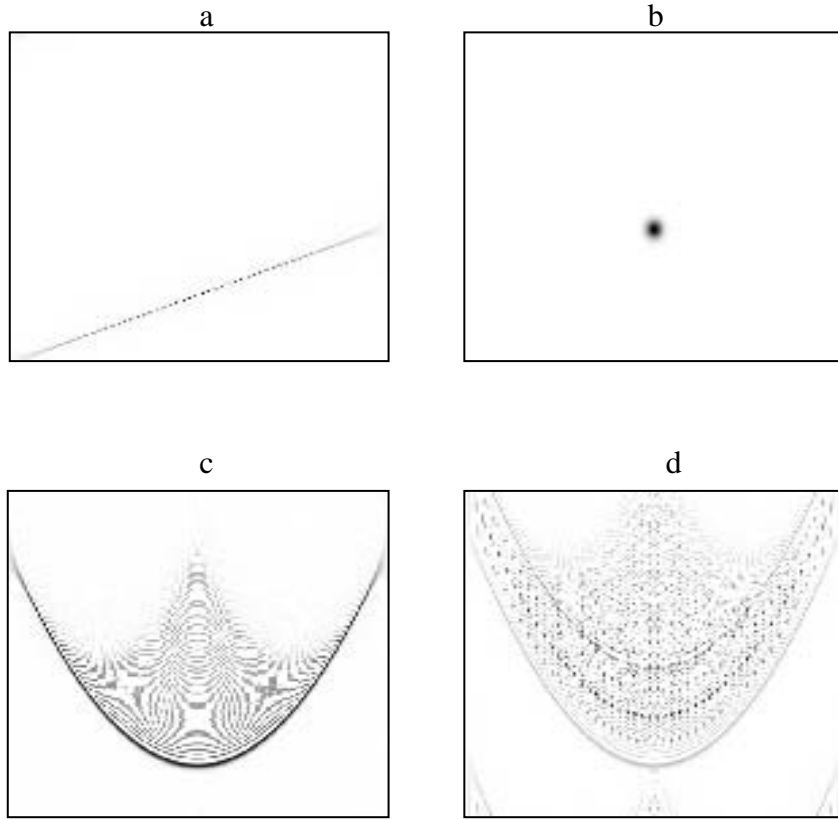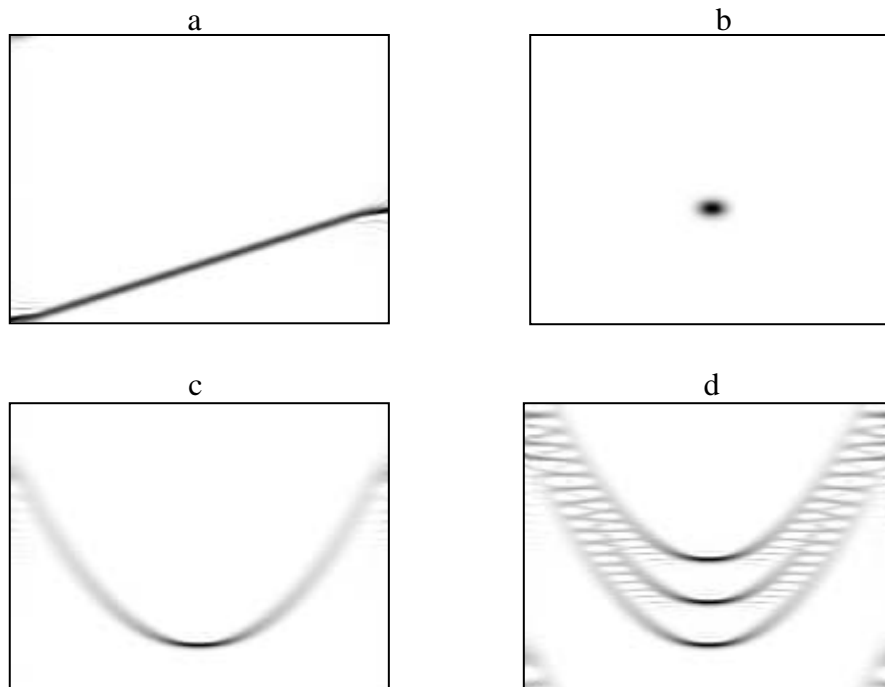

Fig 2.10 RSPWD Analysis of (a) linear component (b) atom or transient (c) quadratic component (d) multiple quadratic components.

2.3.3 Polynomial WD

This technique was proposed in [28] for signals having higher order instantaneous frequency variation. Mathematically,

$$WD_x(t,\omega) = \int_{-\infty}^{\infty} x^2(t+\tau/2)x^{*2}(t-\tau/2)x(t+\tau/2)x^*\ (t-\tau/2)e^{-j\omega\tau}d\tau. \tag{2.39}$$

This method is only used for analysis of mono-component signals and fails in case of multi-component signals due to increasing cross-terms.

2.3.4 Cross-terms suppression by using Bessel function expansion

In this method [27, 29], a multi-component signal is decomposed into mono-component signals by using Fourier Bessel expansion. These mono-components are studied individually by using WD and at the end all WD are summed for a resultant TFR which is cross-term free. The main limitation of this method is that it requires auto-components separation in frequency domain. This method cannot be used for signals whose auto-components can be separable in time-frequency domain. Moreover, this method needs manual input to locate auto-components and is only partially automatic.

2.3.5 Matching Pursuit TFRs

This method [2, 27, 30] decomposes a signal onto a linear sum of time-frequency atoms and computes WD of auto-component which is chosen from a redundant dictionary. Mathematically,

$$x(t) = \sum_{n=1}^{N} \langle x(t)g_{\lambda n}\rangle g_{\lambda n} + R^m x(t). \tag{2.40}$$

In $Eq(2.40)$, R^m represents residual vector and $g_{\lambda n}$ (time frequency atom) is given as:

$$g_\lambda(t) = \frac{1}{\sqrt{x}}g(\frac{t-u}{x})\exp(j\xi t), \tag{2.41}$$

and $\lambda = (x,u,\xi)$. Now WD of the decomposed auto-components is summed up for a cross-term free TFR. Mathematically,

$$TFR_x(t,\omega) = \sum_{n=1}^{N} \langle x(t) g_{\lambda n} \rangle TFR_g(t,\omega). \tag{2.42}$$

The distinguishing feature of this technique is that, it does not suffer from cross-term reduction and auto-components resolution trade off. On the other hand the limitation of this method is that prior knowledge of auto-components of the signal and of dictionary choice is needed.

2.3.6 S-Method

To obtain the best features of both WD and Spectrogram, S-Method was proposed in [31]. Mathematically it is described as,

$$SM(t,\omega) = \int_{-\infty}^{\infty} STFT(t,\omega+\theta) P(\theta) STFT(t,\omega-\theta) \exp(-j\omega\theta) d\theta, \tag{2.43}$$

where $P(\theta)$ controls the cross-term suppression. If $P(\theta)$ is chosen as a delta function $\delta(\theta)$, S-Method is reduces to a spectrogram. For $P(\theta)=1$, S-Method is a WD. In S-Method, proper choice of $P(\theta)$ will make the auto-components' resolution close to WD, but this is only happened when auto-components are distantly placed. To overcome limitations of S-Method, the adaptive S-Method was also proposed by Stankovic et al in [32]. It was shown that the resolution of S-Method can be increased by computing a signal dependent window in fractional Fourier transform domain [18].

2.3.7 Non-Linear Filtering for Cross-terms Suppression of WD

A non-linear filtering method was proposed in [33] to reduce cross-terms of WD. This technique depends upon the statistical behavior of the auto-components regions and cross-terms regions. The proposed non-linear filter behaves like an identity function in auto-components regions and a low pass filter in cross-terms region. This non-linear filtering based technique outperforms the kernel based methods but in regions where cross-terms overlap auto-components this method fails to give high resolution of auto-components.

2.3.8 Cross-term Suppression of WD Using Morphological Operator

It is a non-linear morphological filtering based technique to eliminate cross-terms of WD was proposed in [34]. In this method a marker is obtained through spectrogram which is used for morphological analysis of WD. The technique preserves auto-component's resolution. The non-linear morphological filter performs better than kernel based techniques but this technique also fails to give good results in regions where auto-components overlap cross-terms.

2.4 Fractional Fourier Transform for Analysis of Time Varying Signals

FT is one of the widely used tools in signal processing [35]. The fractional Fourier transforms (FRFT), was introduced in [36] as a generalization of FT. FRFT has established itself as a powerful tool for the analysis of time-varying signals in a very short span of time [34, 37]. FRFT has many applications in filter design, pattern recognition, and communication [34, 38], TFRs [25], etc. FRFT can be used in applications where FT fails to work due to time varying spectrum of signals and its cost of implementation is also adequate. Windows can be analyzed using FRFT [39]. FRFT can be used for detection of cross terns in WD [40]. FRFT can isolate signal components from multi-component signal [41].

Mathematically, FRFT [42] of a signal $x(t)$ is defined as,

$$X_\alpha(u) = \int_{-\infty}^{\infty} K(\alpha,t,u)x(t)dt,$$ (2.44)

where $\alpha = a\pi/2$ and $K(\alpha,t,u)$ is kernel function defined as

$$K(\alpha,t,u) = \sqrt{\frac{1-j\cot\alpha}{2\pi}} e^{(j/2)u^2\cot\alpha - ju\,\csc\alpha + (j/2)t^2\cot\alpha}.$$ (2.45)

Following are some important characteristics of FRFT :

1. FRFT becomes FT when $\alpha = \pi/2$

2. FRFT with $\alpha = 0$ *or* $\alpha = 2\pi$ is equal to identity operation.

3. $(0 < \alpha < 2\pi)$ corresponds to rotation of time-frequency plane.`

4. FRFT is linear, commutative and associative.

In signal analysis we need a wider window to filter a pure sinusoidal signal, while on other hand a narrower window is needed to filter a delta pulse. If the auto-component of signal cannot be aligned either to time axis or to frequency axis, the time–frequency plane is rotated by taking the FRFT of the signal. The reason of this signal's TFR rotation is to find out appropriate concentration of auto-components [43].

The rotation of time-frequency plane by angle α is described mathematically as,

$$\begin{pmatrix} t \\ \omega \end{pmatrix} = \begin{pmatrix} \cos\alpha & -\sin\alpha \\ \sin\alpha & \cos\alpha \end{pmatrix} \begin{pmatrix} u \\ v \end{pmatrix}. \tag{2.46}$$

Now the relationship for the FRFT kernel is given as,

$$K(\alpha,t_o,u-u_o)e^{j2\pi u_o v}e^{-j\pi uv} = [K(-\alpha,u_o,t-t_o)e^{j\omega t_o}e^{-j\omega/2t}]^*. \tag{2.47}$$

Clockwise rotation of WD, GT and GWT is equal to FRFT of these distributions [4, 44]. Mathematically,

$$WD_{x_\alpha}(u,v) = WD_x(u\cos\alpha - v\sin\alpha, u\sin\alpha + v\cos\alpha), \tag{2.48}$$

$$GT_{x_\alpha}(u,v) = GT_x(u\cos\alpha - v\sin\alpha, u\sin\alpha + v\cos\alpha), \tag{2.49}$$

$$GWT_{x_\alpha}(u,v) = GWT_x(u\cos\alpha - v\sin\alpha, u\sin\alpha + v\cos\alpha). \tag{2.50}$$

$Eqs\,(2.48, 2.49\,and\,2.50)$ show that FRFT gives us rotated version of these TFRs. The filtering process by using FRFT [4] is given by following equation,

$$r(t) = O_X^{-\alpha}\{O_X^{\alpha}[x(t)]H(u)\}, \tag{2.51}$$

where $x(t)$ and $r(t)$ are the filter input and the output, $O_X^{\alpha}[x(t)]$ represents FRFT of $x(t)$ and $H(u)$ is the transfer function. For a FRFT filter bank, the signal is filtered in time–frequency domain using a series of rotation angles $\alpha_1, \alpha_2, \alpha_3, \ldots\ldots, \alpha_n$, i.e,

$$x_1(t) = O_X^{-\alpha_1}\{O_X^{\alpha_1}[x(t)]H_1(u)\},$$

$$x_2(t) = O_X^{-\alpha_2}\{O_X^{\alpha_2}[x_1(t)]H_2(u)\},$$

$$x_{n-1}(t) = O_X^{-\alpha_{n-1}}\{O_X^{\alpha_{n-1}}[x_{n-2}(t)]H_{n-1}(u)\} \quad \ldots\ldots$$

$$r(t) = O_X^{-\alpha_n}\{O_X^{\alpha_n}[x_{n-1}(t)]H_n(u)\}. \tag{2.52}$$

$Eq\,(2.52)$ tells that choice of α_n is critical in FRFT domain for successful elimination of noise.

To design a filter in fractional domain, it is necessary to choose

1) proper rotation angle α,

2) selection criteria for cutoff lines [4, 41].

2.4.1 FRFT and Signal Synthesis for Cross-terms Suppression of WD

Signal synthesis from a TFR was proposed in [55]. This technique can be used for time varying filtering and signal separation. In this estimation technique, a signal is generated in such a way that signal's TFR approximates the desired TFR. This method has following main steps.

Suppose $TFR_{x(t)}(t,\omega)$ represents TFR of $x(t)$. The objective is to find out $\hat{x}(t)$ whose $TFR_{\hat{x}(t)}(t,\omega)$ is close to $TFR_{x(t)}(t,\omega)$. To achieve this goal we have to minimize $e(x)$, which is mathematically described as follows,

$$e(x) = \int_{-\infty}^{\infty} \left| TFR_{x(t)}(t,\omega) - TFR_{\hat{x}(t)}(t,\omega) \right| d\omega. \qquad (2.53)$$

$Eq(2.53)$ allows minimization for even ($\hat{x}_e$) and odd ($\hat{x}_o$) samples of $x(t)$

Even (M_e) and odd (M_o) matrices elements are given as:

$$M_e(i+1,j+1) = g(i+j,i-j) + g^*(i+j,j-i),\ wh\ rae\ i,j = 0,......,L_e-1 \quad (2.54)$$
$$M_o(i,j) = g(i+j+1,i-j) + g^*(i+j+1,j-i),\ wh\ rae\ i,j = 0,......,L_o \quad (2.55)$$

In $Eqs(2.54\,and\,2.55)$, $g(i,j)$ is inverse Fourier transform of $TFR_{x(t)}(t,\omega)$, L_o is length of $\hat{x}_e$ and L_e is length of $\hat{x}_o$.

Phase estimation of φ_e (even) and φ_o (odd) is described as follows,

$$\varphi_e = \tan^{-1}\left\{\frac{\mathrm{Re}\left\{\sum_{p=0}^{L_e-1} x(2p)\widehat{x}_e^*(p)\right\}}{\mathrm{Im}\left\{\sum_{p=0}^{L_e-1} x(2p)\widehat{x}_e^*(p)\right\}}\right\}, \tag{2.56}$$

$$\varphi_o = \tan^{-1}\left\{\frac{\mathrm{Re}\left\{\sum_{p=0}^{L_o} x(2p-1)\widehat{x}_e^*(p)\right\}}{\mathrm{Im}\left\{\sum_{p=0}^{L_o} x(2p-1)\widehat{x}_e^*(p)\right\}}\right\}. \tag{2.57}$$

In $Eqs(2.56 \, and \, 2.57)$, $\widehat{x}_e(p)$ and $\widehat{x}_o(p)$ are given as,

$$\widehat{x}_e(p) = \left|\widehat{x}_e(p)\right| e^{j\varphi_e}, \tag{2.58}$$

$$\widehat{x}_o(p) = \left|\widehat{x}_0(p)\right| e^{j\varphi_o}. \tag{2.59}$$

A FRFT and signal synthesis based recursive method to suppress cross-terms of WD without affecting auto-components resolution was proposed in [27, 40]. This method performs better in challenging situations i.e. when auto-components overlap cross-terms. This technique exploits the mismatch of fractionally rotated and aligned back Wigner distributions to detect cross-terms. A simple mask is used to suppress cross-terms. The auto-components are synthesized in time domain. WD of reconstructed auto-components gives high resolution TFR. The main limitation of the process is that it involves several iterations and each iteration includes signal synthesis which itself is an iterative process. Therefore computational cost is too high.

2.4.2 Combination of GT and WD for Cross-terms Suppression

As explained earlier the main feature of WD is its high resolution property of auto-components during the analysis of mono-component signals. But WD has cross-terms in case of multi-component signals. On the other hand the main strength of the GT is its linearity property but it has less resolution of auto-components than WD. For achieving the goals such as, (i) high concentration of auto-components and (ii) elimination of the cross-terms, it is necessary to combines excellent features of both WD and GT [4, 45]. The combination of GT and WD is called as Gabor Wigner Transform (GWT) which is described and evaluated in detail in chapter 4.

2.4.3 FRFT and 2D Signal Processing Techniques for Cross-terms Suppression of WD

Image processing techniques (image thresholding and segmentation) and FRFT can be used for cross-terms suppression of WD [41]. This technique uses support vector machine for classification of auto-components. Auto-components of a multi-component signal are isolated in FRFT domain. WD of isolated components is computed and their superposition gives a readable TFR. The main drawback of this method is auto-component's discontinuity due to image segmentation. Moreover closely placed auto-components are not segmented properly.

2.5 Reduce interference TFRs

For reduce interference TFRs, kernel is designed in ambiguity domain. This kernel acts as a low pass filter to suppress cross-terms. Mathematically ambiguity function [3] $A_x(\theta, \tau)$ is defined as,

$$A_x(\theta, \tau) = \int_{-\infty}^{\infty} x(u + \tau/2) x^* (u - \tau/2) e^{-j\theta u} d \quad . \qquad u \tag{2.60}$$

The reduce interference TFR is of the form:

$$TFR_x(t, \omega) = \frac{1}{4\pi^2} \iint A_x(\theta, \tau) \phi(\theta, \tau) d\tau d\theta. \tag{2.61}$$

In $Eq(2.61)$, $\phi(\theta, \tau)$ defines kernel of reduce interference TFRs. In this category some common examples of TFRs are given in the Table 2.2.

Table 2. 2 Kernel functions of reduce interference TFRs

TFRs	Kernel function ($\phi(\theta, \tau)$)
Born–Jordan TFR [1]	$\phi(\theta, \tau) = \dfrac{\sin(\theta\tau/2)}{\theta\tau/2}$
Choi–Williams TFR [46]	$\phi(\theta, \tau) = e^{(-\frac{\theta^2\tau^2}{\sigma^2})}$, where σ represents scaling factor.
Zhang–Sato TFR [47]	$\phi(\theta, \tau) = e^{(-\frac{\theta^2\tau^2}{\sigma^2})}\cos(2\pi\beta\tau)$, where, σ and β are parameters. When $\beta = 0$, it becomes Choi–Williams TFR.
Radial Butterworth TFR [48]	$\phi(\theta, \tau) = \dfrac{1}{1 + (\dfrac{\theta^2 + \tau^2}{r_0})^M}$, where r_0 and M are tuning parameters
Bessel TFR [49]	$\phi(\theta, \tau) = \dfrac{J_1(2\pi\alpha\theta\tau)}{\pi\alpha\theta\tau}$, where J_1 is order one Bessel function and $\alpha > 0$ shows scaling factor.
Generalized exponential TFR [50, 51]	$\phi(\theta, \tau) = e^{(-(\frac{\theta}{\theta_1})^{2N}(\frac{\tau}{\tau_1})^{2M})}$, where N, M are integers, θ_1 is positive frequency and τ_1 is time scaling, respectively, in such a way that $\phi(\theta_1, \tau_1) = e^{(-1)}$.
S-method [31]	$\phi(\theta, \tau) = P(-\dfrac{\theta}{2}) *_\theta \displaystyle\int_{-\infty}^{\infty} \omega(u + \tau/2)\omega^*(u - \tau/2)e^{-j\theta u}du$, where $*_\theta$ shows a convolution in θ, $\omega(t)$ is window and smoothing function is $P(\theta)$.
TFR for multi-component linear FM signals [52]	$\phi(\theta, \tau) = \Pi(\dfrac{\theta - \chi^\tau}{b})$, where χ shows frequency modulation rate, width in the direction of θ is b and $\Pi(\xi) = 1 \ for |\xi| \leq 1/2$.
A time-lag kernel TFR [53]	$\phi(\theta, \tau) = |\tau|^\alpha \dfrac{2^{2\alpha-1}}{\Gamma(2\alpha)}\Gamma(\alpha + j\pi\theta)\Gamma(\alpha - j\pi\theta)$, where $\Gamma(z)$ is the Gamma function and bounded parameter is α ($0 < \alpha \leq 1$).
Hyperbolic TFR [54]	$\phi(\theta, \tau) = \dfrac{1}{\cosh(\beta\theta\tau)}$, where β controls exponential terms.

In all kernel functions described in Table 2.2, tuning of one or more parameters is essential for cross-terms suppression and high resolution of auto-components (only for specific application in hand). Hence an addition complexity is added in order to select a correct parameter value.

2.6 IF estimation techniques

An important feature of a non-stationary signal is its Instantaneous Frequency (IF) parameter. IF has a key role in motion estimation, biomedical signals and radar [27, 56, 57, 58, 59].

In the case of a mono-component signal, IF can be defined as the derivative of the phase of the signal. Mathematically,

$$\omega(t) = \frac{1}{2\pi} \frac{d}{dt} (\arg(s(t))). \tag{2.62}$$

In $Eq(2.62)$, $s(t)$ is analytic form of $x(t)$ and is defined as,

$$s(t) = x(t) + js(t).\frac{1}{\pi t}. \tag{2.63}$$

$Eq(2.62)$ describes the exact time location of frequency, which is only applicable for a mono-component signal.

Instantaneous Frequency is mostly estimated by identifying the peaks in a TFR at a given time instant. For this purpose WD is mostly used as it gives accurate IF estimation for a linearly-frequency-modulated signal. In case of non-linearly frequency-modulated- signals, WD has biased IF estimation. Windowed WD can overcome this bias. The negative effect of this windowing is the increase in variance of IF estimates as there is always a trade-off between bias and variance. Various techniques proposed for IF estimations are described in the following subsections.

2.6.1 ICI based IF estimation technique

A technique was proposed for IF estimation in [60]. This method is based on Intersection of the confidence interval (ICI) rule, for selection of optimal window to compute the IF of an auto-component. The drawback of this technique is that it is only applicable for mono-component signals.

2.6.2 IF estimation by tracking the maxima of auto-components

A scheme was proposed in [61] for IF estimation which tracks maxima of each auto-component while leaving the local maxima due to cross-terms for a multi-component signal. This method needs knowledge of auto-components location and manual selection of thresholds so it is not automatic.

2.6.3   IF estimation by Viterbi algorithm

It was shown that Viterbi algorithm can be used for IF estimation of multi-component signal buried in high noise [62]. The limitation of this scheme is that it is only applicable for linearly-frequency- modulated signals.

2.6.4   IF estimation by image segmentation

An automatic scheme of IF estimation based on image processing was proposed in [63]. In this method modified B-distribution is used. IF estimation of auto-components is done with the help of image segmentation and auto-component connectivity criteria. This method fails when auto-components have significant frequency modulation.

2.6.5   IF estimation by modified ICI rule

A modified ICI rule based IF estimation technique was proposed in [21]. The main subsections of this technique are auto-components extraction and improved ICI rule. The technique involves modified component extraction method [21] that has following major steps:

(i)   Compute reduce interference TFR of a multi-component signal.

(ii)   Detect highest peak (t_0, ω_0) in time-frequency plane, followed by $(t_0, \omega) = 0$, where $\omega \in [\omega_0 - \Delta\omega,\ \omega_0 + \Delta\omega]$. Now divide vicinity of (t_0, ω_0) in two (t, ω) sub-portion followed by the condition $\omega \in [\omega_0 - W/2,\ \omega_0 + W/2]$, where $t \in [t_0 - 1, t_0]\ and\ t \in [t_0, t_0 + 1]$ for first and second sub-portion. Above procedure will give maximum value (t_0', ω_0') for the both sub-portions.

(iii)   In next stage $(t_0, \omega_0) = (t_0', \omega_0')$, step (ii) is repeated until TFR boundary is reached. These extracted (t_0, ω_0) values form the auto-component. The same procedure is adapted for rest of auto-components of the multi-component signal.

The overall improved ICI rule has following major steps:

(i)   The overlap $C_m(n, l)$ of   two consecutive intervals is defined as,

$$C_m(n, l) = |D_m(n, l) \cap D_m(n, l - 1)|. \tag{2.64}$$

In $Eq(2.64)$, $D_m(n, l)$ and $D_m(n, l - 1)$ are confidence intervals.

(ii) The normalized confidence interval is defined as,

$$O_m(n,l) = \frac{C_m(n,l)}{D_m(n,l)}.$$
(2.65)

In $Eq(2.65)$, $O_m(n,l)\,\varepsilon\,[0,1]$

(iii) Now the threshold O_c criteria for window width is described as,

$$O_m(n,l) \geq O_c.$$
(2.66)

In $Eq(2.66)$, $O_m(n,l)$ is defined as,

$$O_m(n,l) = \begin{cases} 0 & C_m(n,l) = 0 \\ 1 & C_m(n,l) = |D_m(n,l)|. \\ \langle 0,1 \rangle & elsewhere \end{cases}$$
(2.67)

Algorithmic steps of modified ICI rule based IF estimation technique are:

- Compute a set of reduced interference TFRs for different smoothing windows. Extract auto-components for each reduced interference TFR.

- Calculate IF of each auto-component by using following relation,

$$\widehat{\omega}_m(n,h) = \arg[\max_k \, TFR_m(n,k,h)]$$
(2.68)

In $Eq(2.68)$, $TFR_m(n,k,h)$ is the mth auto-component's TFR and h is length of window

- Select best IF estimate (based on modified ICI rule) for each auto-component.

2.6 Conclusion

In this chapter the advantages and disadvantages of most widely used linear and quadratic TFRs are analyzed. Some more techniques which combine signal processing and image processing techniques along with these TFRs are also discussed. The strengths and limitations of each approach are highlighted. Based on mentioned facts it is necessary to combine linear and quadratic TFRs in order to get merits of both linear and quadratic transforms. As we know that significant efforts are required to define algorithms for cross-terms suppression of quadratic TFRs. To overcome this difficulty it is required to define new combinations of linear and quadratic TFRs which are robust against complicated multi-component signals and simple in implementation.

Chapter 3

Performance measures

The choice of a right TFR to analyze a given signal is not straightforward task, even for a mono-component signal, and this choice becomes more difficult while considering a multi-component time-varying signal. A common way of determining the appropriate TFR for a given signal is the visual comparison among the plots of considered TFRs. However selection of a TFR based on visual inspection is generally difficult and requires the introduction of some performance measures [64]. Therefore for detailed performance evaluation of existing and proposed TFRs, these performance measures are important. This chapter discusses these measures as these measures will be used in the comparative analysis given in subsequent chapters.

In literature, TFRs are compared on the basis of following criteria:

- Readability [64]
- CT suppression [68]
- Energy concentration [69]
- Resolution [72]

3.1 Entropy Measures

Entropy measures the information for a given probability density function. The alternative terms used in the meaning of entropy are uncertainty and information. Entropy can be used for TFRs to compute the information by measuring the signal's complexity [65, 66, 67]. According to probability theory, minimization of complexity or information contained in a TFR is equal to maximizing the TFR' peakiness, concentration and resolution [64, 68].

3.1.1 Shannon entropy

Shannon entropy [27, 69] is described as,

$$E_{shanon} = \sum_n \sum_\omega Q(n,\omega) \log_2(Q(n,\omega)). \tag{3.1}$$

Mathematically, unit energy case of Shannon entropy can be described in following equation,

$$\sum_{n} \sum_{\omega} Q(n,\omega) = 1. \tag{3.2}$$

$Eq(3.2)$ cannot be used for TFR having negative values, for such cases absolute values of entropy are used. Mathematically it is described as,

$$E_{shanon} = \sum_{n} \sum_{\omega} |Q(n,\omega)| \log_2(|Q(n,\omega)|). \tag{3.3}$$

$Eq(3.3)$ increases the overall energy of a TFR. Shannon entropy is a strong candidate for estimating the concentration of a TFR and can be viewed as the inverse of a measure of concentration of the TFR in the time-frequency plane. TFRs of signals with high concentration would yield small entropy values and vice versa.

3.1.2 Renyi entropy

Renyi entropy [65] overcomes the limitations of Shannon entropy and is defined as,

$$E_{\mathrm{Re}nyi} = \frac{1}{1-\alpha} \log_2(\sum_{n} \sum_{\omega} Q^{\alpha}(n,\omega)). \tag{3.4}$$

In $Eq(3.4)$, α describes the order of entropy. Now normalized Renyi entropy measure is described as,

$$E_{\mathrm{Re}nyi} = \frac{1}{1-\alpha} \log_2\left(\frac{\sum_{n} \sum_{\omega} Q^{\alpha}(n,\omega)}{\sum_{n} \sum_{\omega} Q(n,\omega)}\right). \tag{3.5}$$

The normalized Renyi entropy measure with the TFR volume is described as,

$$E_{\mathrm{Re}nyi} = \frac{1}{1-\alpha} \log_2\left(\frac{\sum_{n} \sum_{\omega} Q^{\alpha}(n,\omega)}{\sum_{n} \sum_{\omega} |Q(n,\omega)|}\right). \tag{3.6}$$

$Eq(3.6)$ is used to design adaptive kernels design [70].

3.2 Ratio of Norms

Ratio of norms is a measure of TFRs' concentration and is presented in [68]. It divides the fourth power norm of a TFR by its second power norm. Mathematically,

$$E_{jp} = \frac{\sum_n \sum_\omega |Q(n,\omega)|^4}{(\sum_n \sum_\omega |Q(n,\omega)|^2)^2}.$$ (3.7)

Higher value of E_{jp} gives better energy concentration which is opposed to entropy based measures. In equation $Eq(3.7)$ numerator' fourth power describes the peaky TFR. The maximum value of the ratio of norms gives the appropriate TFR for a signal being considered. Mathematically,

$$Q_{optimum}(n,\omega) = \arg \max_Q [E_{jp}].$$ (3.8)

3.3 LJubisa Measure

Energy concentration of time limited signal can be assessed by method proposed in [71]. Consider a signal $x(t)$ is limited in time $[t_1 \ t_2]$, now the length of $x(t)$ is equal to $\lim_{\beta \to \infty} (\int_{-\infty}^{\infty} |x(t)|^{1/\beta} dt)$. For large values of β, Ljubisa measure (J_β) is defined as,

$$J_\beta = \int_{-\infty}^{\infty} \int_{-\infty}^{\infty} |Q(t,\omega)|^{1/\beta} dt d\omega.$$ (3.9)

In discrete form Ljubisa measure is defined as,

$$J[Q(n,\omega)] = (|Q(n,\omega)|^{1/\beta})^\beta.$$ (3.10)

In $Eq(3.10)$, $\beta > 1$ and

$$\sum_n \sum_\omega Q(n,\omega) = 1.$$ (3.11)

TFRs that minimize $J[Q(n,\omega)]$ are considered as better TFRs.

3.4 Boashash Performance Criteria

Boashash performance criteria takes resolution and concentration of auto-components of the signals having closely placed auto-components. The parameters that influence the resolution of a TFR are:

- auto-components concentration
- separation of auto-components

- interference terms.

All above mentioned parameters are used to define Boashash performance criteria [64, 72]

3.4.1 Concentration measure

Consider the time slice ($t = t_0$) of a quadratic TFR of a n-auto-components signal that has the instantaneous bandwidth ($V_{i_n}(t_0)$), the IF ($f_{i_n}(t_0)$), the side lobe amplitude ($A_{x_n}(t_0)$), and the main lobe amplitude ($A_{m_n}(t_0)$) for each of the nth component at time $t = t_0$. The magnitude of cross-terms is represented by $A_x(t_0)$. At any time instant, concentration of a TFR can be improved by minimizing side lobes amplitudes $A_{x_n}(t_0)$ relative to main lobe amplitudes $A_{m_n}(t_0)$ and main lobe bandwidth $V_{i_n}(t_0)$ about the signal IF $f_{i_n}(t_0)$ for each auto- component [72]. As a result, for a given time slice $t = t_0$ of a TFR of n-auto-component signal, which is defined below

$$x(t) = \sum_n x_n(t), \tag{3.12}$$

the TFR concentration parameter $c_n(t)$ is defined as [72],

$$c_n(t) = \frac{A_{x_n}(t_0)}{A_{m_n}(t_0)} \frac{V_{i_n}(t_0)}{f_{i_n}(t_0)}. \tag{3.13}$$

3.4.1.1 Modified concentration measure

This performance measure is an alternative to the performance measure described in $Eq(3.13)$. It is the sum of $\dfrac{A_{x_n}(t_0)}{A_{m_n}(t_0)}$ and $\dfrac{V_{i_n}(t_0)}{f_{i_n}(t_0)}$, and hence it accounts their effects separately. This modified concentration measure $C_n(t)$ is defined as,

$$C_n(t) = \frac{A_{x_n}(t_0)}{A_{m_n}(t_0)} + \frac{V_{i_n}(t_0)}{f_{i_n}(t_0)}. \tag{3.14}$$

If $C_n(t)$ is near to zero then a TFR has a good performance.

3.4.2 Resolution measure

The minimum difference $f_2 - f_1$ of two auto-components tones f_1 and f_2 describes frequency resolution and satisfy following inequality,

$$f_1 + \frac{V_1}{2} < f_2 - \frac{V_2}{2}, \quad f_1 < f_2. \tag{3.15}$$

In $Eq(3.15)$ V_1 is the bandwidth of the first sinusoid and V_2 is the bandwidth of the second sinusoid. For a multi-component signal, $Eq(3.15)$ takes the form $f_{i_2}(t) - f_{i_1}(t) \langle f_{i_2}(t)$, where $f_{i_1}(t)$ and $f_{i_2}(t)$ are IFs of auto-components' main lobes having separation D, which is positive. Components' main lobes separation $D(t)$ is described as,

$$D(t) = \frac{(f_{i_2}(t) - \frac{V_{i_2}(t)}{2}) - (f_{i_1}(t) - \frac{V_{i_1}(t)}{2})}{f_{i_2}(t) - f_{i_1}(t)}. \tag{3.16}$$

Simplified form of $Eq(3.16)$ is given below,

$$D(t) = 1 - \frac{V_i(t)}{\Delta f_i(t)}. \tag{3.17}$$

In $Eq(3.17)$, $V_i(t) = \sum \frac{V_{i_n}}{2}$, $V_i(t)$ is the auto-components' main lobes average bandwidth and $\Delta f_i(t) = f_{i_{n+1}}(t) - f_{i_n}(t)$ is the difference between the components' IFs. For better resolution of quadratic TFRs, it is required to maximize the separation measure D and minimize the interference terms. The resolution measure R [72] of a TFR for a pair of auto-components is described by,

$$R(t) = \frac{A_x(t) A_x(t_0)}{A_m(t) A_m(t_0)} \frac{1}{D(t)}. \tag{3.18}$$

In $Eq(3.18)$, $A_X(t)$, $A_S(t) = \sum \frac{A_{S_n}(t)}{2}$ and $A_M(t) = \sum \frac{A_{m_n}(t)}{2}$ are the cross-terms amplitude of two adjacent auto-components, the average amplitude of the auto-components' side lobes and the average amplitude of the auto-components' main lobes respectively. Good resolution of a TFR is happened when R is near to zero. The $Eq(3.18)$ can be expressed in normalized form [72] as,

$$R_i(t) = 1 - \frac{1}{3}\left[\frac{A_S(t)}{A_m(t)} + \frac{1}{2}\frac{A_X(t)}{A_m(t)} + (1 - D(t))\right], \qquad 0 < R_i(t) < 1. \tag{3.19}$$

In summary, the performance of a proposed TFR is evaluated on the basis of quantative measures like entropy measures, Ljibisa measure and ratio of norms. If the proposed method has a maximum value of ratio of norms and minimum value of entropy and Ljubisa measure then it is considered as a concentrated and high resolution TFR.

Chapter 4

Gabor Wigner Transform

In chapter 2 various time-frequency techniques for analysis of time-varying signals have been critically evaluated. It is observed that most of the TFRs make some kind of compromise between auto-components resolution and cross-terms suppression. Linear TFRs offer no cross-terms but have low resolution of auto-components. Quadratic TFRs offer better resolution of auto-components but have cross-terms [1, 3]. Therefore, there is a need of a TFR that can combines advantages of both linear and quadratic TFRs. In this chapter GWT is studied with the help of some commonly used case studies. Our simulation results show that there is a need to propose further combinations of linear and quadratic TFRs in order to overcome obvious limitations. A modified GWT is also proposed and the results are compared with already existing definitions of GWT.

The combination of GT and WD is called as Gabor Wigner Transform (GWT) [4, 45]. Mathematically some of these combinations are defined as,

$$GWT_x(t,\omega) = GT_x(t,\omega)WD_x(t,\omega), \tag{4.1}$$

$$GWT_x(t,\omega) = \min\{|GT_x(t,\omega)|^2, |WD_x(t,\omega)|\}, \tag{4.2}$$

$$GWT_x(t,\omega) = WD_x(t,\omega)\{|GT_x(t,\omega)| > 0.25\}, \tag{4.3}$$

$$GWT_x(t,\omega) = GT_x^{2.6}(t,\omega)WD_x^{0.6}(t,\omega). \tag{4.4}$$

$Eqs\,(4.1, 4.2, 4.3\,and\,4.4)$ show that there is no unique definition of GWT and choice of GT and WD is critical in order to extract strengths of GT and WD. However different combinations of GWT ($Eqs\,(4.1, 4.2, 4.3\,and\,4.4)$) are only applicable for slowly time varying signals.

4.1 Modified GWT

Here a modified scheme for computing GWT that gives better concentration of auto-components is proposed. The proposed GWT [73] can be written in the form of algorithm based on the following steps.

Step 1. Compute $WD_x(t,\omega)$ of the signal $x(t)$ and its mean value T, where

$$T = mean\ of\ WD_x(t,\omega). \tag{4.5}$$

Step 2. Classify the transformed data into two classes $WD_A(t,\omega)$ and $WD_B(t,\omega)$ as

$$WD_A(t,\omega) \in WD_x(t,\omega) \quad if \quad WD_x(t,\omega) \geq T, \tag{4.6}$$

$$WD_B(t,\omega) \in WD_x(t,\omega) \quad if \quad WD_x(t,\omega) < T. \tag{4.7}$$

Step 3. Compute averages of $WD_A(t,\omega)$ and $WD_B(t,\omega)$ and update T [74] as

$$T = \frac{\mu_{WD_A(t,\omega)} + \mu_{WD_B(t,\omega)}}{2}. \tag{4.8}$$

In *Eq* (4.8), T is updated in each iteration. When T does not change in two consecutive iterations, then   iterations are terminated.

Step 4. Same steps 1 to 3 will be repeated for GT analysis of the signal $x(t)$

Step 5.

Choose

$$WD_x(t,\omega) = \begin{cases} 0 & if \ WD_x(t,\omega) \leq T \\ WD_x(t,\omega) & otherwise. \end{cases} \tag{4.9}$$

Choose

$$GT_x(t,\omega) = \begin{cases} 0 & if \ GT_x(t,\omega) \leq T \\ GT_x(t,\omega) & otherwise. \end{cases} \tag{4.10}$$

Step 6. Multiply $WD_x(t,\omega)$ and $GT_x(t,\omega)$ obtained in step 5 as:

$$GWT_x(t,\omega) = GT_x^{.5}(t,\omega)WD_x(t,\omega). \tag{4.11}$$

All the steps of this proposed technique are shown in the following block diagram.
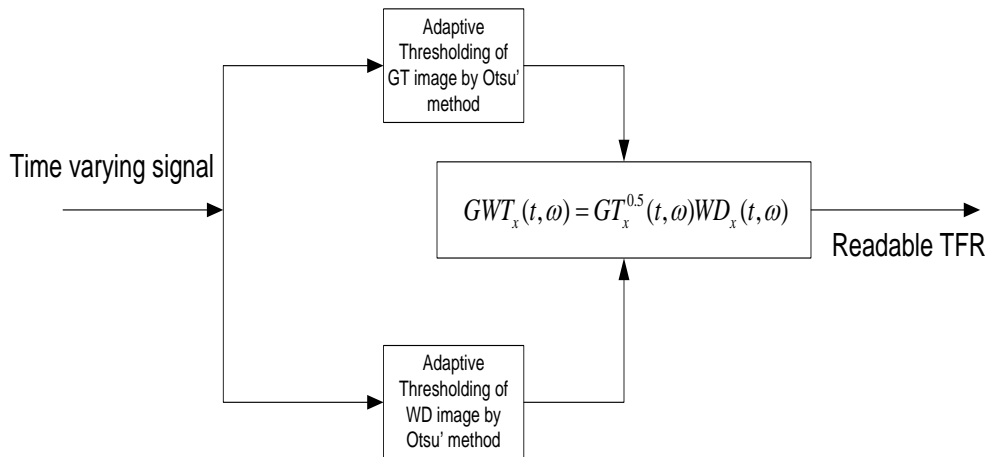
Fig. 4.1 Adaptive threholding based GWT

4.1.1 Numerical Simulations

Five different test examples have been considered to demonstrate the potential of the modified GWT and comparison with existing GWT defined in $Eqs\,(4.1, 4.2, 4.3\,and\,4.4)$. These examples are:

(i)   a Gaussian atom,

$$x(t) = 2\exp(-2\pi j(70t))\exp(-15t^2),\tag{4.12}$$

(ii)   a linear component,

$$x(t) = 2\exp(-2\pi j(7t^2 + 55t)),\tag{4.13}$$

(iii)   a quadratic component,

$$x(t) = 2\exp(-2\pi j(7t^3 + 55t)),\tag{4.14}$$

(iv)   two linear components,

$$x(t) = 2\exp(-2\pi j(7t^2 + 55t)) + 2\exp(-2\pi j(7t^2 + 35t)),\tag{4.15}$$

(v)   three quadratic components,

$$x(t) = 2\exp(-2\pi j(7t^3 + 55t)) + 2\exp(-2\pi j(7t^3 + 35t)) +$$
$$2\exp(-2\pi j(7t^3 + 15t)).\tag{4.16}$$

As shown in Fig 4.2a and Fig 4.3 a, WD is an ideal analysis tool for a linearly modulated mono-component signal and a Gaussian atom. However as shown in Fig 4.4a, WD suffers from inner interferences in case of quadratic component. Since quadratic nature of WD produces cross-terms, therefore in case of multiple components WD has both inner and outer interferences (Fig 4.5a).

GT provides suppression of both inner and outer interferences at the cost of blurring of auto-components (Fig 4.4b).

Analysis of these signals through different variants of GWT show that, these variants of GWT provide high resolution property of WD and linearity of GT as shown in Fig 4.5 (c, d, e, f and g).

In case of three quadratic components, modified GWT extracts successfully three quadratic components and provides better readability as compared to other variants of GWT (Fig 4.6).

In noisy case (SNR=3dB), analysis of Eq (4.16) also proves the potential of modified GWT with respect to auto-component extraction as shown in Fig 4.7. In this case different variants of GWT have very low readability of auto-components as

43

shown in Fig 4.7(c, d, e and f). WD has severe cross-terms (Fig 4.7a), where as GT has blurring in auto-components (Fig 4.7b).

These examples have shown the potential of modified GWT for multi-component signal analysis. Adaptive choice of GT and WD makes the resultant GWT to avoid the cross-term problem while maintaining the resolution of auto-components as good as that of the WD. That is, it can combine the advantages of both GT and WD and will be a powerful tool for analyzing the characteristics of a multi-component signal. Performance analysis of modified GWT reveals that it provides high concentration of auto-components as compared to other variants of GWT.
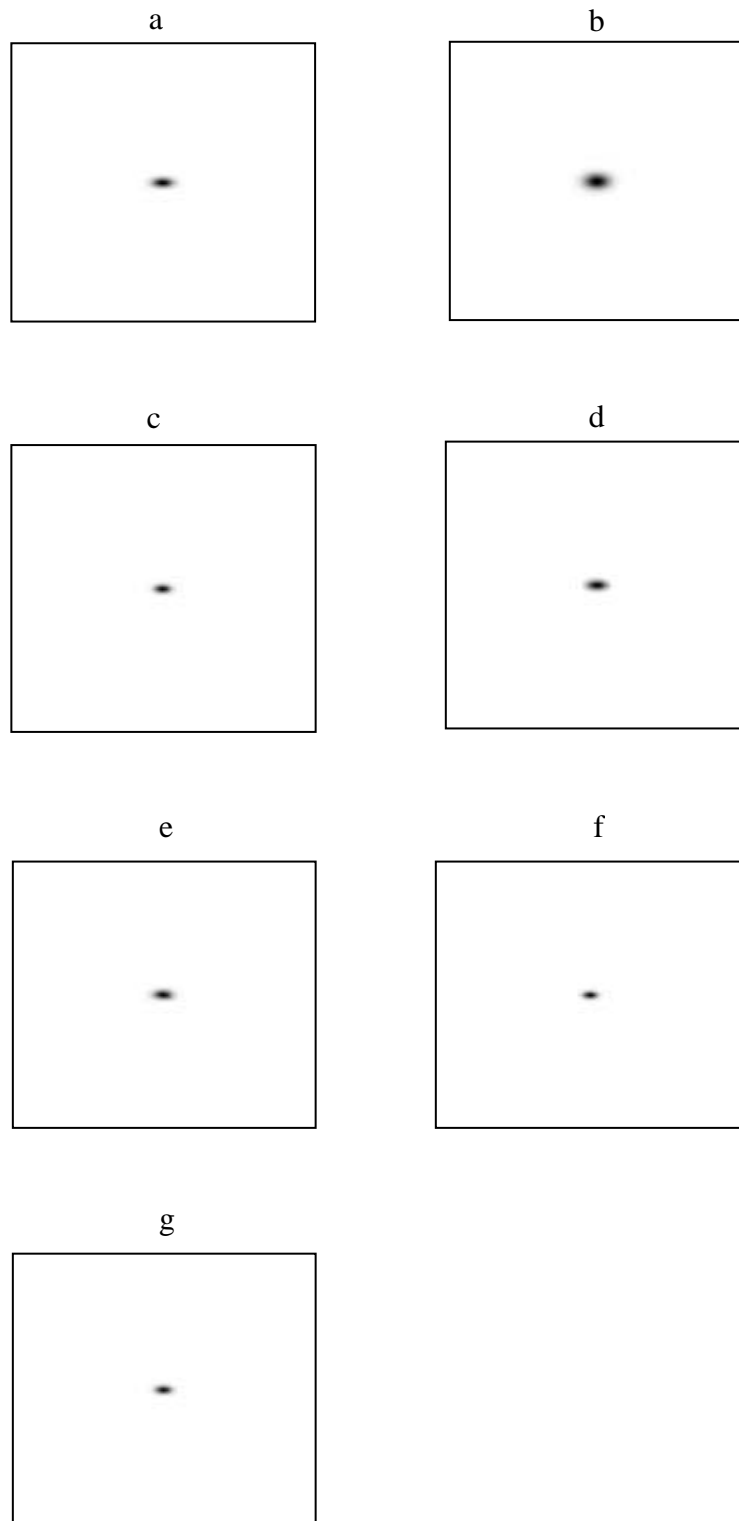
Fig 4.2 Analysis of a Gaussian atom (a) WD, (b) GT, (c) GWT (*Eq. 4.1*), (d) GWT (*Eq. 4.2*), (e) GWT (*Eq. 4.3*), (f) GWT (*Eq. 4.4*) and (g) Modified GWT.
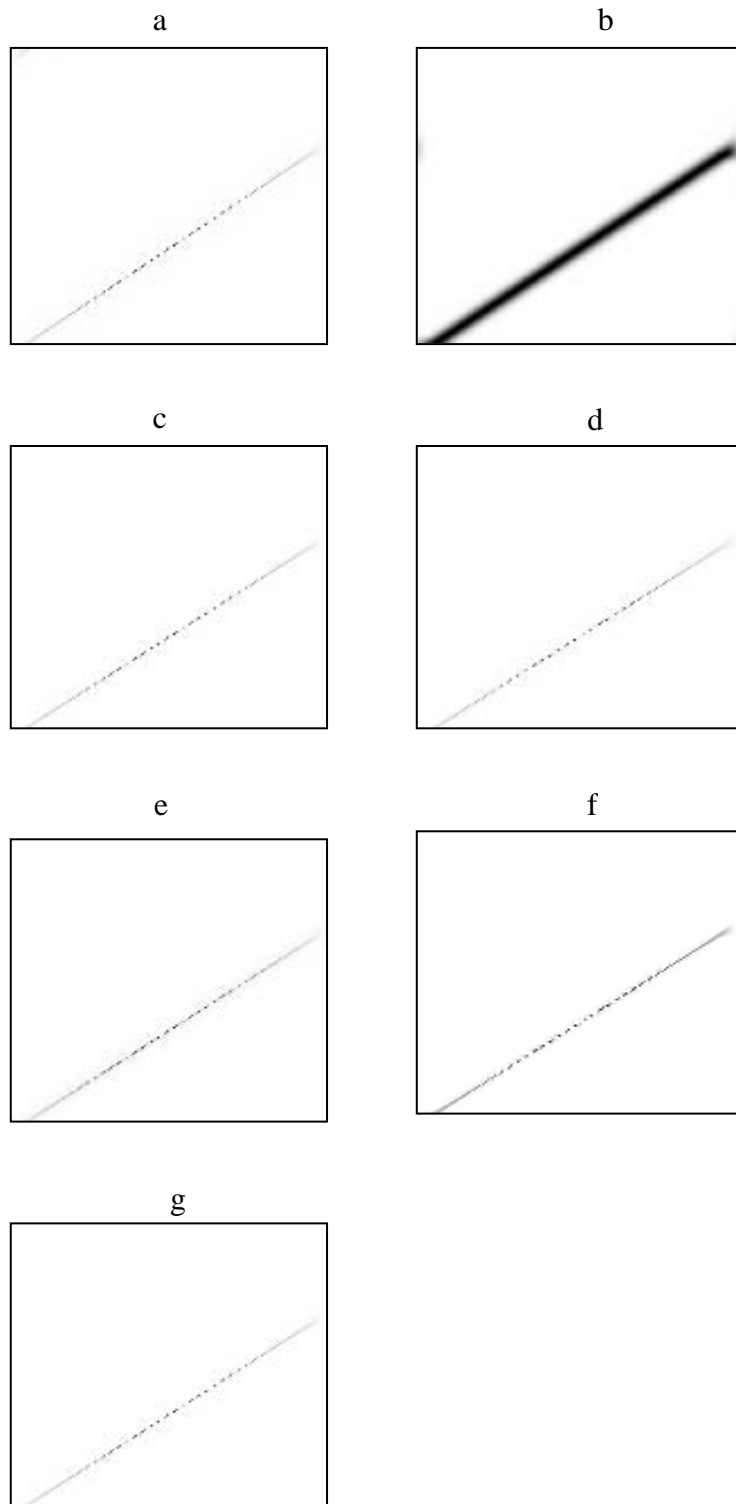
Fig 4.3 Analysis of a linear chirp (a) WD, (b) GT, (c) GWT (*Eq. 4.1*), (d) GWT (*Eq. 4.2*), (e) GWT (*Eq. 4.3*), (f) GWT (*Eq. 4.4*) and (g) Modified GWT.
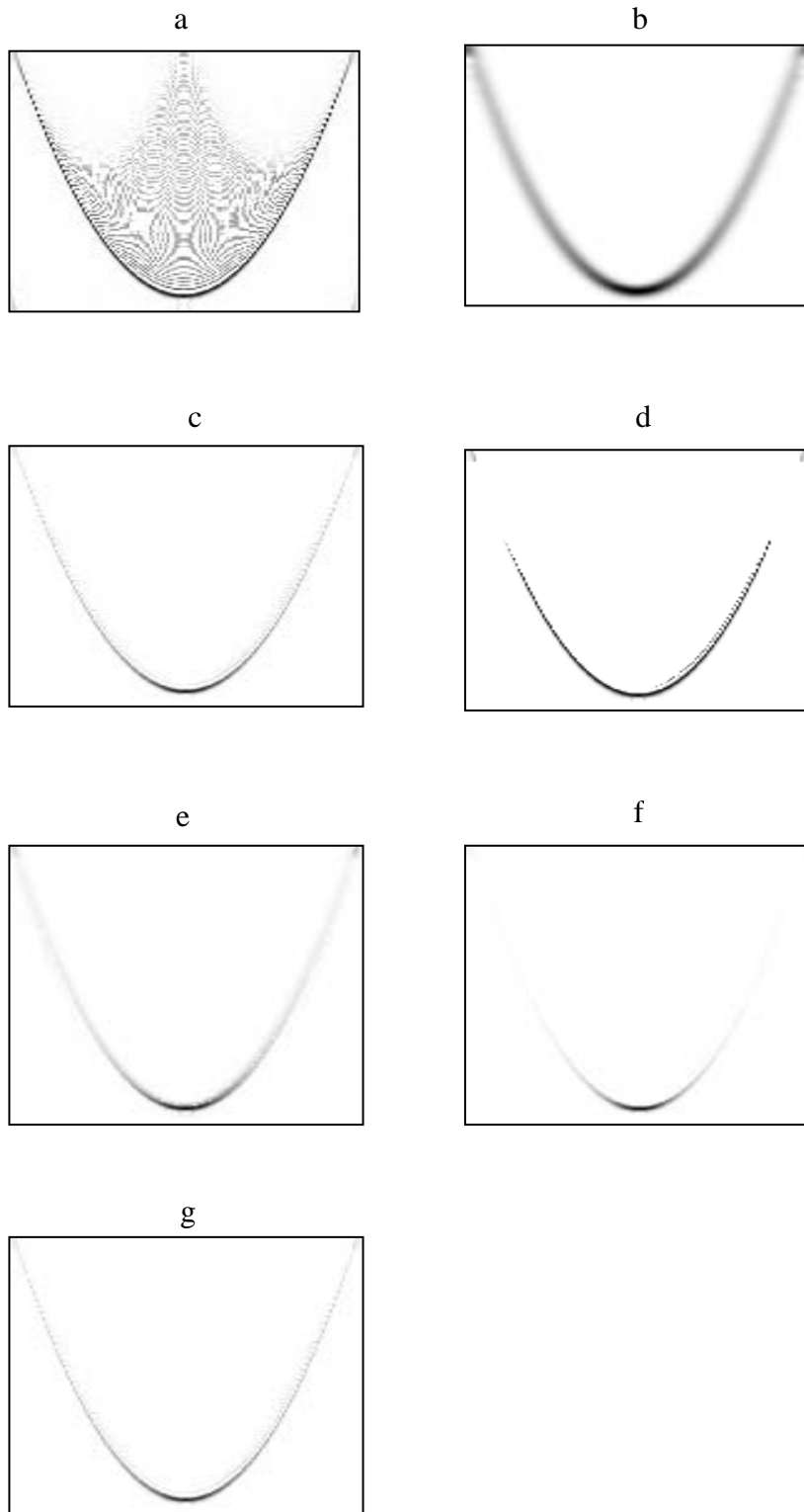
Fig 4.4 Analysis of a quadratic component (a) WD, (b) GT, (c) GWT (*Eq. 4.1*), (d) GWT (*Eq. 4.2*), (e) GWT (*Eq. 4.3*), (f) GWT (*Eq. 4.4*) and (g) Modified GWT.
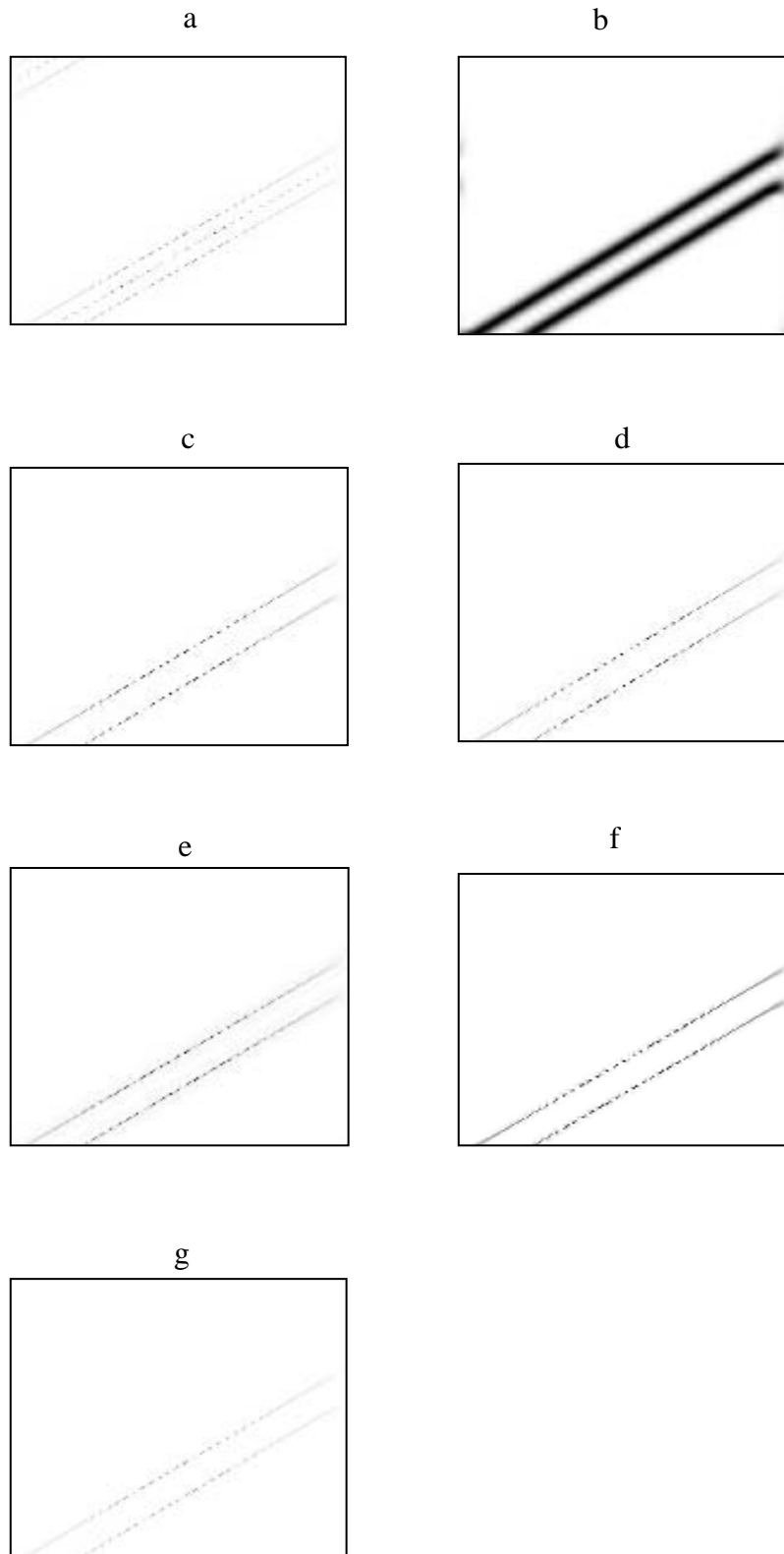
Fig 4.5 Analysis of two linear components (a) WD, (b) GT, (c) GWT (*Eq. 4.1*), (d) GWT (*Eq. 4.2*), (e) GWT (*Eq. 4.3*), (f) GWT (*Eq. 4.4*) and (g) Modified GWT.
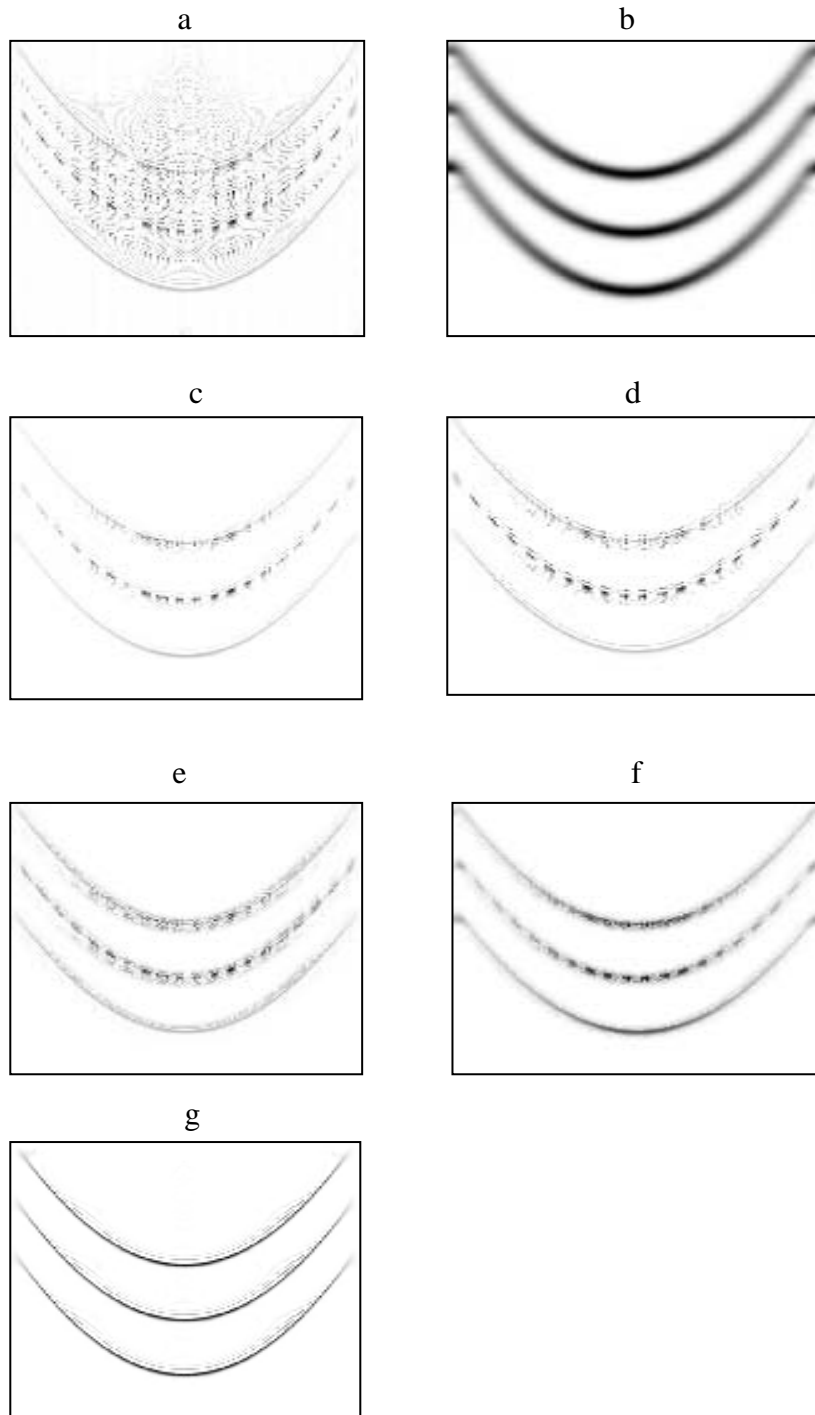
Fig 4.6 Analysis of a three quadratic components (a) WD, (b) GT, (c) GWT (*Eq. 4.1*),
(d) GWT (*Eq. 4.2*), (e) GWT (*Eq. 4.3*), (f) GWT (*Eq. 4.4*) and (g) Modified GWT.
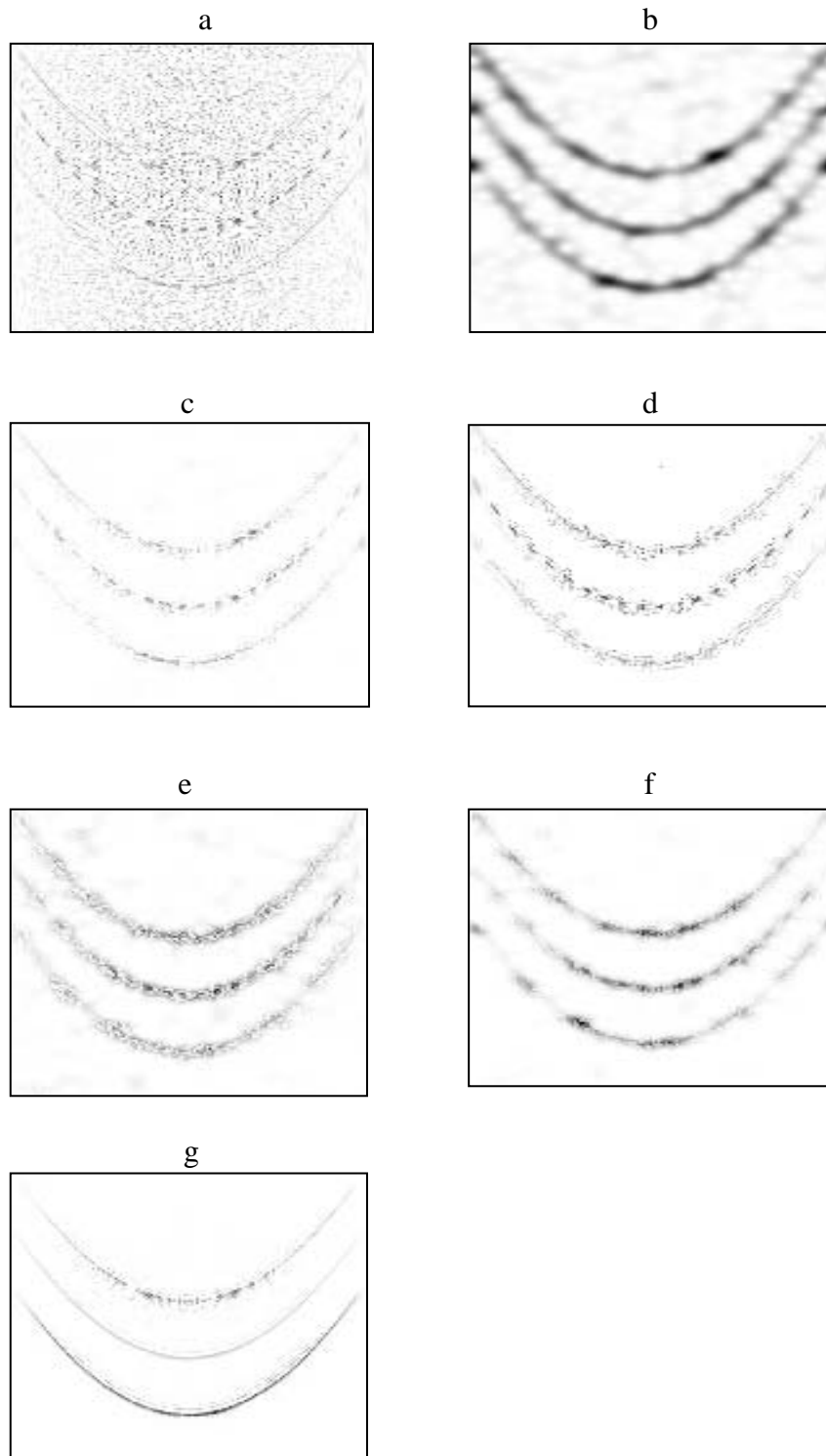
Fig 4.7 Analysis of a three quadratic components (SNR= 3dB) (a) WD, (b) GT, (c) GWT (*Eq. 4.1*), (d) GWT (*Eq. 4.2*), (e) GWT (*Eq. 4.3*), (f) GWT (*Eq. 4.4*) and (g) Modified GWT.

4.1.2 Performance analysis of modified GWT

The performance of a TFR can be evaluated on the basis of its readability, energy concentration and cross-terms suppression. Cross-terms suppression and energy concentration of a TFR can be computed by visual inspection or on the basis of performance measures, like Shannon entropy [69], Renyi entropy [65], ratio of norms [68] and LJubisa measure [71]. Readability of TFRs can only be tested by visual inspection [27].

The performance of modified GWT is evaluated on the basis of quantative measures including entropy measures [65] and ratio of norms [68] as described in last chapter. The proposed method has a maximum value of ratio of norms as shown in table 4.1 and minimum value of entropy as shown in table 4.2. Therefore the modified GWT shows good energy concentration property as compared to other considered TFRs. Hence our analysis shows that, it provides advantages of both WD and GT.

Table 4. 1 Comparison of modified GWT with other TFRs (based on ratio of norms)

Test signal	WD	SPWD	GT	GWT (*Eq 4.1*)	GWT (*Eq 4.2*)	GWT (*Eq 4.3*)	**Proposed GWT**
Gaussian atom	1.7	1.1	0.8	2.4	1.7	1.8	**2.5**
Linear chirp	1.1	0.1	0.1	1.2	1.1	1.1	**1.3**
Quadratic component	0.0198	0.2321	0.0685	0.2701	0.1544	0.3311	**0.3428**
2 linear chirps	0.5559	0.0316	0.0347	0.7716	0.6586	0.6475	**0.8649**
3 quadratic components	0.0261	0.0452	0.0219	0.1599	0.0835	0.0849	**0.2489**

Table 4. 2 Comparison of modified GWT with other TFRs (based on Renyi entropy)

Test signal	WD	SPWD	GT	GWT (*Eq 4.1*)	GWT (Eq 4.2)	GWT (*Eq 4.3*)	**Proposed GWT**
Gaussian atom	9.8955	10.4266	10.9410	9.3150	9.7509	9.7793	**9.3149**
Linear chirp	12.3137	14.2874	14.3732	11.1482	11.3292	11.4733	**10.64**
Quadratic component	16.3826	14.1037	14.7630	13.0494	13.0027	12.8098	**12.5322**
2 linear chirps	13.2392	15.5037	15.2019	11.9084	12.1326	12.3899	**11.3706**
3 quadratic components	16.2640	15.7187	16.1286	14.2950	14.5171	14.8538	**13.5344**

In this chapter, the advantages of the proposed modified GWT are analyzed for multi-component signals. The proposed combination of GT and WD leads to the resultant GWT eliminates cross-terms while keeping the resolution of auto-components closer to WD. Moreover, the proposed TFR provides better concentration of auto-components comparing to other GWT forms.

Chapter 5

Modified FRFT based GWT approach

In chapter 4, we have shown the potential of modified GWT for a multi-component signal analysis. Unfortunately this method and different combinations of GWT given in $Eqs\,(4.1, 4.2, 4.3\,and\,4.4)$ are only applicable for slowly time-varying signals. In multi-component signal analysis where GWT fails to extract auto-components, the combination of signal processing and image processing techniques has proven their potential to extract auto-components. In this chapter a new scheme for TFR of multi-component signals has been described that includes FRFT along with image segmentation techniques to find a cross-term free TFR. The proposed modified fractional GWT is an extension of Nabeel's work [41] which also includes FRFT and image segmentation. The proposed algorithm maintains the resolution of auto-components and it shows that FRFT domain is a powerful tool for signal analysis. Before going to describing modified FRFT based GWT, it is necessary to describe image segmentation and classification processes, which will be later used in the proposed scheme.

5.1 Classification process

Classification based on a TFR is preferred due to the capability of TFRs to discriminate between different auto-components taken as different segments in time-frequency domain. Before going to discuss a particular classification method, let us consider sample auto-component patterns depicted in Fig 5.1. The patterns in Fig.(5.1 a, b and c) are non-overlapping and pattern in Fig. 5.1d is overlapping. Time or frequency domain filtering can be easily used in case of non-overlapping auto-components. However, in case of overlapping auto-component a classification mechanism is required to segment out auto-components of a particular segment.
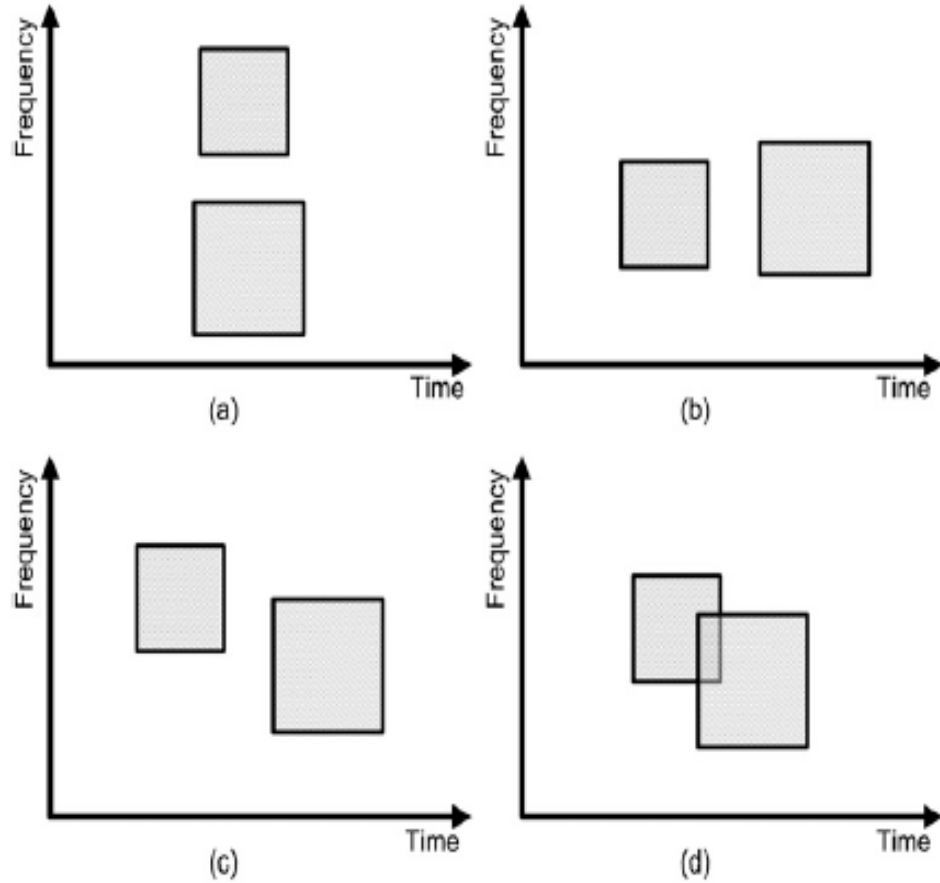
Fig 5.1 Auto-component patterns in the TFR domain: (a) Auto-components (same time band), (b) Auto-components (same frequency band), (c) Non intersecting auto-components (same frequency band), (d) auto-components overlap on some frequency and time bands [76].

5.1.1 Overall segmentation Procedure

The linear TFR (GT) is transformed into a binary image, by assigning the value one to local peaks, and assigning zero value for all other locations. The binary image $B(t,\omega)$ of a TFR is given by:

$$B(t,\omega) = \begin{cases} 1 \;\; if \left\{ \dfrac{\partial(TFR(t,\omega))}{\partial\omega} = 0 \right\} \oplus \left\{ \dfrac{\partial^2(TFR(t,\omega))}{\partial\omega^2} < 0 \right\} \\ 0 \;\; else. \end{cases} \qquad (5.1)$$

In $Eq(5.1)$, $\oplus$ is a and operator. This binary transformation followed by a component- linking procedure [74] defines edges in a image. A linked component in a

binary image is called as a independent object [75]. The problem of a false component linking arises due to large neighboring set. Therefore, it is necessary to define a threshold value to identify true connected and falsely connected components. This threshold value is application dependent [63].

5.1.2 Support vector machine (SVM)

For identification of boundaries among various auto-components we use Support vector machine (SVM). SVM [27, 41, 77] is a powerful classification tool used in signal processing applications and is one of the most widely used algorithm of machine learning. SVM is used to separate boundary between different segments in a time–frequency plane as shown in Fig 5.2. Let us consider a set of data points having the form,

$$D = \left\{ (\mathbf{x}_i, c_i) \,\middle|\, \mathbf{x}_i \varepsilon R^2, \quad c_i \varepsilon \{-1, 1\} \right\}_{i=1}^{n}. \tag{5.2}$$

In $Eq(5.2)$, $c_i = 1\, or\, -1$, represents the segment to which the point belong and $\mathbf{x}_i$ is a two-dimensional vector showing a pixel belonging to image segment in time–frequency plane. The main goal is to find out the line having maximum margin between the points following the condition $c_i = 1$ and $c_i = -1$. Two lines are drawn parallel to the classification line in such a way that they can classify the data points. Mathematically these lines can be described as:

$$\mathbf{w}^T \mathbf{x}_i + b = 1, \tag{5.3}$$

$$\mathbf{w}^T \mathbf{x}_i + b = -1. \tag{5.4}$$

This problem of finding the optimal classifying line is solved by minimizing the objective function (minimize $(\frac{1}{2} \|\mathbf{w}\|^2)$) subjected to the constraint $c_i(w\mathbf{x}_i - b) \geq 1$. Now quadratic programming [27, 41, 77] solves this Lagrangian dual problem as,

$$\text{maximize } \sum_{i=1}^{n} \alpha_i - \frac{1}{2} \sum_{i=1}^{n} \sum_{j=1}^{n} \alpha_i \alpha_j c_i c_j K(\mathbf{x}_i, \mathbf{x}_j), \tag{5.5}$$

such that $0 \leq \alpha_i \leq C$ and

$$\sum_{i=1}^{n} \alpha_i c_i = 0. \tag{5.6}$$

In conditions (5.5 and 5.6), $K(\mathbf{x}_i, \mathbf{x}_j)$ is kernel function, C is the measure of misclassification and α is Lagrange multiplier. The solution of discriminant function is given by

$$g(\mathbf{x}) = \sum_i \alpha_i K(\mathbf{x}_i, \mathbf{x}_j) + b. \qquad (5.7)$$

SVM can use several types of kernel functions (polynomial, linear, sigmoid and Gaussian radial basis function). Mathematical representations of these kernel functions are,

$$K_{linear}(\mathbf{x}_i, \mathbf{x}_j) = \mathbf{x}_i^T \mathbf{x}_j \qquad (5.8)$$

$$K_{polynomial}(\mathbf{x}_i, \mathbf{x}_j) = (1 + \mathbf{x}_i^T \mathbf{x}_j)^d \qquad (5.9)$$

$$K_{radial\,basis\,function}(\mathbf{x}_i, \mathbf{x}_j) = \exp(-\gamma \|\mathbf{x}_i - \mathbf{x}_j\|^2) \qquad (5.10)$$

In $Eqs(5.8, 5.9\ and\ 5.10)$, $\mathbf{x}_i$ represents feature vector, $\mathbf{x}_j$ describes target vector, d represents degree of polynomial and γ represent width of Gaussian funtion. In summary, linear kernel function is computationally efficient than non-linear kernels.

(Segmented Image)	(auto-components classification)
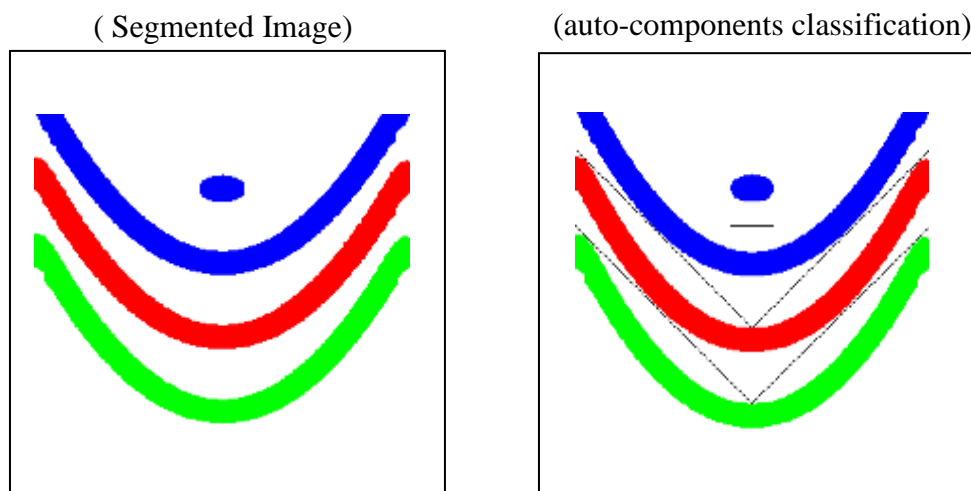
Fig 5.2 Classification of signal described in $Eq(5.16)$.

5.2 Application of FRFT

FRFT is used to isolate the auto-components that are linearly separable in time-frequency plane. SVM is used to draw a boundary between two auto-components. If two auto-components are linearly separable, then single line would be enough. However, for nonlinearly separable auto-components, multiple straight lines are required. Slope and y-intercept of classifying line between auto-components defines two important parameters of fractional filtering. These two parameters are:

➤ Rotation angle α [4, 41]

➤ Selection criteria for cutoff lines [4, 41].

The rotation angle [41] α is defined as,

$$\alpha = \frac{2}{\pi} \tan^{-1}(\frac{m(x_2 - x_1)}{N}).$$ (5.11)

In $Eq(5.11)$, m is defined as,

$$m = \frac{y_2 - y_1}{x_2 - x_1}.$$ (5.12)

The cutoff frequency is defined as,

$$\omega = \pi \frac{y_2 + y_1}{N}.$$ (5.13)

In $Eqs(5.11, 5.12 \text{ and } 5.13)$, α, m, ω, N, x_1, x_2, y_1, y_2 are rotation order, slope, cutoff frequency, starting point on x-axis, ending point on x-axis, starting point on y-axis and ending point on y-axis [41].

5.3 Modified Fractional GWT

The objective of this work is to propose a TFR which should preserve the quality of auto-components for a multi-component dynamic signals and suppress the cross-terms. For this purpose a proper combination of linear and quadratic TFRs such as GT and WD is designed which can achieve better results as compared to already proposed definitions of GWT [78]. Steps of proposed method are given as:

Step 1. Transform the given signal $x(t)$ in 2D using $Eq(2.11)$.

Step 2. Adaptive thresholding (detailed discussion in chapter 4) and image segmentation (8-connectivity criterion) of the process performed in step 1 [19].

Step 3. Classification of auto-components by support vector machine (SVM) of the process performed in step 2 [41]. Location and slope of classification line will determine two important parameters (cut-off lines and rotation angle) for filtering in FRFT domain [4, 41].

Step 4. Isolation of auto-components in FRFT domain, using step 3 [40, 41].

Step 5. Compute GT and WD of isolated auto-components by using step 4.

Step 6. Compute GWT using following relation,

$$GWT_x(t,\omega) = GT_x^{0.5}(t,\omega)WD_x(t,\omega). \tag{5.14}$$

Eq(5.14) will give high readability of auto-components in case of weak components as compared to method proposed in [27, 41].

Now high readable TFR can be obtained by using following relation,

$$TFR_x(t,\omega) = \sum_k GWT_{x_k}(t,\omega) \ where \ k = no \ of \ auto-components. \tag{5.15}$$

All the steps of this proposed technique are shown in the following block diagram.
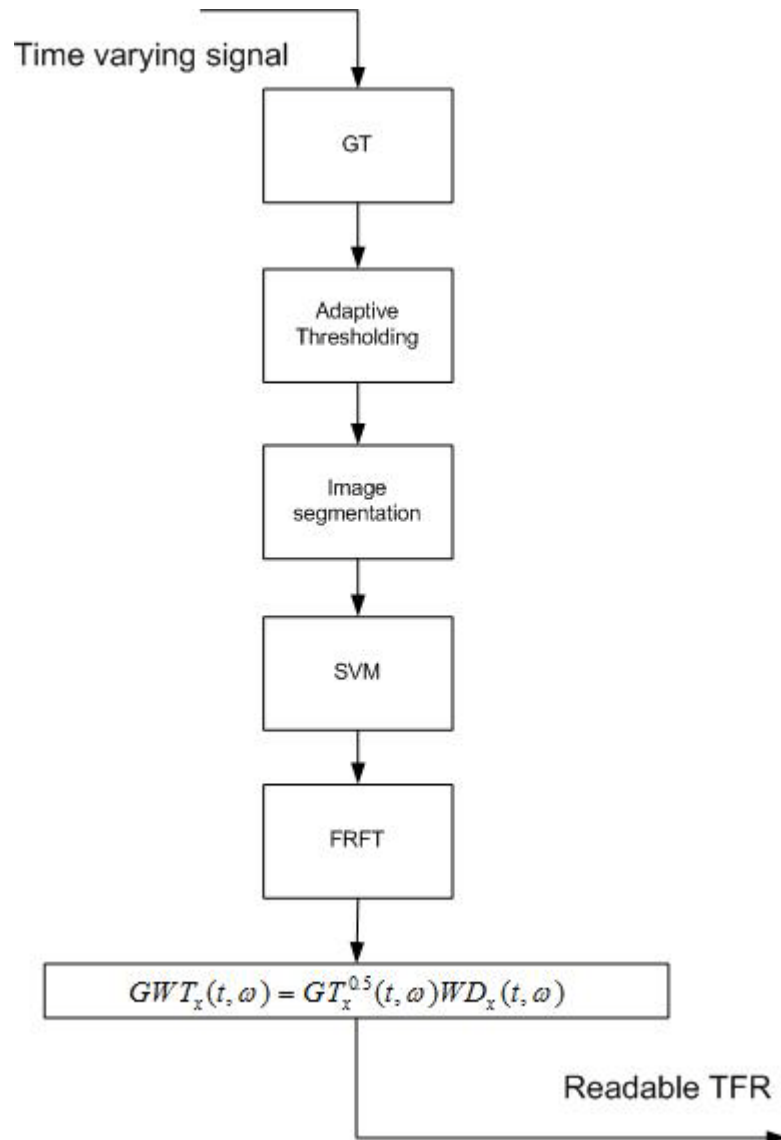
Fig. 5.3 FRFT based GWT

5.3.1 Numerical simulations

To show the strength of modified Fractional GWT two examples are considered, (i) three quadratic components and a Gaussian atom, (ii) amplitude varying bat signal. In both examples, auto-components overlap in frequency or in time and they are also buried in interferences. Thus, these particular case studies show challenging task to isolate auto-components from cross-terms in case of WD.

5.3.1.1 Example 1

$$x(t) = 0.2\exp(-2\pi j(7t^3 + 55t)) + 0.5\exp(-2\pi j(7t^3 + 35t)) +$$
$$0.9\exp(-2\pi j(7t^3 + 15t)) + 0.7\exp(-2\pi j(70t))\exp(-15t^2). \hspace{1cm} (5.16)$$

Consider $Eq(5.16)$, the example of a three quadratic components with time varying amplitude and a Gaussian atom as shown in Fig.5.4 (sampling frequency = 200 Hz, time duration = -1 to 1 seconds). The quadratic nature of WD produces cross-terms (Fig.5.4 a). Analysis of this signal through GT shows that, it provides cross-terms elimination property of GT but auto-components are blurred (Fig.5.4 b). The behavior of different variants of GWT (*Eq 4.1*, *Eq 4.2*, *Eq 4.3*, and *Eq 4.4*) represent issues of readability and missing of auto-components (Fig.5.4 c, d, e, f). By applying proposed algorithm step by step, it proves it's potential to study a multi-component signal (Fig.5.4 g). It provides cross-terms elimination property of GT and high resolution property of WD. It extracts successfully all auto-components and gives highly readable TFR. This example also proves that the combination of signal processing and image processing techniques successfully removes the cross- terms of WD and gives a high resolution TFR which is also shown in Tables 5.1 & 5.2. Fig 5.6 reveals that proposed method completely beats ZAM and PAGE TFRs and its readability is higher than method proposed by Nabeel et al. [41].

5.3.1.2 Example 2

Consider the example of a real life bat signal [23] as shown in Fig.5.5 (sampling frequency = 200 Hz, time duration = -1 to 1 seconds). This signal is commonly used for comparison of TFRs. The quadratic nature of WD produces cross-terms (Fig.5.5 a). Analysis of this signal through GT shows that, it provides cross-terms elimination property of GT but auto-components are blurred (Fig.5.5 b). The behavior of different variants of GWT (*Eq 4.1*, *Eq 4.2*, *Eq 4.3*, and *Eq 4.4*)

represent issues of readability and missing of auto-components (Fig.5.5 c, d, e, f). By applying proposed algorithm step by step it proves its potential to study the behavior of a multi-component signal (Fig.5.5 g). It provides cross-terms elimination property of GT and high resolution property of WD. It extracts successfully all auto-components and gives a highly readable TFR. Fig 5.7 reveals that proposed method completely beats ZAM and PAGE TFRs and its readability is higher than method proposed by Nabeel et al. [41].
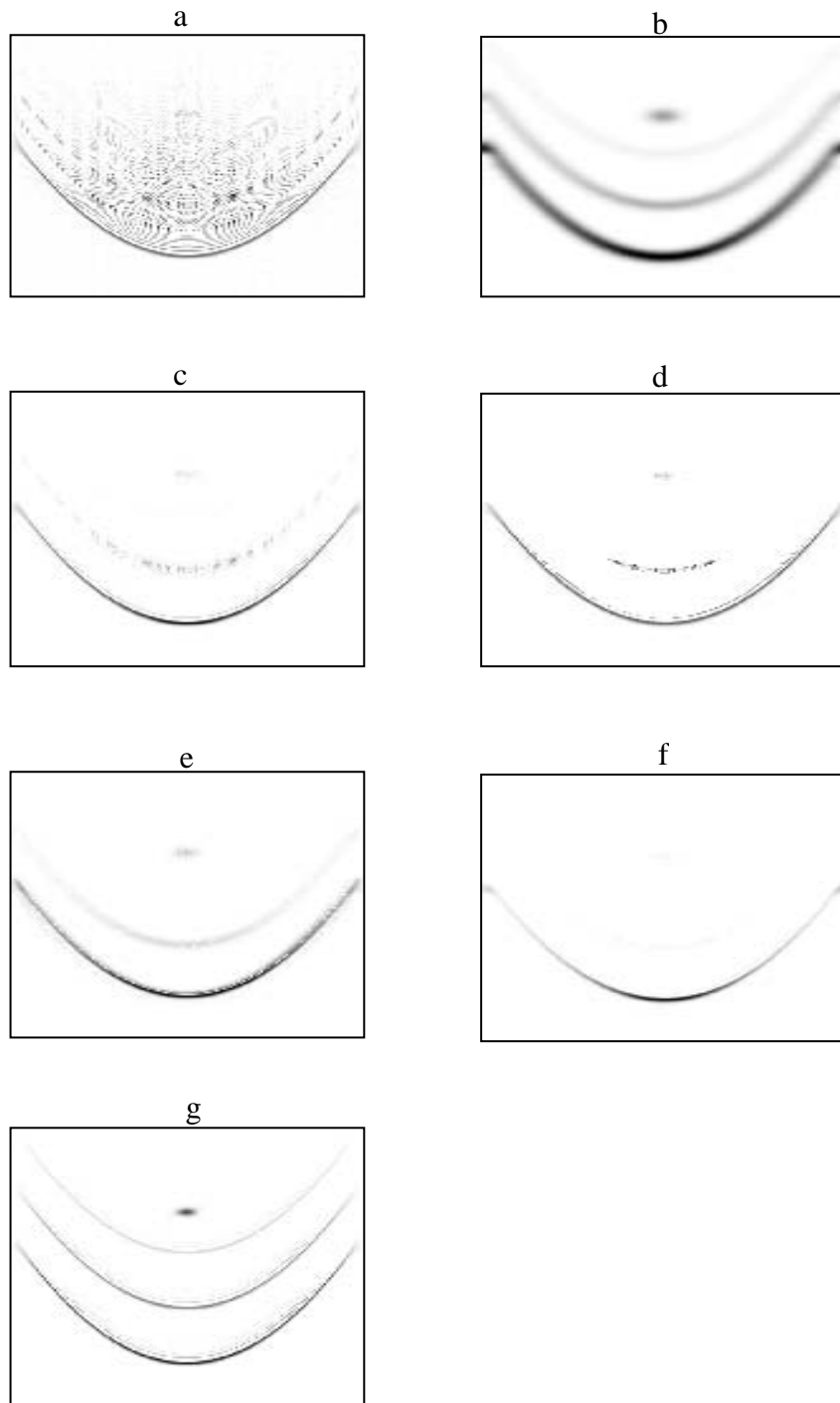
Fig 5.4 Analysis of a three quadratic and a Gaussian atom (a) WD, (b) GT, (c) GWT (*Eq. 4.1*), (d) GWT (*Eq. 4.2*), (e) GWT (*Eq. 4.3*), (f) GWT (Eq. *4.4*) and (g) Modified Fractional GWT.
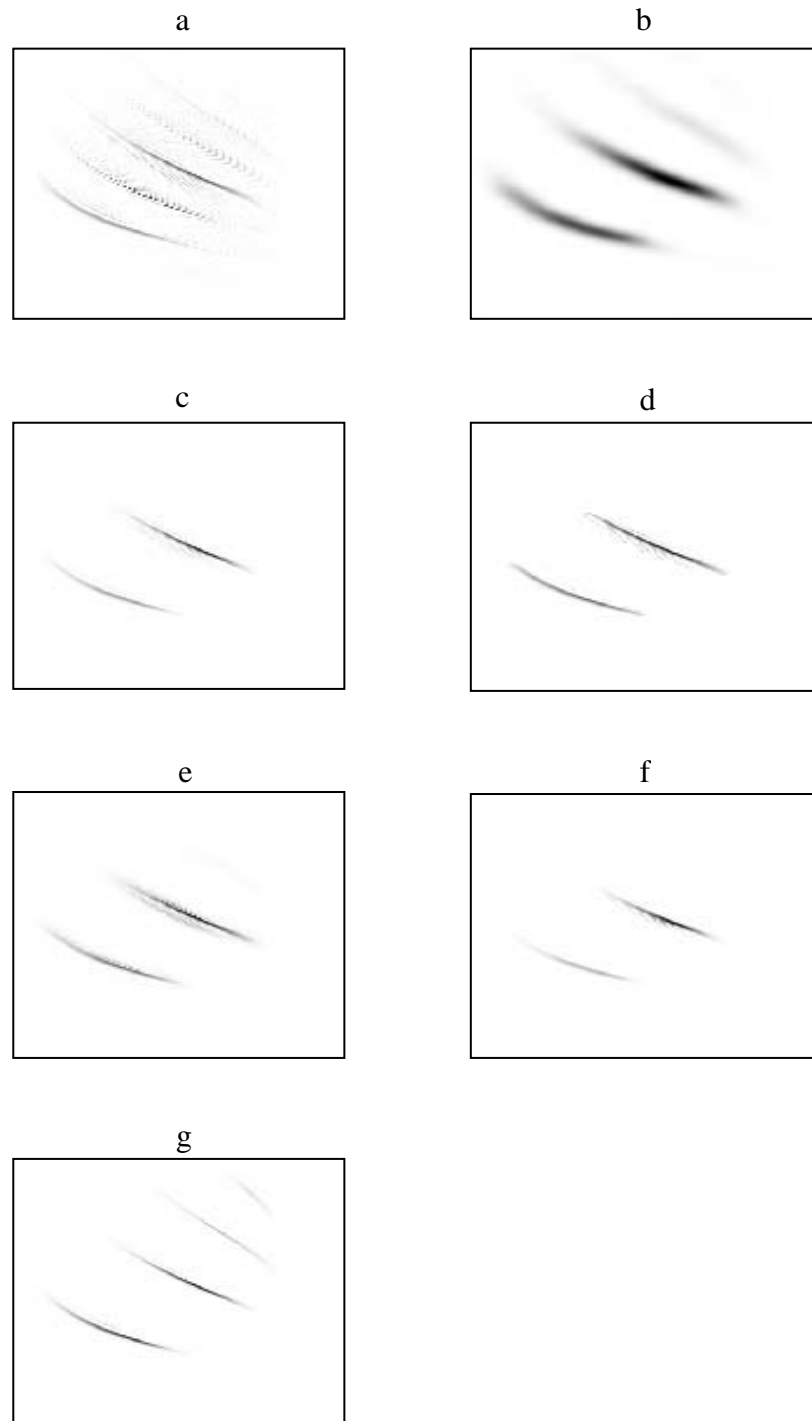
Fig 5.5 Analysis of a bat signal (a) WD, (b) GT, (c) GWT (*Eq. 4.1*), (d) GWT (*Eq. 4.2*), (e) GWT (*Eq. 4.3*), (f) GWT (*Eq. 4.4*) and (g) Modified Fractional GWT.
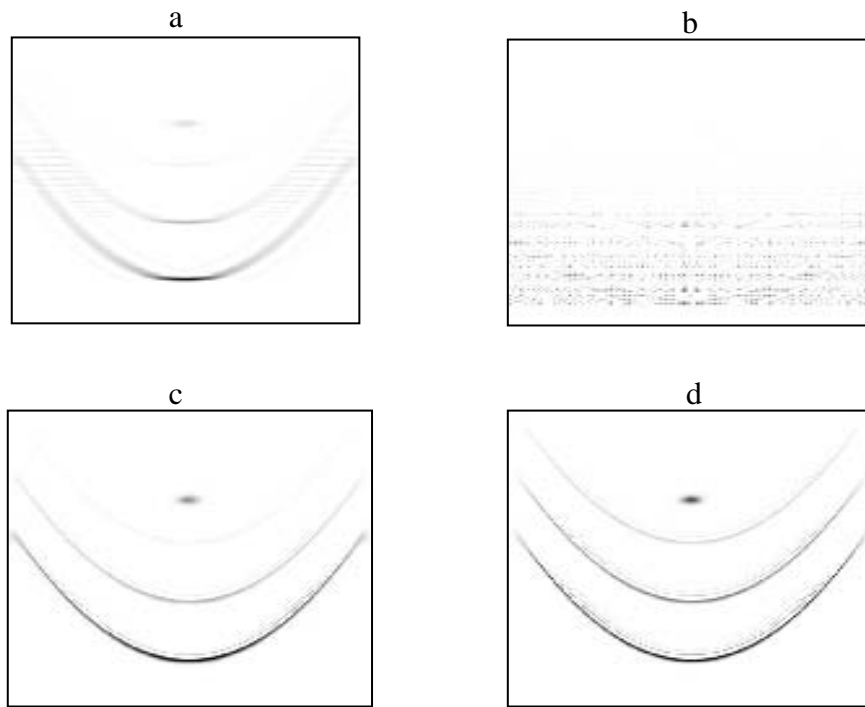
Fig 5.6 Analysis of a three quadratic and a Gaussian atom (a) ZAM, (b) PAGE, (c) Nabeel et al. and (d) Modified Fractional GWT.
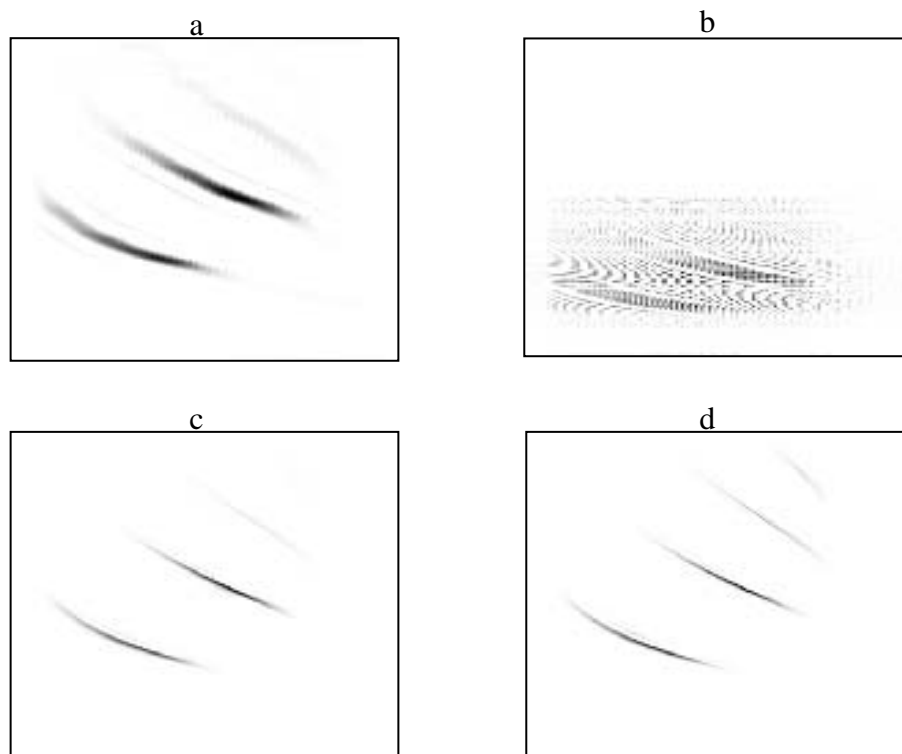
Fig 5.7 Analysis of a bat signal (a) ZAM, (b) PAGE, (c) Nabeel et al. and (d) Modified Fractional GWT.

5.3.2 Performance analysis of Fractional GWT

The performance of a TFR can be evaluated on the basis of its readability, energy concentration and cross-terms suppression. Since modified FRFT based GWT method uses a linear TFR (GT) for allocation of auto-components, and hence, it faces resolution limitation as that of linear TFRs [9]. Cross-terms suppression and energy concentration and of a TFR can be computed by visual inspection or on the basis of performance measures, like Shannon entropy [69], Renyi entropy [65], ratio of norms [68] and LJubisa measure [71]. Readability of TFRs can only be tested by visual inspection [27].

The performance of proposed method is evaluated on the basis of quantative measures like entropy measures [65], LJubisa measure [71] and ratio of norms [68]. The proposed method has a maximum value for ratio of norms for both signals (Table 5.1) and minimum value of entropy and LJubisa measure as shown in table 5.2. Therefore proposed GWT shows good energy concentration property as compared to other TFRs. Hence our analysis show that proposed GWT provides advantages of both WD and GT and also gives solution of cross-terms of WD.

Table 5. 1 Performance measures (three quadratic components and a Gaussian atom)

TFR	Shannon	Renyi	Ratio of Norms ($\times10^{-3}$)	Ljubisa ($\times10^{9}$)
WD	16.1481	15.1764	0.0495	1.4116
GT	15.9242	15.0367	0.0532	1.5082
GWT (*Eq 4.1*)	14.7101	13.3563	0.2066	0.2782
GWT (*Eq 4.2*)	14.8139	13.3118	0.1355	0.2811
GWT (*Eq 4.3*)	14.7700	13.4737	0.1871	0.3052
GWT (*Eq 4.4*)	14.6396	13.3426	0.4077	0.3678
ZAM	16.7161	14.3490	0.2830	1.1864
PAGE	16.7507	15.4222	0.0538	2.0772
Nabeel	14.2968	13.1015	0.2320	0.2675
Modified Fractional GWT	13.8139	12.3426	0.4663	0.2460

Table 5. 2 Performance measures (bat signal)

TFR	Shannon	Renyi	Ratio of Norms	Ljubisa ($\times 10^8$)
WD	15.3288	13.5606	0.0003	2.7967
GT	15.2583	14.2951	0.0001	6.3033
GWT (*Eq 4.1*)	12.3199	10.7382	0.0015	0.0919
GWT (*Eq 4.2*)	11.9194	11.1182	0.0008	0.0519
GWT (*Eq 4.3*)	12.7364	11.3310	0.0009	0.1567
GWT (*Eq 4.4*)	11.6490	10.3088	0.0018	0.1362
ZAM	15.0218	13.5436	0.0002	3.5857
PAGE	15.1744	14.1914	0.0001	3.7244
Nabeel	11.7711	10.6054	0.0012	0.0587
Modified Fractional GWT	11.4099	10.2685	0.0023	0.0426

In this chapter, the advantages of GWT are analyzed in FRFT domain for a multi-component signal. A modified fractional GWT is proposed which is a modified form of Nabeel's work [41]. In the proposed technique, cross-terms are eliminated with minimal distortion in the auto-components through FRFT domain. The combination of signal processing and image processing techniques and by using the new combination of linear and quadratic TFRs($Eq(5.11)$) successfully removes the cross-terms of WD and gives high resolution TFR. Performance analysis of proposed method reveals that it provides solution of cross-terms of WD and low resolution of GT.

Chapter 6

Linear Time Varying filtering based GWT

In this chapter, a new method has been developed by combining Linear Time Varying (LTV) filtering technique [79] with image processing techniques (adaptive thresholding and image segmentation [74]) for cross-terms suppression. In the proposed method a filter in time-frequency domain is designed using an iterative approach in both time-frequency and time domains. This filter is specifically designed in order to suppress cross-terms and enhances concentration of auto-components even weaker ones. The proposed algorithm is applied to extract auto-components of a multi-component signal, to enhance weaker auto-components and to tackle resolution problem faced by linear TFRs. This work shows that this method adopts the merits of both WD and GT.

6.1 Linear Time Varying (LTV) filtering

It can be proved mathematically that FT can be described as a output of LTV signal $x(t)$, Mathematically it is described as,

$$y(t) = \int_{-\infty}^{\infty} h(t, t - \tau) x(\tau) d\tau. \tag{6.1}$$

In *Eq (6.1)*, $h(t, \tau)$ is defined as the impulse response of the time varying system and $y(t)$ is the output of the filter. By putting $h(t, \tau) = e^{-jt(t-\tau)}$ in *Eq 6.1* which takes the form,

$$y(t) = \int_{-\infty}^{\infty} x(\tau) e^{-jt\tau} d\tau. \tag{6.2}$$

By simplification, *Eq 6.2* takes the form

$$y(t) = X(t). \tag{6.3}$$

Similarly we can write

$$y(\omega) = Y(\omega). \tag{6.4}$$

STFT can be interpreted as a LTV filter bank and hence its time varying spectrum can be described as an output of LTV filter [79]. By considering *Eq*(2.5) it

can be shown that for a particular value of $\omega = \omega_1$, STFT has an interpretation of modulated filtering which is described in *Eq (6.1)*. Time varying transfer function $H(t,\omega)$ is described by the following relation,

$$H(t,\omega) == \int h(t,\tau)e^{-j\omega\tau}d\tau. \tag{6.5}$$

$GWT_x(t,\omega)$ can be used as a linear operator if auto-components of WD do not overlap with its cross-components then it is considered as a linear operator. Mathematically it is described as,

$$GWT_x(t,\omega) = \sum_{i=1}^{M} GWT_{x_i}(t,\omega) + \sum_{k=1}^{M-1}\sum_{l=k+1}^{M} 2\,\text{Re}(GWT_{x_k x_l}(t,\omega)). \tag{6.6}$$

By putting $\text{Re}(GWT_{x_k x_l}(t,\omega)) = 0$ in *Eq 6.6*, then $GWT_x(t,\omega)$ is a linear operator and mathematically,

$$GWT_x(t,\omega) = \sum_{i=1}^{M} GWT_{x_i}(t,\omega). \tag{6.7}$$

In order to show the strength of the LTV filtering an example of a synthetic signal having three quadratic components is considered. Fig. 6.1(a, b) shows the time domain and joint time-frequency (*t-f*) domain representations of the signal. Suppose that if we want to filter out two components of the signal through LTV filtering, the desired output signal with only one auto-component is shown in time and *t-f* domain in Fig. 6.1 (c) and (d) respectively. Fig. 6.1 (e) describes the filtering mask in *t-f* domain and finally Fig. 6.1 (f) show the output signal obtained after LTV filtering given in *Eq 6.5*, where the filter $h(t,\tau)$ is obtained by taking the inverse FT of the *t-f* filtering mask. Fig. 6.1 (g) and (h) shows the filtered signal in t-f domain given by its GT and WD respectively. It is clear that the purpose of LTV filtering has been fully achieved as the desired signal and true output signal are nearly similar in time domain as demonstrated in Fig. 6.1 (c) and (f), as well as in *t-f* domain as demonstrated in Fig. 6.1 (d) and (g).
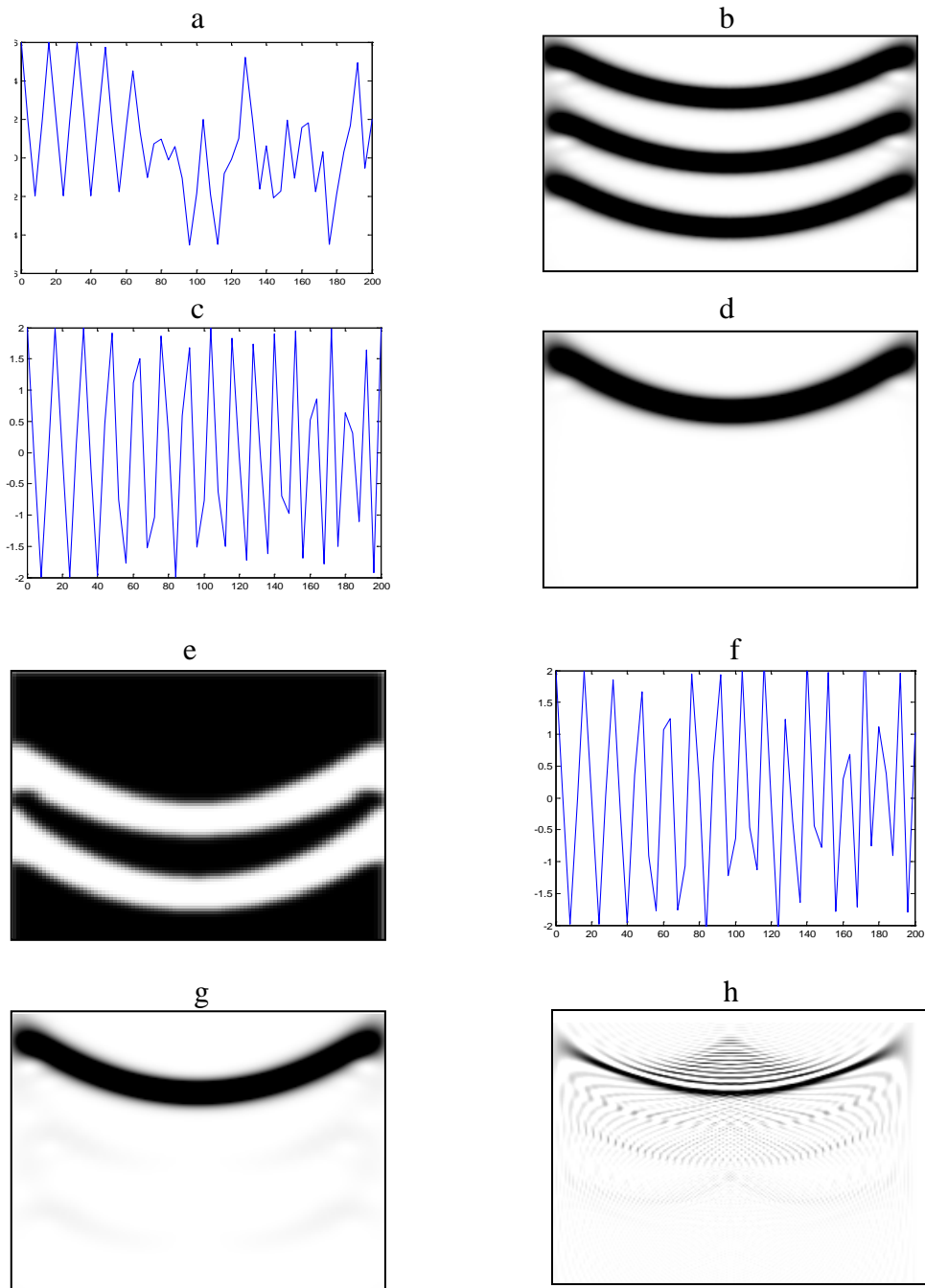
Fig. 6.1. Signal consisting of three quadratic components, (a) time domain representation of the signal, (b) TFR of the signal (GT), (c) time domain representation one auto-component, (d) TFR of the one auto-component (GT), (e) filtering mask in frequency domain, (f) LTV filtering, (g) filtered auto-component (GT) and (h) filtered auto-component (WD)

6.2 The proposed algorithm

Our aim is to obtain a TFR which not only has strong localization but also keeps intact the weak auto-components [80]. For this purpose we propose an algorithm which is based on designing a filter which rejects cross terms and enhances auto-components, even weaker ones. The filter is designed in an iterative way where in each iteration new auto-components are identified (strongest auto-components are identified first). The procedure is given in the following steps.

For the first iteration,

1. Initialize $x^i(t) = x(t)$, where i stands for i^{th} iteration

2. Compute GWT of the given signal $x^i(t)$ by using the following relation [4],

$$X^i(t,\omega) = GWT_{x^i}(t,\omega) = GT_{x^i}(t,\omega)WD_{x^i}(t,\omega). \tag{6.8}$$

3. 2D thresholding and segmentation [78] of $X^i(t,\omega)$ by using the following procedure.

   (i). Calculate the mean T^i of $X^i(t,\omega)$

   $$T^i = mean\left[X^i(t,\omega) \right]. \tag{6.9}$$

   (ii). Thresholding $X_A^i(t,\omega)$ and $X_B^i(t,\omega)$ against T^i and dividing it into two portions

   $$X_A^i(t,\omega) \in X^i(t,\omega) \quad if \quad X^i(t,\omega) \geq T^i, \tag{6.10}$$

   $$X_B^i(t,\omega) \in X^i(t,\omega) \quad if \quad X^i(t,\omega) < T^i. \tag{6.11}$$

   (iii). Calculate means of $X_A^i(t,\omega)$ and $X_B^i(t,\omega)$ separately and update

   T^i as $T^i = \dfrac{\mu^i_{X_A^i(t,\omega)} + \mu^i_{X_B^i(t,\omega)}}{2}. \tag{6.12}$

   Go back to (ii). Repeat (ii) & (iii) until T^i does not change further.

   (iv). Now the binary representation of $X^i(t,\omega)$ is taken out as

   $$X_T^i(t,\omega) = \left\{ \begin{array}{ll} 0 & if \quad X^i(t,\omega) \leq T^i \\ 1 & else. \end{array} \right. \tag{6.13}$$

   (iv). The number of auto-components identified in i^{th} iteration (N_X^i) are calculated by using 2-D 8-connectivity criteria for a component linking [75].

Two points j and k in $X_T{}^i(t,\omega)$ are connected if the following two conditions are fulfilled:

(a) $X^i_{T_j}(t,\omega) = X^i_{T_k}(t,\omega) = 1,$ $\quad$ (6.14)

(b) both are within eight neighbors of each other as follows.

$$8-neighborhood = \{ (t-1,\omega-1),(t-1,\omega),(t-1,\omega+1),(t,\omega-1),$$
$$(t,\omega+1),(t+1,\omega-1),(t+1,\omega),(t+1,\omega+1) \ \}. \quad (6.15)$$

5. For obtaining a smooth transition, 2D Gaussian smoothing is performed on the $X_T{}^i(t,\omega)$ by masking operation with mask $M(t,\omega)$. The smoothing is given by

$$\hat{X}^i_T(t,\omega) = X^i_T(t,\omega) * M(t,\omega). \quad (6.16)$$

6. The identified signal components in the ith iteration are then suppressed by LTV filtering [described in section 6.1] of the original signal $x^i(t)$ by using the following equations. The filtered signal is used in the next iteration.

$$H^i(t,\omega) = 1 - \hat{X}^i_T(t,\omega), \quad (6.17)$$

$$h^i(t,\tau) = \int H^i(t,\omega)e^{j\omega\tau}d\omega, \quad (6.18)$$

$$x^{i+1}(t) = \int x^i(t) * h^i(t,\tau)d\tau. \quad (6.19)$$

Repeat 1-4 until all auto-components are extracted and the total energy of $x^i(t)$ is less than predetermined threshold.

7. The final filter is given as:

$$H_{TFR}(t,\omega) = \left[\sum_i a.i.\hat{X}^i_T(t,\omega) \right]^n. \quad (6.20)$$

In (*Eq 6.20*), i shows the iteration number, i.e. for first iteration it is 1, for second it is 2 and so on, *a* is a scaling factor the value of which depend on how much we want to scale up the weaker components and *n* is the order of the filter and we can set $n = 1$, 2, 3, or 4, depending on how much concentration is required in a given TFR.

It should be noted that the number of iteration is not equal to the number of auto-components. The number of iterations depends on how much variation is present in the strength of different auto-components. In most cases all auto-components are detected within 2~3 iterations.

Finally the highly readable TFR is obtained as follows:

$$TFR_{readable}(t,\omega) = TFR_{x(t)}(t,\omega)H_{TFR}(t,\omega)$$
$$where \ TFR_{x(t)}(t,\omega) = GT \ or \ WD \ or \ GWT \ or \ etc.$$

<div style="text-align: right">(6.21)</div>

All the steps of this proposed technique are shown in the following block diagram.
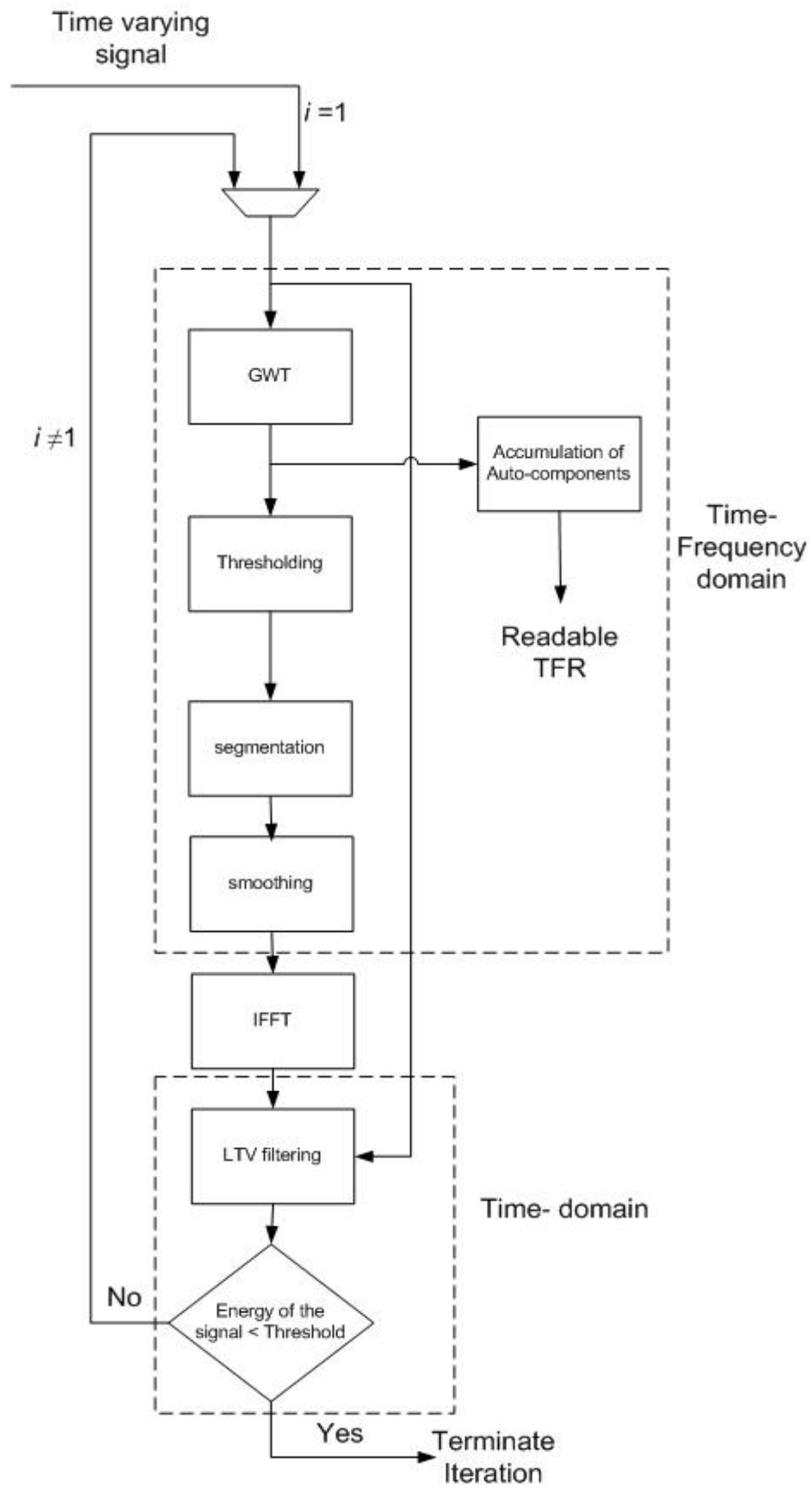
Fig. 6.2 LTV filtering based GWT

6.2.1 Numerical simulations

In order to demonstrate the effectiveness of the proposed technique, an example of the synthetic signal having three quadratic components (with same and varying strengths of auto-components) is considered. The analysis of this signal through WD, GT, GWT (*Eq 4.1*), GWT (*Eq 4.2*), GWT (*Eq 4.3*) and GWT (*Eq 4.4*) is illustrated in Figs. (6.3 to 6.10 by taking noise free and noisy cases (SNR=1dB). The steps of the proposed algorithm for filter design are followed exactly as shown in the previous section and in the final step only, these TFRs are filtered by the designed filter as given in *Eq* 6.21.

Figs. (6.3 (a, c), 6.4 (a, c)) describe WD of the signal for noise free and noisy cases. Figs. (6.3 (b, d), 6.4 (b, d)) clearly represent the effectiveness of the proposed technique where cross-terms of WD are highly suppressed.

Figs. (6.5 (a, c), 6.6 (a, c)) show GT of the signal for noise free and noisy cases. Fig. Figs. (6.5 (b, d), 6.6 (b, d)) clearly represents the effectiveness of the proposed technique where resolution of GT is highly improved.

Figs. (6.7 (a, c, e, g), 6.8(a, c, e, g)) show GWT (*Eq 4.1*), GWT (*Eq 4.2*), GWT (*Eq 4.3*) and GWT (*Eq 4.4*) of the signal. Figs. (6.7 (b, d, f, h), 6.8 (b, d, f, h)) clearly represents the effectiveness of the proposed technique where readability of different variants of GWT is highly improved.

Figs. (6.9 (a, c, e, g), 6.10(a, c, e, g)) show GWT (*Eq 4.1*), GWT (*Eq 4.2*), GWT (*Eq 4.3*) and GWT (*Eq 4.4*) of the signal for the noisy cases. It is cleared in Figs. (6.9 (b, d, f, h), 6.10 (b, d, f, h)) that in the noisy case the proposed filter works very well to represent the complicated signals in a noise free manner.
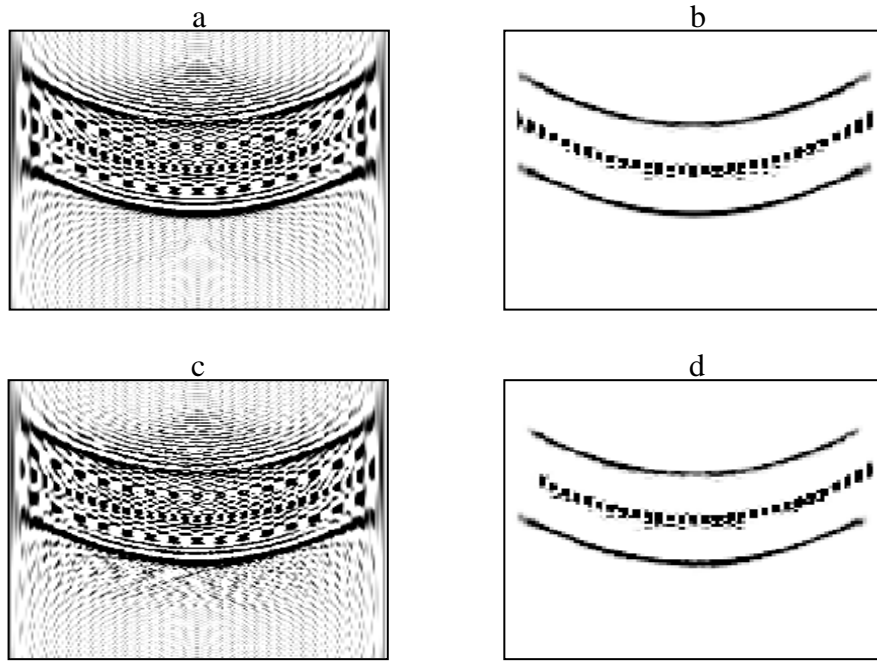
Fig. 6.3. Results of three quadratic-components (same strengths) by using proposed filtering scheme (a) WD, (b) WD after proposed filtering, (c) WD (noisy case >1dB) and (d) WD after proposed filtering.
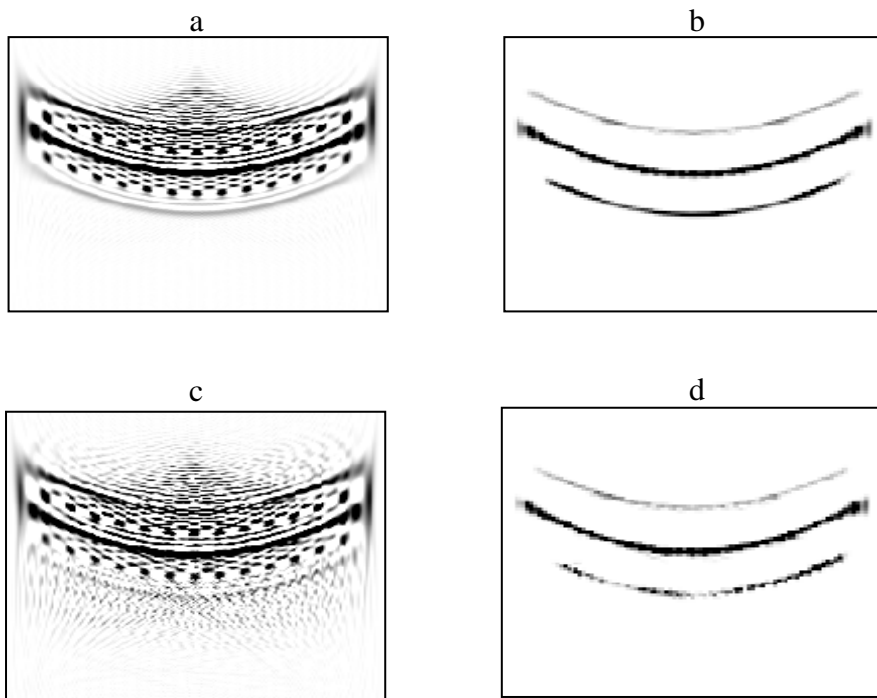
Fig. 6.4. Results of three quadratic-components (varying strengths) by using proposed filtering scheme (a) WD, (b) WD after proposed filtering, (c) WD (noisy case >1dB) and (d) WD after proposed filtering.
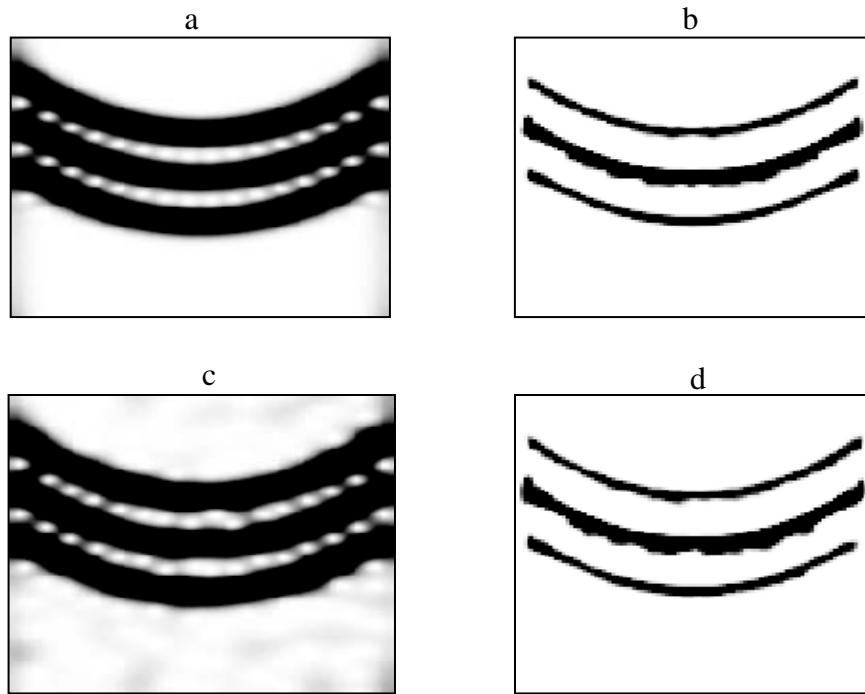
Fig. 6.5. Results of three quadratic-components (same strengths) by using proposed filtering scheme (a) GT, (b) GT after proposed filtering, (c) GT (noisy case >1dB) and (d) GT after proposed filtering.
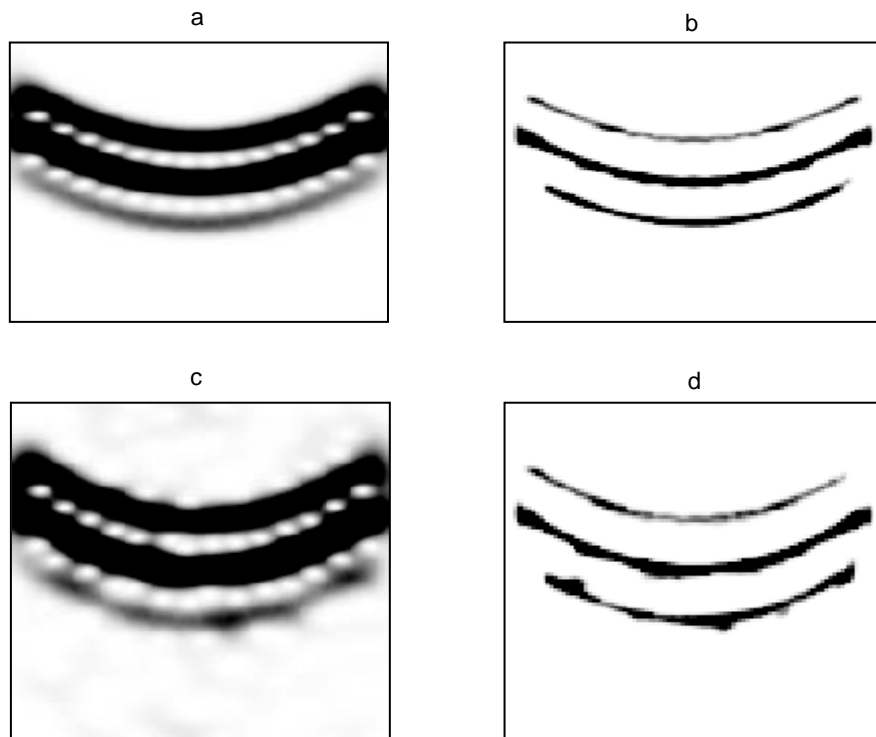
Fig. 6.6. Results of three quadratic-components (varying strengths) by using proposed filtering scheme (a) GT, (b) GT after proposed filtering, (c) GT (noisy case >1dB) and (d) GT after proposed filtering.
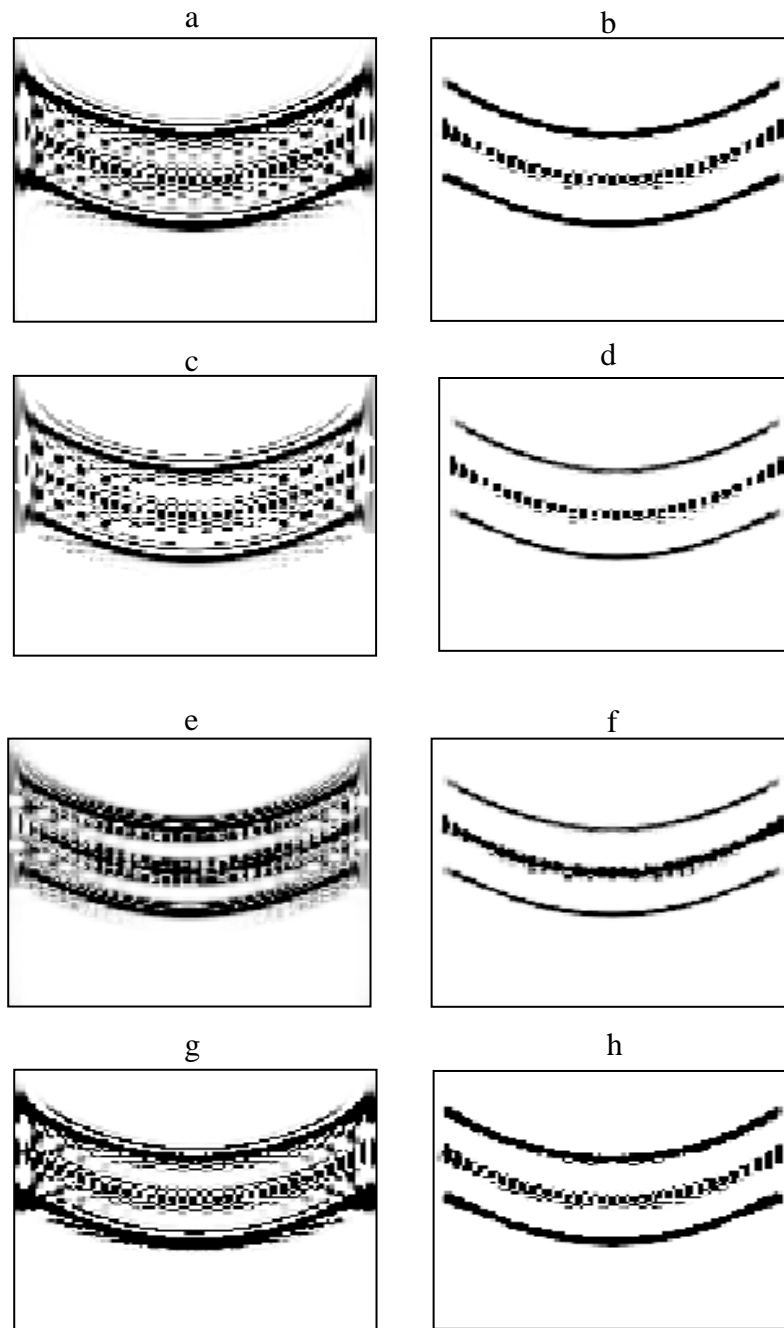
Fig. 6.7. Results of three quadratic-components (same strengths) by using proposed filtering scheme (a) GWT (*Eq 4.1*), (b) GWT (*Eq 4.1*) after proposed filtering, (c) GWT (*Eq 4.2*), (d) GWT (*Eq 4.2*) after proposed filtering, (e) GWT (*Eq 4.3*), (f) GWT (*Eq 4.3*) after proposed filtering (g) GWT (*Eq 4.4*) and (h) GWT (*Eq 4.4*) after proposed filtering.
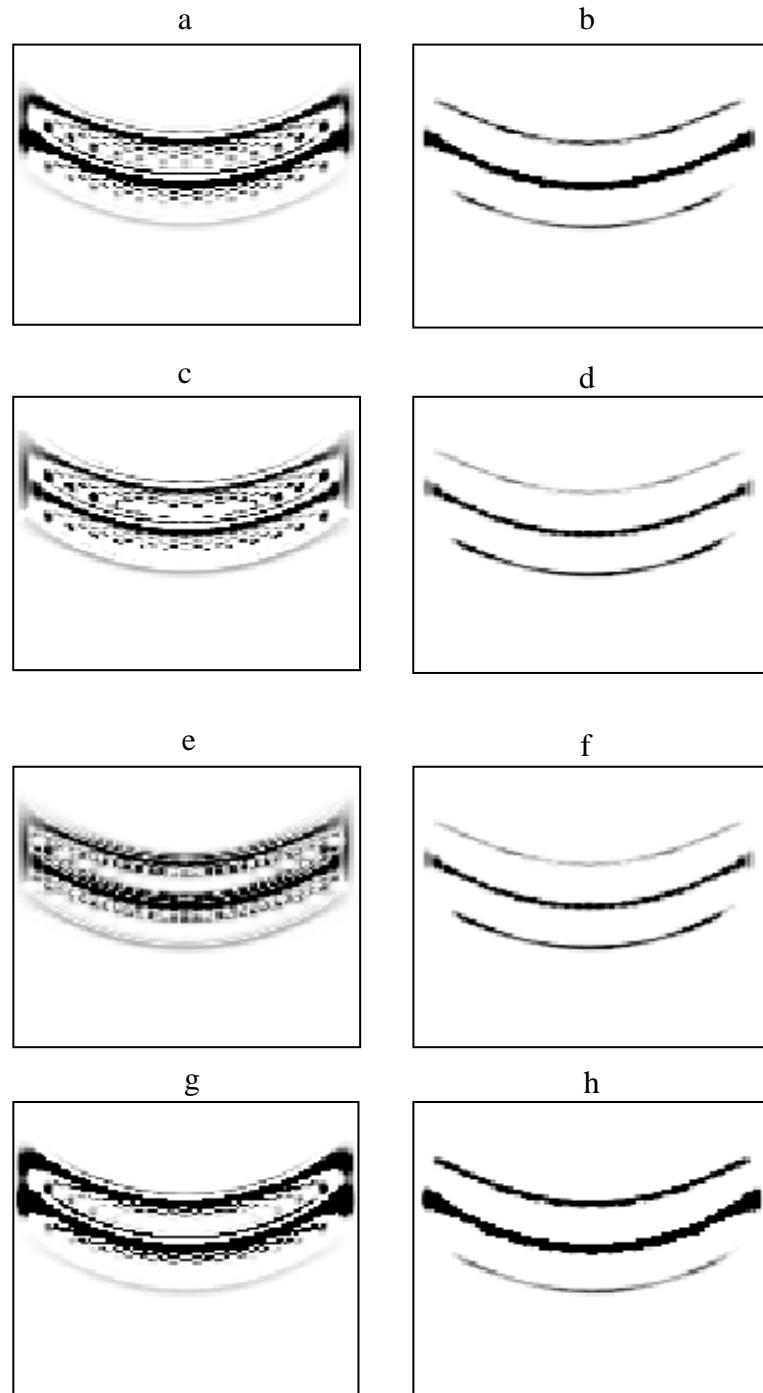
Fig. 6.8. Results of three quadratic-components (varying strengths) by using proposed filtering scheme (a) GWT (*Eq 4.1*), (b) GWT (*Eq 4.1*) after proposed filtering, (c) GWT (*Eq 4.2*), (d) GWT (*Eq 4.2*) after proposed filtering, (e) GWT (*Eq 4.3*), (f) GWT (*Eq 4.3*) after proposed filtering (g) GWT (*Eq 4.4*) and (h) GWT (*Eq 4.4*) after proposed filtering.
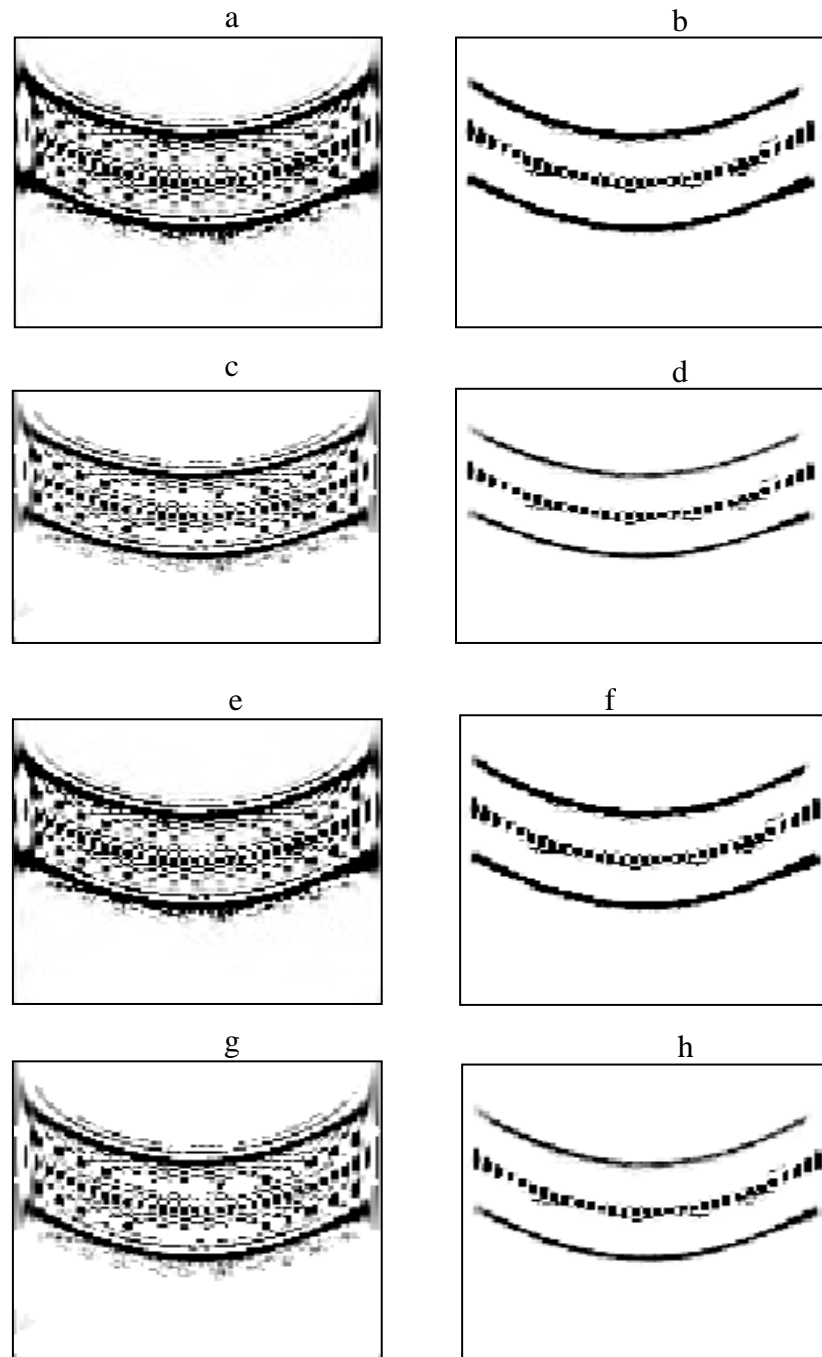
Fig. 6.9. Results of three quadratic-components (same strengths) by using proposed filtering scheme (noisy case >1dB) (a) GWT (*Eq 4.1*), (b) GWT (*Eq 4.1*) after proposed filtering, (c) GWT (*Eq 4.2*), (d) GWT (*Eq 4.2*) after proposed filtering, (e) GWT (*Eq 4.3*), (f) GWT (*Eq 4.3*) after proposed filtering (g) GWT (*Eq 4.4*) and (h) GWT (*Eq 4.4*) after proposed filtering.
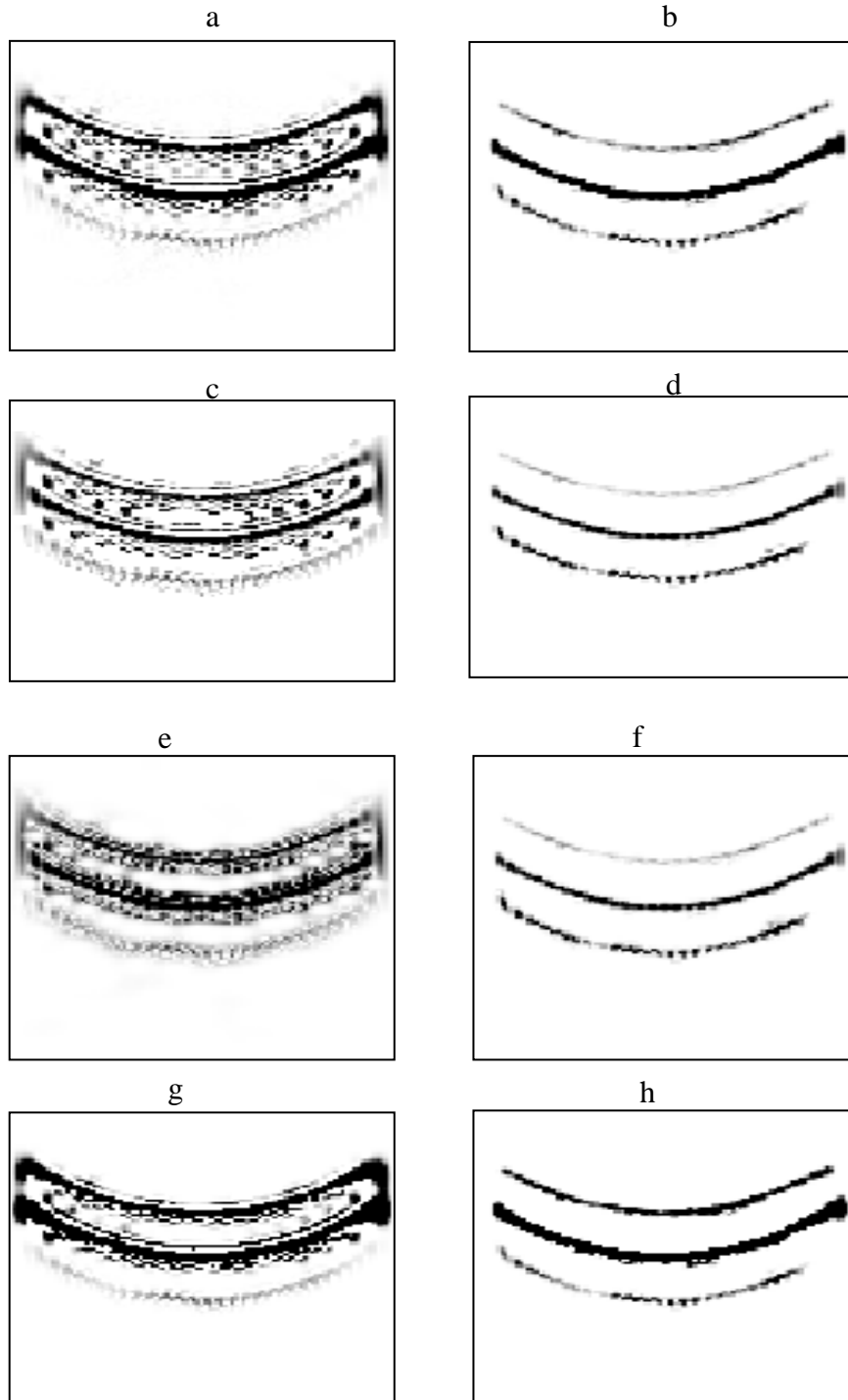
Fig. 6.10. Results of three quadratic-components (varying strengths) by using proposed filtering scheme (noisy case >1dB) (a) GWT (*Eq 4.1*), (b) GWT (*Eq 4.1*) after proposed filtering, (c) GWT (*Eq 4.2*), (d) GWT (*Eq 4.2*) after proposed filtering, (e) GWT (*Eq 4.3*), (f) GWT (*Eq 4.3*) after proposed filtering (g) GWT (*Eq 4.4*) and (h) GWT (*Eq 4.4*) after proposed filtering.

6.2.2 Performance analysis of proposed scheme

It is discussed in detail in chapter 3 that the performance of a TFR can be evaluated on the basis of its readability, energy concentration and cross-terms suppression. Cross-terms suppression and energy concentration of a TFR can be computed by visual inspection or on the basis of performance measures, like Shannon entropy [69], Renyi entropy [65], ratio of norms [68] and LJubisa measure [71]. Readability of TFRs can only be tested by visual inspection [27].

The performance of proposed method is evaluated on the basis of quantative measures like entropy measures [65], Ljubisa measure and ratio of norms [68]. Table 6.1 reveals that after LTV filtering the considered TFRs have high concentration of auto-components (high value of ratio of norm and low value of Ljubisa measure and entropy). Figs. 6.3-6.10 also describe concentration of auto-components which is due to proposed filtering mechanism.

Table 6. 1 Performance measures (test signal: three amplitude varying quadratic components)

Ratio of norms		
TFRs	Before LTV filtering	After LTV filtering
WD	0.0013	0.0075
GT	0.0005	0.0017
GWT (*Eq 4.1*)	0.0034	0.0063
GWT (*Eq 4.2*)	0.0018	0.0075
GWT (*Eq 4.3*)	0.0024	0.0075
GWT (*Eq 4.4*)	0.0026	0.0035

Ljubisa measure (($\times 10^{7}$)		
TFRs	Before LTV filtering	After LTV filtering
WD	1.1687	0.0594
GT	2.4494	0.2395
GWT (*Eq 4.1*)	0.7858	0.1093
GWT (*Eq 4.2*)	0.4713	0.0570
GWT (*Eq 4.3*)	0.4643	0.0548
GWT (*Eq 4.4*)	2.0957	0.4361

Renyi Entropy measure		
TFRs	Before LTV filtering	After LTV filtering
WD	10.6598	8.6888
GT	11.3305	9.9068
GWT (*Eq 4.1*)	9.5237	8.6453
GWT (*Eq 4.2*)	10.2094	8.6827
GWT (*Eq 4.3*)	9.9949	8.6596
GWT (*Eq 4.4*)	9.4888	9.0290

Shannon Entropy measure		
TFRs	Before LTV filtering	After LTV filtering
WD	11.7506	10.2604
GT	11.8067	10.6997
GWT (*Eq 4.1*)	10.8421	9.9585
GWT (*Eq 4.2*)	11.1737	10.2357
GWT (*Eq 4.3*)	11.1965	10.1912
GWT (*Eq 4.4*)	10.4488	9.9515

In this chapter, the advantages of GWT are analyzed by using LTV filtering for a multi-component signal. In our proposed technique, we introduce a novel strategy to eliminate cross terms with minimal distortion in the auto-components through image processing techniques. The combination of signal processing and image processing techniques successfully removes the cross- terms of WD and gives a high resolution TFR. Performance analysis of proposed method reveals that it provides solution of cross-terms of WD and resolution problem faced by linear TFRs.

Chapter 7

Conclusion and future direction

As discussed in previous chapters, time representation of one dimensional signal does not contain the frequency description of the signal. Similarly frequency domain representation of the signal have no information of frequency content of the signal changes with respect to time. Therefore, the basic goal of a time frequency representation (TFR) is to find out the energy concentration along the frequency axis at a given time [1]. A TFR provides simultaneously, time and frequency information and therefore is used to study the behavior of non-stationary signals. It provides the information which is unavailable in time or frequency representation alone. Time frequency representations (TFRs) provide information, such as number of auto-components, time duration, frequency band and relative amplitude of the considered signal [2].

TFRs are classified as Linear TFRs and Quadratic TFRs. Linear TFRs obey the principle of superposition. Linear TFRs offer no cross-terms but have low resolution of auto-components. Quadratic TFRs offer better resolutions of auto-components but have cross-terms [1, 3]. This discussion shows that there is a no unique TFR that tackles every kind of non-stationary signals. Therefore, the selection of a particular TFR is highly dependent upon specific application at hand. However, TFRs have proven themselves in successful identification, extraction and classification of signals' auto-components in various applications. TFRs are often compared in terms of their ability to suppress cross-terms, resolution performance and mathematical properties [2].

7.1 Main Contributions

This thesis contributes in the field of time-frequency signal analysis as follows:

- **Review of most widely used linear and quadratic TFRs**

    This part of the thesis contains most widely used linear and quadratic TFRs [81], including their merits and demerits. In this section, a brief

discussion on fractional Fourier transform (FRFT) and signal synthesis techniques are also given, which is used for time varying filtering. This part also provides critical analysis of some of recent cross-terms suppression techniques.

- **Modified Gabor Wigner transform**

  Gabor Wigner transform consists of two time-frequency transforms GT and WD, and hence GWT takes the advantages of both transforms (high resolution of WD and cross-terms free GT). Different ways to combine GT and WD are proposed in [4]. A modified form of Gabor Wigner Transform (GWT) has been developed by using adaptive thresholding in GT and WD [73]. The proposed GWT combines the advantages of both GT and WD and proves itself as a powerful tool for analyzing multi-component signals. Performance analysis of modified GWT shows to have high resolution as well as cross-terms suppression of WD. These different variants of GWT are applicable for slowly time varying signals [73].

- **Comparison of different variants of GWT and Modified Fractional GWT**

  In multi-component signal analysis where GWT fails to extract auto-components, the combination of signal processing techniques (FRFT) and image processing techniques (image thresholding and segmentation) have proved their potential to extract auto-components. A Modified Fractional GWT scheme was proposed which maintained the resolution of auto-components. This work also shows that FRFT domain is a powerful tool for signal analysis. Performance analysis and comparison of Modified fractional GWT reveals that it provides solution of cross-terms of WD and worst resolution faced by linear TFRs [78].

- **LTV filtering based GWT**

  In this part of the thesis, the advantages of GWT are analyzed by using the LTV filtering to study a multi-component signal. In our proposed technique [80], we introduce a novel strategy to eliminate cross-terms with minimal distortion in the auto-components through image processing techniques. In this approach a filter in time-frequency domain is designed by using an iterative approach in both time-frequency and time domains.

This filter is specifically designed in order to suppress cross-terms and enhances concentration of auto-components even weaker ones. The combined effect of signal processing and image processing techniques have shown their strength to successfully removes the cross-terms of WD and gives high resolution TFR.

7.2 Future work

- **New combinations of linear and quadratic TFRs**

  We have discussed in detail that time frequency representations (TFRs) are used for non-stationary signal analysis. TFRs are generally classified as linear TFRs and quadratic TFRs. The linear TFRs provide cross-terms free representation but with low time-frequency resolution. The time-frequency resolution is improved by using quadratic TFRs. However significant efforts are made to define algorithms for cross-terms suppression, which appear due to quadratic nature of these distributions. To overcome this difficulty it is required to define new combinations of linear and quadratic TFRs with respect to applications.

- **Use of signal synthesis techniques to study GWT**

  Signal synthesis based techniques can be used for time varying filtering and signal separation [56]. For the analysis of more complicated signals (overlapping cross-terms and auto-components), it is necessary to use advanced synthesis method instead of technique described in [56].

- **Intelligent image segmentation in proposed TFR [78]**

  The proposed method [78] can be applied to signals having crossing auto-components by intelligent image segmentation methods. In this way continuity of time-frequency signature of auto-components can be maintained [27].

- **Use of de-blurring techniques**

  The modified FRFT based GWT technique [78] initially processes the signal through linear TFR (GT), and hence suffers from resolution limitation in case of closely placed auto-components [9, 41]. This limitation can be solved by de-blurring techniques [27]. To improve

resolution of linear TFR a 2-D de-convolution operator is applied on the STFT spectrogram in [16], but this technique is highly dependent upon de-convolution method. Another method to improve resolution of the linear TFRs is based on de-blurring of spectrogram by using neural networks is described in [17].

- **Local adaptive thresholding**

  The proposed algorithm described in [78, 80] forms a binary image by using global adaptive thresholding technique. Good result can be achieved by using region based adaptive thresholding [27].

- **Modified ICI rule for IF estimation of auto-components**

  The proposed method [78, 80] can be modified to computes IF of separated auto-components by using modified ICI rule [21].

- **Analysis of more complicated signals**

  The proposed techniques [78, 80] can be modified to study the behavior of signals' auto-components with complicated IF laws by using other methods including approximation of the IF by applying Hough transform [82] and combined Wigner Hough transform [83, 84] for cross-terms reduction [64].

7.3 Applications

TFRs are used to separate and extract signal's auto-components which are buried in noise [85] and also used to estimate instantaneous frequency of a multi-component signal in low SNR [21]. Many TFRs, like wavelet transform, short time Fourier transform and GWT have been used for detection, identification and classification of power quality disturbances [45, 85].

- **New Born EEG Seizure**

  The multi-component behavior of a newborn EEG was proposed in [86] and its detail are given in [87]. There are two important features which completely describes the new born EEG seizure:

  ➤ Number of auto-components

  ➤ IF of auto- components

It was discussed in [87, 88] that raw EEG data has energy concentration in frequency band having range 0.4 to 8Hz. The proposed TFR methods [78, 81] can be extended for IF estimation of auto-components of EEG Seizure.

- **Power quality disturbances**

  Many TFRs have been used for detection, identification and classification of power quality disturbances [45, 85]. The modified GWT [73] can be used in electromagnetic phenomena (voltage sag, voltage swell, transients, harmonics, inter-harmonics, voltage change and flicker).

- **Synthetic aperture radar (SAR) imaging**

  Synthetic aperture radar (SAR) image processing is a hot research field. SAR is widely used in the military, accessing of space information and remote sensing. TFRs are used for SAR image processing [89]. The method proposed in [89] uses adaptive thresholding and adaptive selection of frequency window width to obtain highly focused radar images. The proposed techniques [78, 81] can be extended for SAR imaging in order to get focused images .

References

[1]   L. Cohen, *Time-Frequency Analysis*, Prentice Hall, Englewood Cliffs, NJ, 1995.

[2]   I. Shafi, J. Ahmad, S. I. Shah, and F. M. Kashif, "Techniques to Obtaian Good Resolution and Concentrated Time-Frequency Distributions: A Review," *EURASIP Journel on Advances in Signal processing*, vol. 2009, pages 43, 2009.

[3]   B. Boashash, *Time-Frequency Signal Analysis and Processing*, Prentice-Hall, Upper   Saddle River, NJ, USA, 2003.

[4]   S. C. Pei and J. J. Ding, "Relations between Gabor transforms and fractional Fourier transforms and their applications for signal processing," *IEEE Trans. on Signal Process.*, vol. 55, no. 10, pp. 4839-4850, Oct. 2007

[5]   L. Cohen, "Time-frequency distributions-A review," *Proc. IEEE*, vol. 77, no. 7, pp. 941-981, July 1989.

[6]   K. Gröchenig, *Foundations of Time-Frequency Analysis*, Birkhäuser, Boston, 2001.

[7]   S.G. Mallat, *A Wavelet Tour of Signal Process*, second ed., Academic Press, San Diego, 1999.

[8]   I. Daubechies, *Ten Lectures on Wavelets*, Society for Industrial and Applied Mathematics, Philadelphia, 1992.

[9]   O.Rioul and M.Vetterli, "Wavelets and Signal Processing," *IEEE Signal Processing Magazine*, vol. 8, no. 4, pp.14-38, Oct. 1991.

[10]   R. L. Allen and D. W. Mills*, Signal Analysis: Time, Frequency, Scale, and Structure*, New York: Wiley-Interscience, 2004.

[11]   R. Wilson, A.D. Calway, and E.R.S. Pearson, "A generalized wavelet transform for Fourier analysis: The multiresolution Fourier transform and its application to image and audio signal analysis," *IEEE Trans. on Inform. Theory*, vol. 38, no. 2, pp. 674–690, 1992.

[12]   R.G. Stockwell, L. Mansinha, and R.P. Lowe, "Localization of the complex spectrum: The S-transform," *IEEE Trans. on Signal Process.*, vol. 44, no. 4, pp. 998–1001, 1996.

[13]   V. Chen and H. Ling, *Time-Frequency Transforms for Radar Imaging and Signal Analysis*, Artech House, Boston-London, 2002

[14]   F. Hlawatch and G. F. Boudreaux-Bartels, "Linear and quadratic time frequency signal representations," *IEEE Signal Processing Magazine*, vol. 9, no. 2, pp. 21-67, Apr. 1992.

[15]   W.J. Williams and J. Jeong, "New time-frequency distributions: Theory and applications," *in Proc. of IEEE International Symposium on Circuits and Systems*, vol. 2, pp. 1243–1247, 1989.

[16]   Wkai Lu and Q. Zhang, "Deconvolutive short-time fourier transform spectrogram," *IEEE Signal Processing Letters,* vol. 16, no. 7, pp. 576 –579, July 2009.

[17]   I. Shafi, J. Ahmad, S. Shah, and F. Kashif, "Evolutionary time-frequency distributions using bayesian regularised neural network model," *IET Signal Processing,* vol. 1, no. 2, pp. 97 –106, June 2007.

[18]   C. Capus and K. Brown, "Short-time fractional fourier methods for the time frequency representation of chirp signals," *The Journal of the Acoustical Society of America,* vol. 113, no. 6 , pp. 3253–3263, 2003.

[19]   S. Kadambe and G. F. Boudreaux-Bartels, "A comparison of the existence of "cross terms" in theWigner distribution and the squared magnitude of the wavelet transform and the short time fourier transform," *IEEE Trans. on Signal Process.*, vol. 40, no. 10, Oct. 1992.

[20]   T. A. C. M. Classen and W.F.G. Mecklenbrauker, "The Wigner distribution-a tool for time-frequency signal analysis, part I: Continuous time signals," *Philips J. Res.*, vol. 35, pp. 217-250, 1980.

[21]   J. Lerga, V. Sucic, and B. Boashash: "An Efficient Algorithm for Instantaneous Frequency Estimation of Nonstationary Multicomponent Signals in Low SNR," *EURASIP J. on Adv. in Signal processing*, vol. 2011, pages 16, 2011.

[22]   F. Hlawatsch and P. Flandrin, "The interference structure of the Wignerdistribution and related time-frequency signal representations, in The Wigner Distribution-Theory and Applications in Signal Processing," *Elsevier,* pp. 59-133, 1997.

[23]   F. Hlawatsch, "Interference terms in the Wigner distribution," *Proc. Int. Conf. on Digital Signal Processing*, pp. 363-367, Sep 5-8, 1984.

[24]   S. Qian, *Introduction to Time-Frequency and Wavelet Transforms*, Upper Saddle River, New Jersey: Prentice-Hall, 2002.

[25]   F. Hlawatsch, T. G. Manickam, R. L. Urbanke, and W. Jones, "Smoothed pseudo-Wigner distribution, choi-williams distribution, and cone-kernel representation: Ambiguity-domain analysis and experimental comparison," *Signal Process.*, vol. 43, no. 2, May 1995.

[26]   F. Auger and P. Flandrin, "Improving the readability of time-frequency and time-scale representations by the reassignment method," *IEEE Trans. on Signal Process.,* vol. 43, no. 5, pp. 1068–1089, 1995.

[27]   N. A. Khan, *Cross-term Suppression in Wigner Distribution*, Ph.D. dissertation, M.A.J.U., Pakistan, 2010.

[28]   B. Boashash and P. O'Shea, "Polynomial Wigner-ville distributions and their relationship to time-varying higher order spectra," *IEEE Trans. on Signal Process.*, vol. 42, no. 1, pp. 216 –220, Jan. 1994.

[29]   R. B. Pachori and P. Sircar, "A new technique to reduce cross terms in the Wigner distribution," *Digit. Signal Process.,* vol. 17, no. 2, pp. 466–474, 2007.

[30]   S. Mallat and Z. Zhang, "Matching pursuits with time-frequency dictionaries," *IEEE Trans. on Signal Process.*, vol. 41, no. 12, pp. 3397 –3415, Dec 1993.

[31]   L. Stankovic, "A method for time-frequency analysis," *IEEE Trans. on Signal Process.*, vol. 42, no. 1, pp. 225 –229, Jan. 1994.

[32]   S. Stankovic and L. Stankovic, "An architecture for the realization of a system for time-frequency signal analysis Circuits and Systems II: ," *IEEE Transactions on Analog and Digital Signal Processing*, vol. 44, no. 7, pp. 600 –604, July 1997.

[33]   G. R. Arce and S. R. Hasan, "Elimination of interference terms of the discrete wigner distribution using nonlinear filtering," *IEEE Trans. on Signal Process.*, vol. 48, no. 8, pp. 2321 –2331, Aug. 2000.

[34]   E. Sejdic, I. Djurovic, and L. Stankovic, "Fractional Fourier trnansform as a signal processing tool: An over view of recent developments," *Signal Processing*, vol. 91, no. 6, pp. 1351-1369, 2011.

[35]   R. N. Bracewell, *The Fourier transforms and its applications*, McGraw-Hill 1986.

[36]   V. Namias, "The fractional order Fourier transform and its applications to quantum mechanics," *J. Inst. Math Appl.*, vol. 25, no. 3, pp. 241–265, 1980.

[37]   D. Mendlovic and H. M. Ozaktas, "Fractional Fourier transforms and their optical implementation," *J. Opt. Soc. Am. A.*, vol. 10, no. 10, pp. 1875–1881,1993.

[38]   M. A. Kutay, H. M. Ozaktas, O. Arikan, and L. Onural, "Optimal filter in fractional Fourier domains," *IEEE Trans. on Signal Process.*, vol. 45, no. 5, pp. 1129–1143, May 1997.

[39]   R. Saxena and K. Sing "Fractional Fourier transform: A novel tool for signal processing," *J. Indian Institute of Science*, vol. 85, no. 1, pp. 11-26, Jan. 2005.

[40]   S. Qazi, A. Georgakis, L. K. Stergioulas, and M. S. Bahaei, "Interference suppression in the Wigner distribution using fractional Fourier transformation and signal synthesis," *IEEE Trans. on Signal Process.*, vol. 55, no. 6, pp. 3150–3154, June 2007.

[41]   N. A. Khan, I. A. Taj, N. Jaffri, and S. Ijaz, "Cross-term elimination in Wigner distribution based on 2D signal processing techniques," *Signal Processing,* vol. 91, no. 3, pp. 590-599, 2011.

[42]   L. B. Almeida, "The fractional Fourier transform and time–frequency representations," *IEEE Trans. on Signal Process.*, vol. 42, no. 11, pp. 3084–3091, 1994.

[43]   L. J. Stankovic´ , T. Alieva, M. J. Bastiaans, "Time–frequency signal analysis based on the windowed fractional Fourier transform," *Signal Processing,* vol. 83, no. 11, pp. 2459–2468, 2003.

[44]   S. C. Pei and J. J. Ding, "Relations between the fractional operations and the Wigner distribution, ambiguity function," *IEEE Trans. on Signal Process.*, vol. 49, no. 8, pp. 1638–1655, Aug. 2001.

[45]   S.H. Cho, G. Jang, and S.H. Kwon, "Time-Frequency Analysis of Power-Quality Disturbances via the Gabor-Wigner Transform," *IEEE Trans. on Power Deliver.*, vol. 25, no. 1, pp. 494–499, Jan. 2010.

[46] H. I. Choi and W.J. Williams, "Improved time-frequency representation of multicomponent signals using exponential kernels," *IEEE Trans. on Acoust. Speech Signal Process.,* vol. 37, no. 6, pp. 862–871, 1989.

[47]   B. Zhang and S. Sato, "A time-frequency distribution of Cohen's class with a compound kernel and its application to speech signal processing," *IEEE Trans. on Signal Process.*, vol. 42, no. 1, pp. 54–64, 1994.

[48]   D. Wu and J.M. Morris, "Time-frequency representations using a radial Butterworth kernel," in Proc. of IEEE-SP International Symposium on Time-Frequency and Time-Scale Analysis, *Philadelphia*, pp. 60–63, 1994.

[49]   Z. Guo, L.-G. Durand, and H.C. Lee, "The time-frequency distributions of nonstationary signals based on a Bessel kernel," *IEEE Trans. on Signal Process.,* vol. 42, no. 7, pp. 1700–1707, 1994.

[50] A. Papandreou and G.F. Boudreaux-Bartels, "Generalization of the Choi–Williams distribution and the Butterworth distribution for timefrequency analysis," *IEEE Trans. on Signal Process.,* vol. 41, no. 1, pp. 463–472, 1993.

[51]   E.J. Diethorn, "The generalized exponential time-frequency distribution," *IEEE Trans. on Signal Process.,* vol. 42, no. 5, pp. 1028–1037, 1994.

[52]   N. Ma, D. Vray, P. Delachartre, and G. Gimenez, "Time-frequency representation of multicomponent chirp signals," *Signal Process.,* vol. 56, no. 2, pp. 149–155, 1997.

[53] B. Barkat and B. Boashash, "A high-resolution quadratic time-frequency distribution for multicomponent signals analysis," *IEEE Trans. on Signal Process.*, vol. 49, no. 10, pp. 2232–2239, 2001.

[54]   K.N. Le, K.P. Dabke, and G.K. Egan, "Hyperbolic kernel for time-frequency power spectrum," *Opt. Eng.*, vol. 42, no. 8, pp. 2400–2415, 2003.

[55] G. F. Boudreaux-Bartels and T. Parks, "Time-varying filtering and signal estimation using Wigner distribution synthesis techniques," *IEEE Trans.on Acoust., Speech, Signal Process.*, vol. 34, no. 3, pp. 442–451, Jun. 1986.

[56] B. Boashash and M. Mesbah, "A time–frequency approach for newborn seizure detection," *IEEE Eng. Med. Biol. Mag.*, vol. 20, no. 5, pp. 54–64, 2001.

[57] B. Boashash, "Estimating and interpreting the instantaneous frequency of a signal fundamentals," *Proceedings of the IEEE*, pp. 520–538, 1992.

[58] I. Djurovic and S. Stankovic, "Estimation of time-varying velocities of moving objects by time-frequency representations," *IEEE Trans. on Image Processing,* vol. 12, no. 5, pp. 550 – 562, May 2003.

[59] C. Wang and M. Amin, "Performance analysis of instantaneous frequencybased interference excision techniques in spread spectrum communications," *IEEE Trans. on Signal Process.*, vol. 46, no. 1, pp. 70 –82, Jan 1998.

[60] V. Katkovnik and L. Stankovic, "Instantaneous frequency estimation using the Wigner distribution with varying and data-driven window length," *IEEE Trans. on Signal Process.*, vol. 46, no. 9, pp. 2315 –2325, Sep 1998.

[61] Z. Hussain and B. Boashash, "Adaptive instantaneous frequency estimation of multicomponent fm signals using quadratic time-frequency distributions," *IEEE Trans. on Signal Process.*, vol. 50, no. 8, pp. 1866 –1876, Aug 2002.

[62] Wang Bai-he and J.g.H., "Instantaneous frequency estimation of multicomponent chirp signals in noisy environments," *Journal of Marine Science and Application,* vol. 6, no. 4, pp. 13–17, 2007.

[63] L. Rankine, M. Mesbah, and B. Boashash, "IF estimation for multicomponent signals using image processing techniques in the time-frequency domain," *Signal Process.*, vol. 87, no. 6, pp. 1234–1250, 2007.

[64] I. Shafi, *Time -Frequency Analysis Using Neural Networks*, Ph.D. dissertation, C@SE, Pakistan, 2009.

[65] W. J. Williams, M. Brown, and A. Hero, "Uncertainty, information and time. frequency distributions," *in SPIE, Advanced Signal Processing Algorithms,* vol. 1556, pp. 144-156, 1991.

[66] R. G. Baraniuk, P. Flandrin, A. J. E. M. Janssen, and O. Michel, "Measuring time frequency information content using the Rényi entropies," *IEEE Trans. on Info. Theory*, vol. 47, no. 4, pp. 1391-1409, May 2001.

[67] C. Arndt, *Information Measures: Information and its Description in Science and Engineering*, Springer, Berlin, 2001.

[68] D. Jones and T. Park, "A resolution comparison of several time-frequency representations," *IEEE Trans. on Signal Process.,* vol. 40, no. 2, pp. 413-420, Feb. 1992.

[69] C. E. Shannon, "A mathematical theory of communication Part I," *Bell Sys. Tech J.*, vol. 27, pp. 379-423, July 1948.

[70] T. H. Sang and W. J. Williams, "Renyi information and signal dependent optimal kernel design," *Proc. IEEE ICASSP,* pp. 997-1000, May 1995.

[71] L. Stankovic, "A Measure of Some Time Frequency Distributions concentration," *Signal Processing*, vol. 81, no. 3, pp. 212-223, Mar. 2001.

[72] B. Boashash and V. Sucic, "Resolution Measure Criteria for the Objective Assessment of the Performance of Quadratic Time-Frequency Distributions," *IEEE Trans. on Signal Process.*, vol. 51, no. 5, pp. 1253-1263, May 2003.

[73] M. Ajab, I. A. Taj , I. Shafi and S.Stankovic, "A new form of Gabor Wigner Transform by adaptive thresholding in Gabor Transform and Wigner Distribution and the power of signal synthesis techniques to enhance the strengths of GWT," *Metrology and Measurement Systems*, vol. 20, no. 1, pp. 99-106, 2013 (ISSN 0860-8229, Impact Factor 0.764).

[74] T. Acharya, A. Ray, *Image Processing: Principles and Applications*, Wiley Interscience, Hoboken, NJ, 2005.

[75] A. Farag and E. Delp, "Edge linking by sequential search," *Pattern Recognition,* vol. 28, no. 5, pp. 611–633, 1995.

[76] E. Sejdic, I. Djuroviv and J. Jiang, "Time-frequency feature representation using energy concentration: An overview of recent advances," *Digital signal Processing,* vol. 19, no. 2009, pp. 153-183, 2009.

[77] C. Hsu, C.Chang, and C.Lin, *A practical guide to support vector classification*, Technical report, Department of Computer science and Information Engineering National Taiwan University Taipei, Taiwan, 2003.

[78] M. Ajab, I. A. Taj and N. A. Khan, "Comparative Analysis of Variants of GWT for Cross-Terms Reduction," *Metrology and Measurement Systems*, vol.19, no. 3, pp. 499-508, 2012 (ISSN 0860-8229, Impact Factor 0.764).

[79] P. K. Ghosh and T. V. Sreenivas, "Time-varying filter interpretation of Fourier transform and its variants," *Signal Processing,* vol. 86, no. 11, pp. 3258-3263, 2006.

[80] M. Ajab, I. A. Taj and N. A. Khan, "A highly localized time-frequency representation scheme for dynamic signal with multiple components of

varying strengths," *Signal Processing*, (submitted, ISSN 0165-1684, Impact Factor 1.503).

[81]   M. Ajab, I. A. Taj and N. A. Khan, "On efficacy of combining linear and quadratic time frequency representations for time-varying signal analysis: A Review," *Metrology and Measurement Systems*, (accepted, ISSN 0860-8229, Impact Factor 0.764).

[82]   R. Suleesathira and L.F. Chaparro, "Interference Mitigation in Spread Spectrum Using Discrete Evolutionary and Hough Transforms," *Proc. IEEE ICASSP*, pp. 2821-2824, June 2000.

[83]   S. Barbarossa, A. Scaglione, S. Spalletta, and S. Votini, "Adaptive suppression of wideband interferences in spread.spectrum communications using the Wigner.Hough transform," *Proc. IEEE ICASSP*, pp. 3861-3864, April 1997.

[84]   S. Barbarossa, "Analysis of Multicomponent LFM Signals by a Combined Wigner.Hough Transform," *IEEE Trans. on Signal Process.*, vol. 46, no. 6, pp. 1511-1515, 1995.

[85]   M. Szmajda, K. Jang, and S.H. Kwon, "Gabor Transform, SPWVD, Gabor-Wigner Transform and Wavalet Transform – Tools For Power Quality Monitoring," *Metrol. Meas. Syst.,* vol. 17, no. 3, pp. 383-396, 2010.

[86]   H. Hassnpour, "A time-frequency approach for noise reduction," *Digital Signal Processing,* vol. 18, no. 5, pp. 728-738, 2008.

[87]   L. Rankine, N. Stevenson, M. Mesbah, and B. Boashash, "A nonstationary model of newborn EEG," *IEEE Trans. on Biomed. Eng.,* vol. 54, no. 1, pp. 19-28, 2007.

[88]   M. Scher, M. Sun, D. Steppe, R. Guthrie, and R. Sclabassi, "Comparison of EEG spectral and correlation measures between healthy term and preterm infants," *Pediatr. Neurol.*, vol. 10, no. 2, pp. 104–108, 1994.

[89]   L. Stankovic, T. Thayaparan, V. Popovic, I. Djurovic, and M. Dakovic, "Adaptive S-Method for SAR/ISAR Imaging," *EURASIP Journel on Advances in Signal processing*, vol. 2007, pages 10, 2007.